

2-9-2010

Design, optimization and analysis of reconfigurable antennas

Joseph Costantine

Follow this and additional works at: https://digitalrepository.unm.edu/ece_etds

Recommended Citation

Costantine, Joseph. "Design, optimization and analysis of reconfigurable antennas." (2010). https://digitalrepository.unm.edu/ece_etds/57

This Dissertation is brought to you for free and open access by the Engineering ETDs at UNM Digital Repository. It has been accepted for inclusion in Electrical and Computer Engineering ETDs by an authorized administrator of UNM Digital Repository. For more information, please contact disc@unm.edu.

**DESIGN, OPTIMIZATION AND ANALYSIS OF RECONFIGURABLE
ANTENNAS**

BY

JOSEPH COSTANTINE

Diploma in Electrical and Electronics Engineering-Computer and
Communications, Lebanese University, 2004
Master of Engineering-Computer and Communication Engineering, The
American University of Beirut, 2006

DISSERTATION

Submitted in Partial Fulfillment of the
Requirements for the Degree of

Doctor of Philosophy

Engineering

The University of New Mexico
Albuquerque, New Mexico

December, 2009

Joseph Costantine

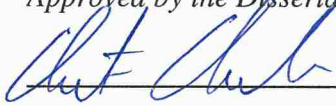
Candidate

Electrical and Computer Engineering Department

Department

This dissertation is approved, and it is acceptable in quality and form for publication:

Approved by the Dissertation Committee:



Dr. Christos Christodoulou, Chairperson



Dr. Chaouki Abdallah



Dr. Mark Gilmore

Dr. Dimitris Anagnostou



©2009, Joseph Costantine

To the carpenter after whom I was named

To the silent praying soul

To the endless tenderness and care

To my Late Grandfather, YOUSSEF

To the never breaking wings that keep me flying

To the rocks that keep me standing

To the guiding light and embodied love

To my parents, MILAD and SAIDI COSTANTINE

ACKNOWLEDGMENTS

I heartily acknowledge Dr. Christos Christodoulou, my Advisor and mentor for all his support and advice throughout this work. I thank him for believing in me and in my “ambitious” ideas.

I thank Dr. Chaouki Abdallah for all his insight, experience, great knowledge and constant care. I greatly acknowledge both Dr. Christodoulou and Dr. Abdallah for the initiation of the idea of using graphs to model reconfigurable antennas.

I thank Dr. Mark Gilmore for his experience, honesty, sincerity and for everything he taught me. I thank Dr. Dimitris Anagnostou for all his support, experience, great ideas and feedback.

I also thank Dr. Karim Kabalan and Dr. Ali el Hajj for introducing me to the world of electromagnetism and antenna design. I acknowledge Dr. Max Costa for the great information theory discussions and ideas.

I also thank my parents “Milad and Saidi” for their infinite support and sacrifice, my two brothers “Maged and Mazen” and their families for their constant presence by my side. I am thankful to all my friends for their continuous encouragement wherever they were in the world.

**DESIGN, OPTIMIZATION AND ANALYSIS OF RECONFIGURABLE
ANTENNAS**

BY

JOSEPH COSTANTINE

ABSTRACT OF DISSERTATION

Submitted in Partial Fulfillment of the
Requirements for the Degree of

Doctor of Philosophy

Engineering

The University of New Mexico
Albuquerque, New Mexico

December, 2009

DESIGN, OPTIMIZATION AND ANALYSIS OF RECONFIGURABLE ANTENNAS

by

Joseph Costantine

Diploma in Electrical and Electronics Engineering-Computer and
Communications, Lebanese University, 2004

M.E.Computer and Communication Engineering, The American University of
Beirut, 2006

Ph.D., Engineering, University of New Mexico, 2009

ABSTRACT

The ability of reconfigurable antennas to tune resonances, change polarization and modify their radiation patterns, made their development imperative in modern telecommunication systems. Their agility and diversity created new horizons for different types of applications especially in cognitive radio, Multiple Input Multiple Output Systems, satellites and many other applications. Reconfigurable antennas satisfy the requirements for increased functionality, such as direction finding, beam steering, radar, control and command, within a confined volume.

Since their rise in the last decade, reconfigurable antennas have made use of many reconfiguration techniques. The most common techniques utilized revolved around switching mechanisms. By combining low-loss, high-isolation switches such as MEMS or PIN diode switches with compatible antenna elements, we can physically reconfigure antennas and their feed structures providing frequency and polarization diversity. Other

techniques such as the incorporation of variable capacitors, varactors and physical structure alteration surfaced recently to overcome many problems faced in using switches and their biasing.

The aim of this work is to develop not only new reconfigurable antenna designs but to also establish guidelines for the design and optimization of these types of antennas. In this work a new approach for reducing redundancies in reconfigurable antennas structures using graph models as optimization tools is presented. The characteristics of various reconfigurable antennas are grouped, categorized and graph modeled according to a set of proposed rules. The optimized configurations of these antennas are presented and discussed to verify the validity of the new proposed approach. In addition to the use of graph models for the optimization approach their algorithms can be used to program field programmable gate arrays (FPGAs) to control reconfigurable antennas and automate their process.

Moreover, in this work the level of uncertainties in a reconfigurable antenna structure, the reliability and correlation between the reliability and complexity of reconfigurable antennas are mathematically formulated. Information theory is used to predict the probability of error in a reconfigurable antenna system. This work also presents the different methods that can be utilized to adjust to failures of an antenna part and to ensure a smooth functioning of the defected reconfigurable antenna.

TABLE OF CONTENTS

LIST OF FIGURES	xiv
LIST OF TABLES.....	xxii
CHAPTER 0 MOTIVATION	1
CHAPTER 1 INTRODUCTION TO RECONFIGURABLE ANTENNAS	3
1.1 Introduction:	3
1.2 Reconfigurable Antennas Classifications and Categories:	3
1.3 Reconfigurable Antennas Functional Mechanism:	5
1.4 Reconfigurable Antennas Applications:.....	6
CHAPTER 2 REVIEW OF PREVIOUSLY DESIGNED RECONFIGURABLE ANTENNAS.....	8
2.1 Introduction:	8
2.2 Review of Previously Designed Reconfigurable Antennas:.....	8
2.2.1 Reconfigurable Antennas Using Switches (Group 1):	8
2.2.2 Reconfigurable Antennas Using Capacitors or Varactors (Group 2):.....	16
2.2.3 Reconfigurable Antennas Using Physical Angular Alteration (Group 3):.....	18
2.2.4 Reconfigurable Antennas Using Different Biasing Networks (Group 4):.....	19
2.2.5 Reconfigurable Antenna arrays (Group 5):.....	20
2.2.6 Antennas Using Reconfigurable Feeding Networks (Group 6):.....	21

2.3 Biasing of Switches in Reconfigurable Antenna Structures:.....	23
2.3.1 The biasing of RF MEMS:.....	23
2.3.2 Biasing of p-i-n and Schotky diodes:.....	25
2.4 Comparison Between Different Reconfiguration Techniques:.....	27
CHAPTER 3 NEW RECONFIGURABLE ANTENNA DESIGNS.....	29
3.1 Introduction:	29
3.2 A New Reconfigurable Antenna Based on a Rotating Feed:.....	29
3.2.1 Antenna Structure and Properties:	29
3.2.2 Reconfigurable Antenna Design:	33
3.2.3 Rotation Process Control:.....	38
3.3 A Star Shaped Reconfigurable Antenna:	38
3.3.1 Antenna Structure:	38
3.3.2 Antenna Reconfiguration:	39
3.4 A Reconfigurable Multi-Band Microstrip Antenna based on open ended microstrip lines :	44
3.4.1 Antenna Design Procedure:	44
3.4.2 Antenna Structure:	46
3.4.3 Antenna Reconfiguration:	50
3.5 The Use of FPGAs to Control Reconfigurable Antennas:.....	53
3.5.1 Field Programmable Gate Arrays :	53
3.5.2 Reconfigurable Antenna Structure, Design and Tuning :	54
3.5.3 Reconfigurable Antenna Fabrication, Measurement and FPGA control:.....	55
3.5.4 Applying Neural Networks on FPGA:.....	62
3.6 Discussion:.....	63

CHAPTER 4 GRAPH MODELING RECONFIGURABLE ANTENNAS	65
4.1 Introduction:	65
4.2 Graph Outlines:	66
4.2.1 The Definition of a Graph:	66
4.2.2 The Properties of a Graph:.....	67
4.2.3 The Adjacency Matrix Representation of a Graph:	70
4.2.4 Paths and Cycles of a Graph:	71
4.3 Review of Graph applications in control systems such as robotics:	72
4.4 Rules and Guidelines for Graph Modeling Reconfigurable Antennas:	73
4.5 Dijkstra’s Shortest Path Algorithm:	93
4.5.1 Introduction to Dijkstra’s algorithm:.....	93
4.5.2 Dijkstra’s Algorithm Mechanism:.....	94
4.5.3 Applying Dijkstra’s Algorithm to The Control Process of Reconfigurable Antennas:.....	97
4.6 Discussion:	100
 CHAPTER 5 A RECONFIGURABLE ANTENNA DESIGN APPROACH USING GRAPH MODELS	 101
5.1 Introduction:	101
5.2 Proposed Reconfigurable Antenna Design Steps.....	101
5.3 Designing Reconfigurable Antennas Using Proposed Design Steps	110
5.4 Discussion:	120
 CHAPTER 6 OPTIMIZING RECONFIGURABLE ANTENNAS USING GRAPH MODELS	 121

6.1 Introduction and Optimization Techniques Review:	121
6.2 Structure Redundancy Optimization:	122
6.2.1 The Total Number of Edges In a Complete Graph:	124
6.2.2 Deriving Equations For Redundancy Reduction in Multipart Antennas of Groups (1,2,4,5,6):.....	125
6.2.3 Deriving Equations For Redundancy Reduction in Single-Part Antennas of Groups (1,2,4,5,6):.....	128
6.2.4 Deriving Equations For Redundancy Reduction in Antennas of Group 3: .	128
6.3 Examples:	129
6.4 A Chart Representation of The Optimization Approach.....	156
6.5 A Comparison Between the Optimization Approach of Section 6.2 and The Iterative Approach of Section 5.2 :.....	157
6.6 A Comparison Between The Application of Graph Models and Neural Networks On Reconfigurable Antennas:	158
6.6 Discussion:	162
CHAPTER 7 RECONFIGURABLE ANTENNAS UNCERTAINTIES, RELIABILITY AND COMPLEXITY ANALYSIS	163
7.1 Introduction:	163
7.2 Review of Reliable Circuits Using Less Reliable Relays [73]:.....	164
7.3 Review of Switches Used On Reconfigurable Antennas:	166
7.4 Reconfigurable Antennas Switches Uncertainties:	167
7.5 The Effect of The Optimization Approach On The Reconfigurable Antennas’ Reliability:.....	170
7.5.1 Reconfigurable Antenna Equivalent Configurations:.....	171

7.5.2 The Effect of The Optimization Technique On The Equivalent Configurations:.....	172
7.5.3 How To Increase The Robustness of A Reconfigurable Antenna:.....	176
7.5.4 The Reliability Assurance Algorithm:.....	179
7.6 Reconfigurable Antenna Reliability Formulations:.....	180
7.7 Reconfigurable Antenna General Complexity:.....	184
7.8 The Correlation Between The Complexity and The Reliability of A Reconfigurable Antenna:	187
7.9 Applying Fano's Inequality to Switch-Reconfigured Antennas:	190
7.10 Discussion:.....	191
CHAPTER 8 CONCLUSIONS AND FUTURE WORK	192
8.1 Conclusions:.....	192
8.2 Future Work:	194
APPENDIX A APPLICATIONS NOTES FOR P-I-N DIODES [80]	195
A.1 Application Notes:.....	195
A.2 Minority Carrier Lifetime :.....	199
REFERENCES	202

LIST OF FIGURES

Fig. 2.1 Open configuration for the antenna structure in [18].....	9
Fig. 2.2 Reconfigurable Yagi array in [16].....	9
Fig. 2.3 Reconfigurable antenna structure in [31]	10
Fig. 2.4 Reconfigurable pixel-patch antenna schematics for a) RHCP (mode 24); and b) LHCP (mode 25) at 4.1 GHz [27]	11
Fig. 2.5 The reconfigurable fractal antenna structure in [7-10].....	11
Fig. 2.6 The reconfigurable planar monopole structure in [20].....	12
Fig.2.7 Multi-part antenna in [29] with switches used to extend the spiral microstrip line length and achieve a circular polarization.....	13
Fig.2.8 The reconfigurable antenna structure in [17].....	14
Fig. 2.9 Reconfigurable antenna geometry in [36].....	14
Fig. 2.10 Reconfigurable antenna structure in [38]. a) Radiating Patch b) Ground Plane Metallisation c) Complete Antenna	15
Fig.2.11 Reconfigurable antenna in [39] a) ASA loaded with 2 p-i-n diodes b) Reconfigurable Matching Network	15
Fig.2.12 The antenna system in [40]	16
Fig.2.13 Reconfigurable OPOMEX array structure in [26]	17
Fig. 2.14 Reconfigurable antenna geometries in [12]. a) Planar Version b) Volumetric Version	18

Fig. 2.15 Antenna in [3] where the patch was bent to achieve reconfiguration	18
Fig. 2.16 Structure in [37].....	19
Fig. 2.17 Reconfigurable antenna in [4] using different biasing networks	20
Fig.2.18 Reconfigurable Antenna Array [25]	21
Fig. 2.19 Reconfigurable antenna structure in [14]	21
Fig. 2.20 Reconfigurable antenna structure [24]	22
Fig.2.21 Feeding network for the reconfigurable antenna in [24]	23
Fig. 2.22 The biasing lines and current distribution at 7 GHz as discussed in [41]	24
Fig. 2.23 The antenna layout with biasing lines and RF MEMS as in [41]	25
Fig. 2.24 Antenna in [42] with biased Schottky diodes	26
Fig. 2.25 The antenna in [36] with biasing lines for the corresponding p-i-n diodes.....	27
Fig. 3.1 Antenna structure in [44-45] with initial slot position.....	30
Fig. 3.2 Surface current distribution at 4.66 GHz on the antenna structure. a. Without Slots b. With Slots.....	31
Fig. 3.3 Antenna return loss in dB at initial slot position	32
Fig. 3.4 Antenna input reactance as a function of frequency at the initial slot position.....	32
Fig. 3.5 Antenna 3-D radiation pattern at 4.6 GHz when slot is at the initial slot position	33
Fig. 3.6 VSWR for 3 different slot positions.....	35
Fig. 3.7 Front and back view of the fabricated prototype	35

Fig. 3.8 a. The removal of the cylinder holding the Chebychev slots. b. The re-insertion of the cylinder holding the Chebychev slots through the cavity to the extended copper	36
Fig. 3.9 Comparison between simulated and measured S11 for slot at 90 deg.	36
Fig. 3.10 Radiation pattern for different slot positions. a. Phi =90 deg. cut at 1.6 GHz. b. Phi =0 deg. cut at 4.29 GHz	37
Fig. 3.11 Comparison between measured results for different slot positions	37
Fig. 3.12 Antenna structure [47]	39
Fig. 3.13 Comparison between simulated and measured return loss for all open switches	40
Fig. 3.14 The fabricated antenna	41
Fig. 3.15 Electric field distribution for the antenna for the two different switches propositions	41
Fig. 3.16 E and H plane electric field simulated radiation pattern in dB when no switch is activated at 2.8 GHz	42
Fig. 3.17 E and H plane electric field simulated radiation pattern in dB when all switches are activated at 2.8 GHz	43
Fig. 3.18 S11 comparison for different antenna configurations	43
Fig. 3.19 Two stubs with spacing S and length $\lambda/2$ [48]	45
Fig. 3.20 The S11 parameter for the 2 stubs patch with S=2 mm and S = 5 mm [48]	45
Fig. 3.21 The 4 stubs patch [48]	46
Fig. 3.22 The S11 results for the 4 lines patch with S= 2 mm	46
Fig. 3.23 The proposed antenna structure	48

Fig. 3.24 Different S11 for different stubs lengths [48]	48
Fig. 3.25 The fabricated prototype	49
Fig. 3.26 A comparison between the measured and simulated return loss [48]	49
Fig. 3.27 The antenna structure. a) Switches ON. b) Switches OFF.....	51
Fig. 3.28 S11 resonance tuning for different configurations [48].....	51
Fig. 3.29 E plane radiation pattern reconfigurability [48]	52
Fig. 3.30 H plane radiation pattern reconfigurability [48].....	52
Fig. 3.31 Schematic representation of the reconfigurable antenna	57
Fig. 3.32Antenna resonance for different diodes states 0- Diode OFF, 1 Diode ON	58
Fig. 3.33 Simulated 3-D radiation pattern at 4.875 GHz.....	59
Fig. 3.34 E and H plane cuts at 4.875 GHz.....	59
Fig. 3.35 The fabricated prototype	60
Fig. 3.36 The parallel III cable with FPGA board	60
Fig. 3.37 The S11 measurement setup	61
Fig. 3.38 A comparison between actual measurements and simulation for an antenna state	61
Fig. 3.39 A comparison between actual measurements and simulations for an antenna state	62
Fig. 3.40 Whole system diagram.....	62
Fig. 4.1 A graph G with five vertices and eight edges [55].....	67
Fig. 4.2 An example of an undirected as well as directed graph with weighted edges	69
Fig. 4.3 A graph with 5 vertices [55].....	69
Fig. 4.4 A graph representation with 6 vertices.....	70

Fig. 4.5 The antenna structure in [7-10]	75
Fig. 4.6 Graph model for different configurations of the antenna in [8]	76
Fig. 4.7 a. Antenna structure in [5] with different configurations. b. Graph modeling	78
Fig. 4.8 Illustration of Rule 2.a.....	80
Fig. 4.9 Antenna structure in [12].....	81
Fig. 4.10 Graph model of the antenna in [12]	81
Fig. 4.11 Antenna structure in [6].....	83
Fig. 4.12 Graph modeling for the antenna in [6]	84
Fig. 4.13 Antenna structure in [3].....	86
Fig. 4.14 Graph modeling of the antenna in [3].....	86
Fig. 4.15 The antenna structure in [4].....	87
Fig. 4.16 Antenna graph model	88
Fig. 4.17 The antenna array in [25].....	90
Fig. 4.18 Graph model of the array antenna in [25].....	90
Fig. 4.19 The feeding network of the antenna in [24].....	92
Fig. 4.20 The graph model for the antenna in [24]	93
Fig. 4.21 The shortest path shown in red as calculated by Dijkstra's algorithm for a weighted graph.....	94
Fig. 4.22 All possible configurations represented by all possible edges [43]	99
Fig. 5.1 The proposed structure a) Switches ON . b) Switches OFF	103
Fig. 5.2 The graph model showing all possible connections	105

Fig. 5.3 The graph model of the iteratively optimized structure.....	107
Fig. 5.4 The iteratively optimized antenna	108
Fig. 5.5 Comparison between the S11 results for the non-optimal and the optimal antenna when the switches are activated.....	108
Fig. 5.6 The radiation pattern for the non optimal and the optimal antenna when the switches are open	109
Fig. 5.7 A comparison between the simulated and tested S11 results for the optimal antenna.....	109
Fig. 5.8 The fabricated antennas.....	110
Fig. 5.9 A chart representation of the proposed design technique.....	111
Fig. 5.10 Antenna structure in [20] with parts numbered	113
Fig. 5.11 Graph modeling before designing the antenna showing the different antenna configurations	114
Fig. 5.12 Graph modeling for the optimal antenna design	115
Fig. 5.13 a. Different antenna configurations. b. Corresponding graph models	117
Fig. 5.14 The graph model of the proposed optimized topology	118
Fig. 5.15 Graph model for all possible configurations	119
Fig. 6.1 An example of possible unique paths in a given graph.....	123
Fig. 6.2 A complete graph with 3 vertices	124
Fig. 6.3 A complete graph with 7 vertices	125
Fig. 6.4 Antenna structure in [48] and its graph model	129

Fig. 6.5 Graph model with 4 vertices.....	130
Fig. 6.6 The optimized antenna structure when the switches are all ON or all OFF	131
Fig. 6.7 The radiation pattern for the non optimal and the optimal antenna when the switches are open, thus proving that the removal of redundant parts did not disturb the antenna radiation characteristics.....	132
Fig. 6.8 Different S11 for 4 different configurations of the optimized antenna. The activated parts are shown in Blue on the left	132
Fig. 6.9 Antenna in [23] and its graph model.....	133
Fig. 6.10 The optimized structure with its graph model	135
Fig. 6.11 The S11 plot for required configurations. The activated parts are shown in red on the left.....	135
Fig. 6.12 The E-plane radiation pattern for the antenna at 2.8 GHz when all switches are OFF	136
Fig. 6.13 Structure of the multifunctional MEMS-reconfigurable pixel antenna (antenna1) [71].....	138
Fig. 6.14 Flattered 3-D radiation pattern with respective antenna configurations [71] ...	138
Fig. 6.15 The antenna structure with all possible connections	139
Fig. 6.16 Different configurations required from the antenna [71].....	139
Fig. 6.17 The graph model of the antenna in [71] for all possible configurations	140
Fig. 6.18 Different antenna sections in different colors . The black parts represent the idle parts (parts never connected to achieve polarization diversity)	152

Fig. 6.19 A comparison of the S11 parameter between the original antenna and the antenna with reduced number of switches for the mode $n=0$ a. Reduced number of switches b. Original antenna	153
Fig. 6.20 The Antenna radiation pattern at 5.83 GHz for $\phi=0$ deg. and 90 deg.....	153
Fig. 6.21 Structure and graph model of the antenna in [20].....	154
Fig. 6.22 Optimized antenna graph model for all switches ON.....	154
Fig. 6.23 Antenna structure in [5] and graph model for all possible connections.....	155
Fig. 6.24 Graph of the optimized antenna topology for all possible connections.....	156
Fig. 6.25A chart representing the optimization approach	156
Fig. 6.26 A schematic representation of the antenna in [7-10] with different switches ...	159
Fig. 6.27 Antenna's frequency response's cluster 2.....	159
Fig. 6.28 Antenna's different cluster representations (current paths representations)	160
Fig. 6.29 Graph model for the antenna in [7-10].....	162
Fig. 7.1 Schematic representation of the transition probabilities	165
Fig. 7.2 Schematic representation of the transition probabilities	169
Fig. 7.3 Schematic representation of the transitional probabilities for multiple switches.	171
Fig. 7.4 Antenna structure in [23].....	172
Fig. 7.5 S11 plot for the antenna in [23] for the different configurations in Table 7.1 a. Zoomed Out. b. Zoomed In at 5 GHz.....	173
Fig. 7.6 The optimized antenna	175
Fig. 7.7 Antenna in Back-Up switch 2.05 GHz equivalent configuration.....	178

Fig. 7.8 Graph model of the equivalent configuration in Fig.7.7.....	178
Fig. 7.9 The antenna's return loss showing clear operation at 2.05 GHz.....	179
Fig. 7.10 A schematic representation of the algorithm	181
Fig. 7.11 The antenna in [71] as well as its graph model for all possible configurations .	185
Fig. 7.12 Different antenna sections.....	186
Fig. 7.13 Redundant structure in [20].....	187
Fig. A.1 Basic p-i-n diode structure [80]	195
Fig. A.2.a Basic structure [80]	196
Fig. A.3 Switching transient of a p-i-n diode [80].....	200

List of Tables

Table 3.1 Antenna dimensions.....	58
Table 4.1 A summary of section 4.4 rules for the graph modeling of reconfigurable antennas.....	95
Table 4.2 The illustration of the step by step operation of Dijkstra's algorithm.....	97
Table 5.1 Graph models for possible antenna configurations.....	120
Table 6.1 Adjacency matrix representation of the different antenna configurations.....	143
Table 6.2 The different matrices composing the adjacency matrices of Table 6.1	150
Table 7.1 The different configurations of the antenna in [23] leading to operation at 5 GHz	174
Table 7.2 Different antenna configurations for different resonances (All frequencies are in GHz).....	176

CHAPTER 0

MOTIVATION

This work was motivated by the increasing importance and development of reconfigurable antennas as well as the need for new reconfiguration techniques, the lack of clear designing guidelines, the need for an easy to grasp optimization approach and the absence of any study addressing the reliability and complexity of reconfigurable antenna systems. The major contribution of this work to these topics resides in the following points:

- Development and fabrication of new reconfigurable antenna designs
- Development of new reconfiguration techniques and their control mechanisms
- Proposition of graphs to model reconfigurable antennas
- Proposition of guidelines for the graph modeling of reconfigurable antennas and introducing algorithms that help in the control and automation of such structures
- Introduction and assessment of a new reconfigurable antenna design technique
- Establishment and test of a new optimization technique for reconfigurable antennas based on graph models
- Study the level of uncertainties in reconfigurable antennas
- Study the reliability and complexity of reconfigurable antenna topologies and their correlation

- Development of an algorithm for reliability insurance and overcoming system failure
- Prediction of the probability of error in a reconfigurable antenna system

This work includes the following eight chapters. The first chapter introduces reconfigurable antennas and explores their functional mechanism, their importance and applications. Chapter 2 reviews a variety of previously designed reconfigurable antennas. Chapter 3 introduces some of the new designs and reconfiguration techniques, and discusses the reconfiguration control process using Field Programmable Gate Arrays (FPGAs). Chapter 4 introduces graph models and proposes some guidelines to model reconfigurable antennas. Chapter 5 introduces a new reconfigurable antenna designing technique. Chapter 6 initiates a new optimization technique for reconfigurable antennas. In Chapter 7, information theory is used in conjunction with graph models to investigate the reliability and complexity of reconfigurable antennas. Overcoming failures and proposing a reliability assurance algorithm is also discussed in Chapter 7. The last chapter discusses conclusions drawn from this work with propositions for future extension.

CHAPTER 1

INTRODUCTION TO RECONFIGURABLE ANTENNAS

1.1 Introduction:

Reconfigurable antennas firstly introduced in 1998 [1], extend the functional possibilities of regular antennas by changing their configurations upon request. The reconfiguration of such antennas is achieved through an intentional redistribution of the currents or, equivalently, the electromagnetic fields of the antenna's effective aperture, resulting in reversible changes in the antenna impedance and/or radiation properties [2].

The reconfiguration of an antenna may be achieved through many techniques. Some designers resort to circuit elements while others rely on mechanical alteration of the structure such as rotating or bending of one or more of its parts [3]. Yet other approaches bias different antenna parts at different times, reconfigure the feeding networks or appropriately excite the antenna arrays [4]. All such approaches have significantly contributed to the evolution of reconfigurable antennas during the last decade. More recently, antenna designers have used electrically-actuated switches and variable capacitors in order to achieve reconfiguration [5-6]. p-i-n diodes and RF MEMS are some of the most widely used electrically-actuated devices

1.2 Reconfigurable Antennas Classifications and Categories:

Although reconfigurable antennas come in a large variety of different shapes and

forms [2], we group them into *4 main categories* based on their reconfigurability function as:

- A frequency reconfigurable antenna
- A reconfigurable radiation pattern antenna
- A reconfigurable polarization antenna
- Combinations of the above stated categories

In the case of frequency reconfigurable antennas, frequency tuning occurs for different antenna configurations [7-23]. This frequency tuning is shown in resonance shifting in a return loss data. In the case of reconfigurable radiation pattern antennas, radiation patterns change in terms of shape, direction or gain [24-26]. In the case of a reconfigurable polarization antenna, polarization types change for every antenna configuration [27-28]. In the last category, antennas exhibit many properties combined together to yield for example a reconfigurable return loss with reconfigurable polarization [29-32].

Reconfigurable antennas can also be further classified into *6 main groups* based on their present reconfiguration techniques:

- *Group 1:* Antennas using switches [5]
- *Group 2:* Antennas using capacitors or varactors [6]

- *Group 3: Antennas using physical angular alteration* [3]
- *Group 4: Antennas using different biasing networks* [14]
- *Group 5: Antenna arrays* [25]
- *Group 6: Antennas using reconfigurable feeding networks* [24]

1.3 Reconfigurable Antennas Functional Mechanism:

Reconfiguration of an antenna can be achieved based on the following basic principles or statements.

Statement 1: In order to design an antenna with frequency as the reconfigurable parameter, the designer must alter the surface current distribution on the antenna [7-23].

Statement 2: In order to design an antenna with a reconfigurable radiation pattern, the designer must alter the radiating edges, slots or the feeding network accordingly [24-26].

Statement 3: In order to design an antenna with reconfigurable polarized fields, the designer must alter the surface structure of the antenna or the feeding network accordingly [27-28].

Statement 4: In order to design an antenna with joint reconfigurable properties, the designer must use all of the above principles simultaneously [29-32].

In this work, an antenna is called a multi-part antenna if it is composed of an array of identical or different elements (triangular, rectangular,...parts). Otherwise it is called a single-part antenna. Reconfigurable antennas of group 1 use switches to connect different parts to each other in multi-part antennas as in [20] or to bridge over slots

existing in single part antennas as detailed in [5]. In multi-part antennas, switches are used to extend the length of an antenna element or to achieve specific radiation characteristics such as circular polarization [29]. However in single-part antennas switches bridging over incorporated slots are used to redirect the surface currents distribution in different directions and so reconfiguring the antenna's performance.

Reconfigurable antennas of group 2 use capacitors or varactors in multi-part as well as in single-part antennas to reconfigure the capacitances between different antenna elements or over slots incorporated in the antenna structure [6]. Reconfigurable antennas of group 3 use physical alteration like bending or rotating a part to redistribute the surface currents and change the radiation properties [3]. Reconfigurable antennas of group 4 use different biasing networks to bias different parts of multi-part antennas as in [14]. Group 5 reconfigurable antennas activate different antennas at different times in an antenna array as in [25]. Reconfigurable antennas of group 6 reconfigure the feeding network instead of reconfiguring the antenna structure as in [24].

1.4 Reconfigurable Antennas Applications:

Reconfigurable antennas find applications in many areas especially when multiple radiation properties are required from a single element. These areas are stated below:

- Cognitive radio
- Plug and play reconfigurable satellites

- Multiple Input Multiple Output (MIMO) communication systems
- Cellular and personal communication systems
- Military applications

As examples to these applications, the antennas in [34] can be used for GSM, DCS, PCS, UMTS, Bluetooth, and wireless local-area network (LAN). The antenna in [35] can reconfigure its radiation patterns by altering its structure, while the resonant frequency and polarization remain unchanged. A lot of the previously stated applications require different radiation pattern changes without affecting the frequency and polarization response. Cognitive radio applications can benefit from the antenna discussed in [36].

CHAPTER 2

REVIEW OF PREVIOUSLY DESIGNED RECONFIGURABLE ANTENNAS

2.1 Introduction:

In this chapter many previous reconfigurable antenna designs are presented and compared to show the differences in the techniques used. Details about the designs as well as their functioning mechanisms and results are shown. The biasing of electronic components used for reconfiguration such as RF MEMS switches and p-i-n diodes is also discussed through examples.

2.2 Review of Previously Designed Reconfigurable Antennas:

2.2.1 Reconfigurable Antennas Using Switches (Group 1):

The antenna shown in Fig. 2.1 [18], is composed of different patches connected together by switches. The reconfigurable antenna is fabricated as two separated prototypes (OPEN and CLOSED configurations). This antenna achieves resonance tuning.

A reconfigurable antenna based on a Yagi array [16] is shown in Fig.2.2. This antenna is designed using a basic reconfigurable dipole to work at two frequencies with double the number of reflectors and directors at the higher frequency than the lower one. For each of the two configurations of the antenna there exists a resonant frequency.

The PASS concept [31] used to realize dual band circularly polarized (CP) performance is applied to the antenna shown in Fig.2.3. A probe fed square patch antenna with a pair of tuning stubs is designed for CP performance and two orthogonal switchable slots are incorporated into the patch to control the resonant frequency. This design achieves a reconfigurable return loss with a reconfigurable polarization between Right Hand Circular Polarization (RHCP) and Left Hand Circular Polarization (LHCP).

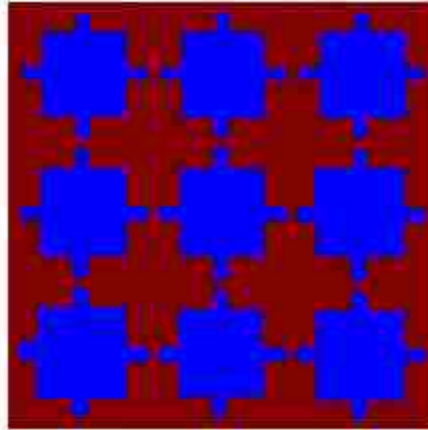


Fig. 2.1 Open configuration for the antenna structure in [18]

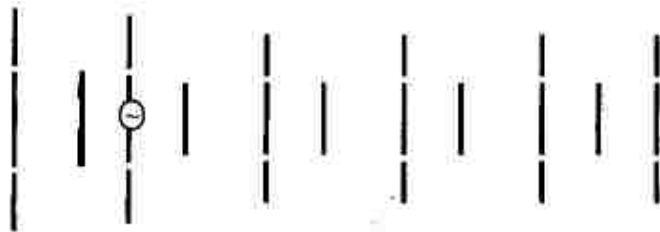


Fig. 2.2 Reconfigurable Yagi array in [16]

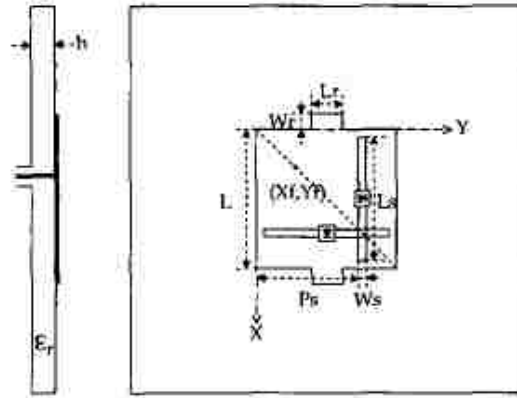


Fig. 2.3 Reconfigurable antenna structure in [31]

A pixilated structure [27] is shown in Fig. 2.4. The proposed reconfigurable pixel-patch antenna architecture is built on a number of printed rectangular shaped metallic pixels interconnected by RF MEMS actuators on a microwave-laminated substrate. The antenna provides 10 different reconfigurable modes of operation corresponding to the combination of two operating frequencies (4.1 and 6.5 GHz) and five reconfigurable polarizations of the radiated field (linear X, linear Y, dual linear, right hand circular, and left hand circular).

The fractal structure [7-10] shown in Fig.2.5 is reconfigured using RF MEMS. The basic antenna is a 130° balanced bowtie. A portion of the antenna corresponds to a two iteration fractal Sierpinski dipole. The remaining elements are added (three elements on each side) to make the antenna a more generalized reconfigurable structure.

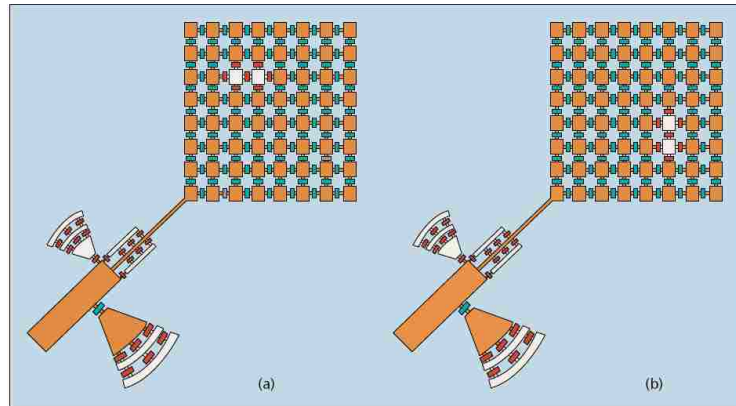


Fig. 2.4 Reconfigurable pixel-patch antenna schematics for a) RHCP (mode 24); and b) LHCP (mode 25) at 4.1 GHz [27]

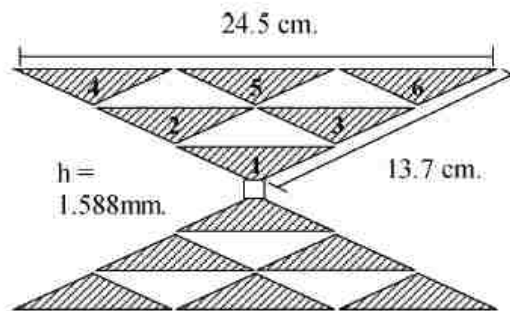


Fig. 2.5 The reconfigurable fractal antenna structure in [7-10]

A planar monopole with attached sleeves [20] is shown in Fig. 2.6. A sleeve is attached to each side of the monopole. Switches are used to connect two additional patches to each sleeve. An extra patch is also connected to the monopole via a switch.

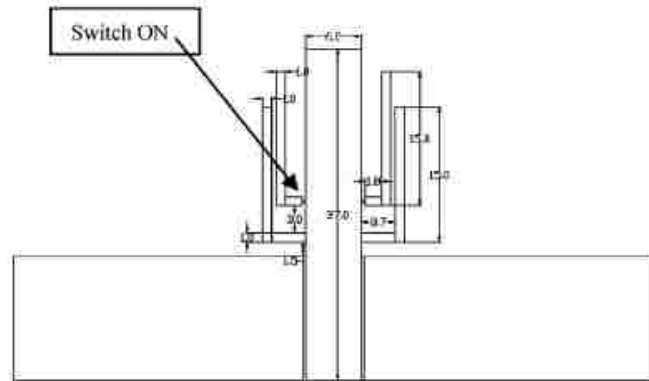


Fig. 2.6 The reconfigurable planar monopole structure in [20]

Two designs based on a spirally shaped patch [29-30] use switches to extend or shorten the length of a spiral arm. The spiral arm shaped patch antenna [29] is shown in Fig. 2.7. This spiral shaped patch is printed on the dielectric substrate and is fed in the center through a coaxial cable. Using the coaxial feed, the antenna is excited through a vertical probe, which is formed by extending the inner conductor of the coaxial line while the external side of the coax is connected to the ground plane in the back of the substrate. The spiral antenna consists of five sections that are connected with four RF-MEMS switches. The location of switches is determined such that the axial ratio and gain of the antenna are optimum at the frequency of interest. This antenna achieves resonance tuning and reconfigurable polarization.

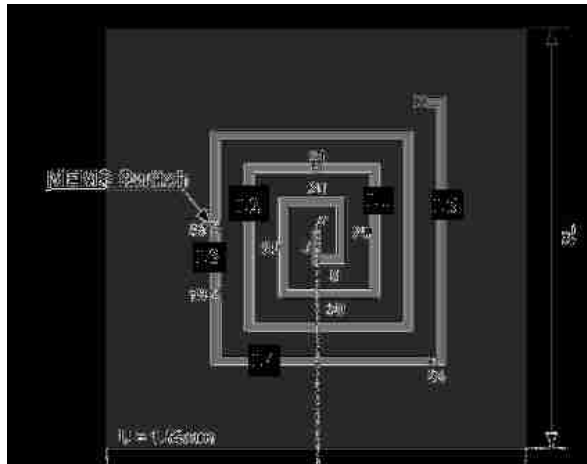


Fig.2.7 Multi-part antenna in [29] with switches used to extend the spiral microstrip line length and achieve a circular polarization

A planar inverted F antenna (PIFA) [17] is shown in Fig.2.8. The antenna structure can be capacitively loaded to reduce its size. The antenna is developed on a standard FR-4 epoxy printed circuit board substrate. The grounded side of the PIFA structure is cut into multiple straps which were, in turn, soldered to separate pads on the FR4 PCB that are connected to ground via surface-mount packaged switches. The state of the switches (open or closed) controls which straps are connected to ground (becoming part of the radiating structure) and which straps are left floating. Effectively, the location and size of the ground path can be controlled via the state of the switches.

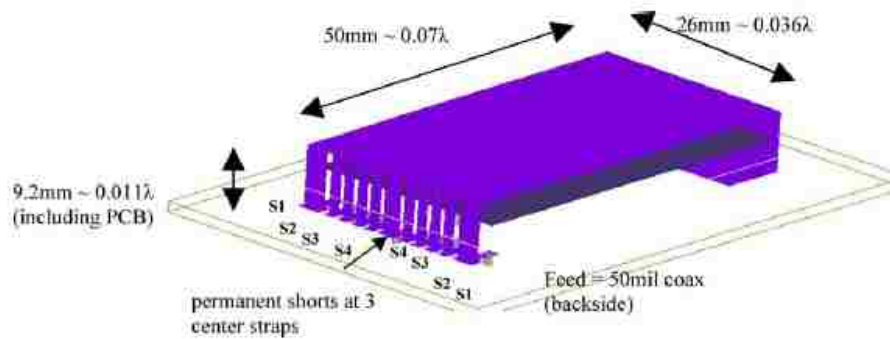


Fig.2.8 The reconfigurable antenna structure in [17]

A lot of switch reconfigured antenna designs targeted cognitive radio applications such as the antennas shown in Fig. 2.9, 2.10 and 2.11 [36,38,39]. Cognitive Radio (CR) is a new paradigm which promises to yield an improved quality of service for the user whilst also enabling more intensive use of the available radio frequency spectrum. CR requires integrated wide-narrowband antennas for performing the search and communications functions.

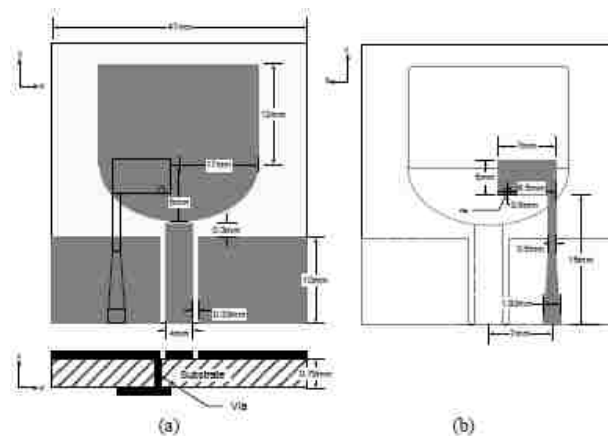


Fig. 2.9 Reconfigurable antenna geometry in [36]

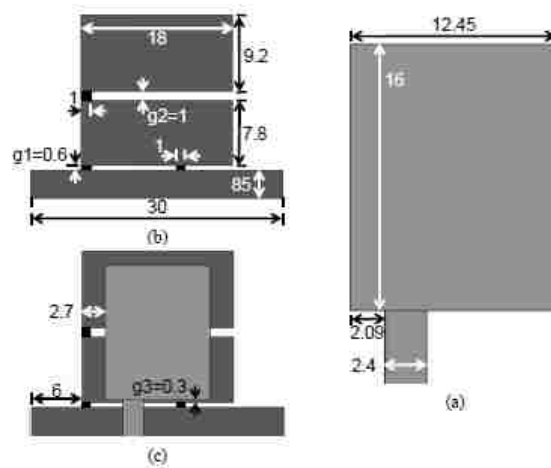


Fig. 2.10 Reconfigurable antenna structure in [38]. a) Radiating Patch b) Ground Plane Metallisation c) Complete Antenna

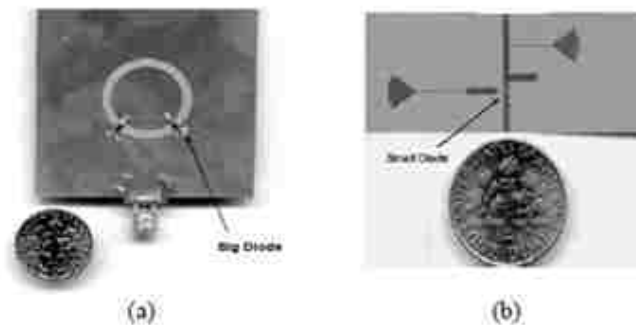


Fig.2.11 Reconfigurable antenna in [39] a) ASA loaded with 2 p-i-n diodes b) Reconfigurable Matching Network

Another switch reconfigured design represents a combination between microwave and optical techniques. This design [40], shown in Fig.2.12, exhibits reconfigurability on two levels: 1-The photonic level, 2- The RF level. Laser pulses directly generate electrical pulses via a metal-semiconductor –metal photoconductor. These pulses are routed by a coplanar waveguide to a reconfigurable fractal bow-tie antenna. The antenna’s geometry is

then reconfigured with MEMS switches. It is tuned to resonate at the quantum dot laser (QDL) mode-lock frequency.

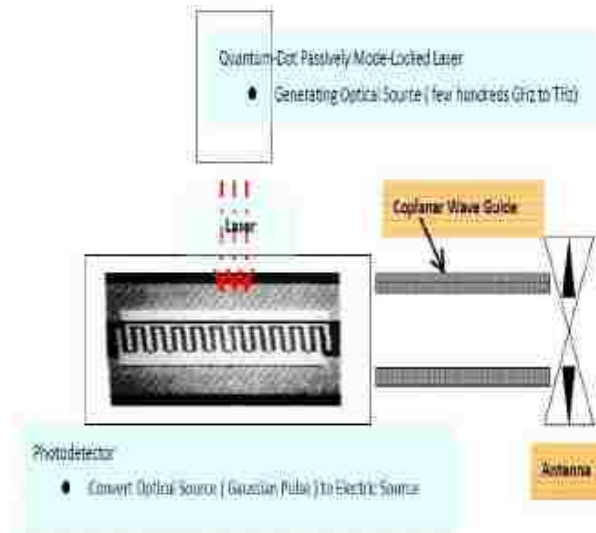


Fig.2.12 The antenna system in [40]

2.2.2 Reconfigurable Antennas Using Capacitors or Varactors (Group 2):

A printed 10 element OPOMEX reconfigurable array [26] is shown in Fig. 2.13. The thick and thin strips form a half-wavelength long transmission line. Therefore, the generator voltage appears at all points that are multiples of $\lambda/2$ from the feed point. The thick and thin lines are physically switched every half wavelength to unbalance the guided-mode currents, allowing for radiation. In order to make the OPOMEX antenna reconfigurable, variable capacitors are added in shunt at the “virtual” feed points as shown in Fig. 2.13. The ultimate goal of

varying the capacitance at each virtual feed is to generate a linearly independent set of radiation patterns that exploit the spatial diversity of the multipath channel. The capacitors can be implemented, with varactor diodes and by adding bias lines to the design [26].

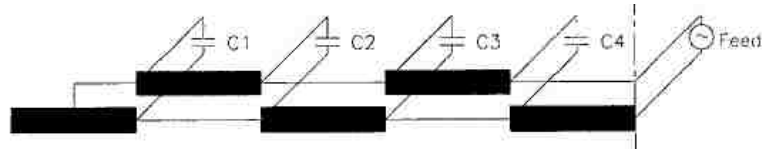


Fig.2.13 Reconfigurable OPOMEX array structure in [26]

Another design reconfigured by variable capacitors [12] is shown in Fig.2.14. The antenna is a 2x2 reconfigurable planar wire grid antenna designed to operate in free space. Variable capacitors are placed in the centers of 11 of the 12 wire segments that comprise the grid. The center of the 12th segment, located on the edge of the grid, is reserved for the antenna feed. An antenna size of 4cm x 4cm is assumed for this design. The values of the variable capacitors are constrained to lie between 0.1pF and 1 pF. These capacitors are then adjusted using a robust Genetic Algorithm (GA) optimization technique in order to achieve the desired performance characteristics for the antenna. This antenna exhibits resonance tuning.

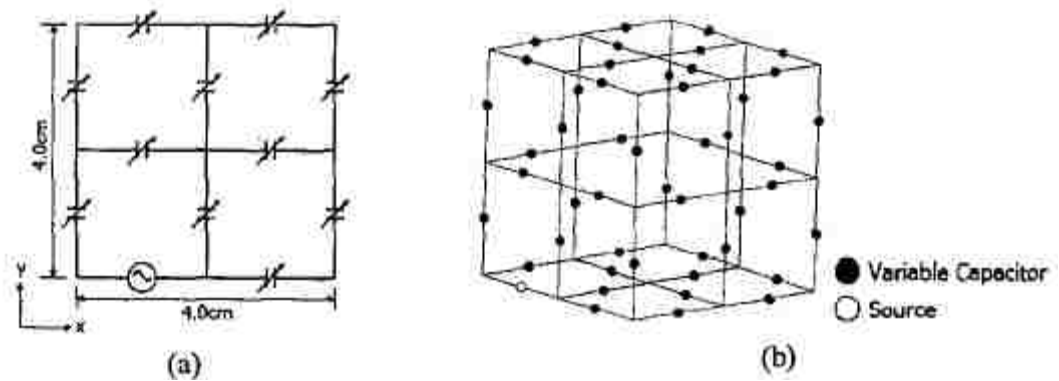


Fig. 2.14 Reconfigurable antenna geometries in [12]. a) Planar Version b)

Volumetric Version

2.2.3 Reconfigurable Antennas Using Physical Angular Alteration (Group 3):

The first design that used a mechanical structural change to achieve reconfiguration [3] is shown in Fig.2.15. The antenna is fabricated over a sacrificial layer residing on the substrate. A thin layer of magnetic material is then electroplated on the antenna surface. By etching away the sacrificial layer between the antenna and substrate, the antenna is released and connected only by its feed line.



Fig. 2.15 Antenna in [3] where the patch was bent to achieve reconfiguration

When an external field is applied, the flexible region created at the junction between the released and unreleased microstrip line is plastically deformed and the structure is bent by an angle. After this plastic deformation, the antenna remains at a certain rest angle above the substrate even after the field is removed. This antenna exhibits resonance tuning.

An example of a reconfigurable frequency selective surface [37] provides a new variation by incorporating magnetically actuated dipole elements that are capable of being tilted away from the supporting surface. This design is shown in Fig.2.16.



Fig. 2.16 Structure in [37]

2.2.4 Reconfigurable Antennas Using Different Biasing Networks (Group 4):

A reconfigurable antenna using different biasing segments [4] is shown in Fig.2.17. The antenna's reconfiguration is achieved by turning ON or OFF various sections, to change the active length of the assembled monopole antenna structure.

As expected, as more sections are turned ON, the operating frequency shifts to lower values [4].

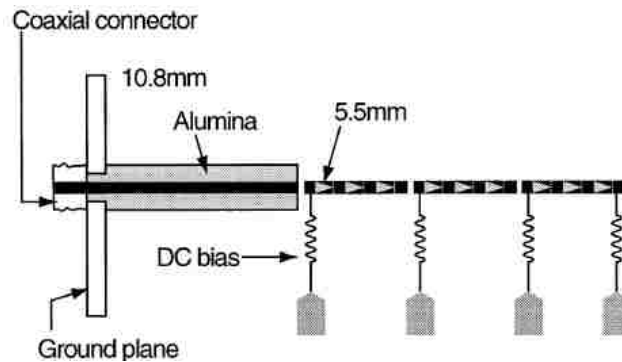


Fig. 2.17 Reconfigurable antenna in [4] using different biasing networks

2.2.5 Reconfigurable Antenna arrays (Group 5):

The antenna shown in Fig. 2.18 is a cube model [25]. Four cube faces are chosen to reside in the same plane, facing the + x-direction and + y-direction in a Cartesian coordinate system. All four antennas are similarly oriented with respect to the four cube faces, with the primary plane and primary polarization coincident to the plane of integration. The bottom face (-z-direction) is used to feed the structure and the top face (+z-direction) is not used in this work. The antennas are mechanically fastened to the structure using nylon screws and appropriately tapped receptacles on the cube faces. This antenna exhibits reconfigurable radiation pattern [25].

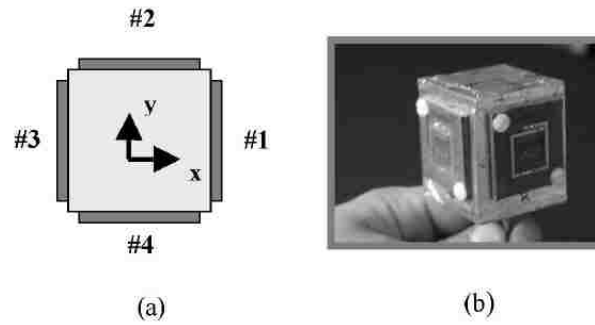


Fig.2.18 Reconfigurable Antenna Array [25]

2.2.6 Antennas Using Reconfigurable Feeding Networks (Group 6):

One of the first antenna designs that resorted to switch-reconfigured feeding [14] is the one shown in Fig.2.19. The antenna consists of an element with a slot, a ground plane, and an active switching network, which can select the location of the feeding point (either location 0 or location 1). Different resonances were obtained for each feeding position.

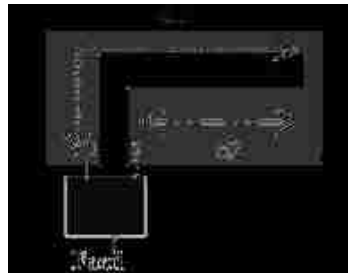


Fig. 2.19 Reconfigurable antenna structure in [14]

Another design using reconfigurable feeding [24] is shown in Fig.2.20. This antenna is based on the parasitic antenna concept and it realizes pattern diversity. Only the driven element is fed while the parasitic elements are strongly coupled to

the driven element and loaded by a switched reactance, usually a switched stub in practice.

The different combinations of switched loads yield a set of switched radiation patterns. The prototype is a three-element parasitic antenna array where aperture-coupled square patches are used as radiating elements. The slot selection results either in an E-plane or H-plane coupling of the central patch with the adjacent parasitic patches. The selected slot also enforces one of the two linear orthogonal polarizations. To realize the pattern diversity, each of the slot pairs in the parasitic patches is loaded by a switchable stub. The stub lengths are adjusted by p-i-n diodes which allow four different patterns for one of the polarization state [24]. The feeding configuration is shown in Fig. 2.21.

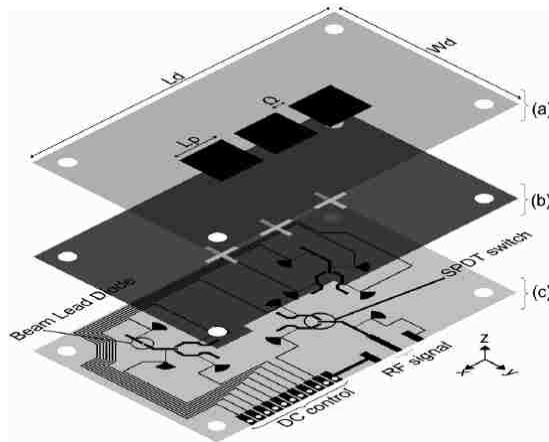


Fig. 2.20 Reconfigurable antenna structure [24]

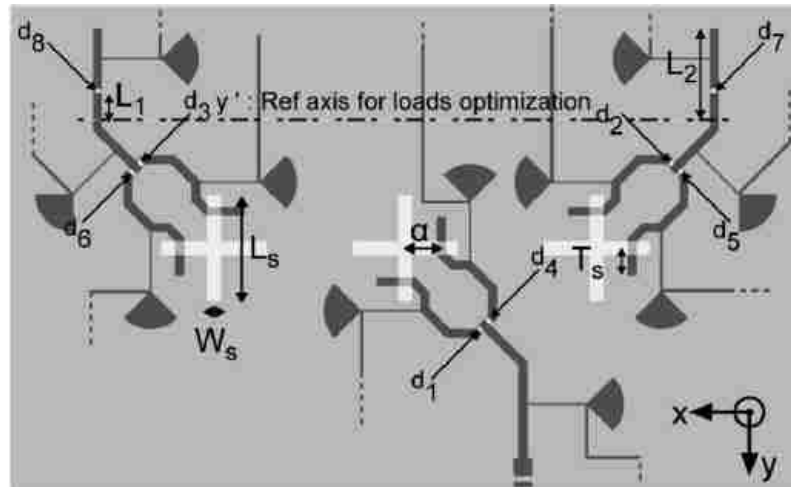


Fig.2.21 Feeding network for the reconfigurable antenna in [24]

2.3 Biasing of Switches in Reconfigurable Antenna Structures:

Most antenna designers resort to RF MEMS and diodes to achieve switching in their reconfigurable antenna designs. In this section the biasing of such switching elements is discussed briefly.

2.3.1 The biasing of RF MEMS:

The bias lines are connected on the side of each switch providing the necessary potential difference between the bottom electrode and the membrane [41]. In this section the antenna in [7-10] is taken into consideration and the biasing lines are applied to this antenna as discussed in [41]. The lines extend away from the furthest upper or lower metal part of the antenna up to where the biasing probe pads connect.

To ensure the accuracy of the applied potential difference between the suspended membrane and the bottom electrode, two more biasing lines provide the DC ground at the areas where the membrane contacts the antenna [41]. The connections of the bias lines to a switch are shown in Fig. 2.22. The bias lines pass close to the antenna and are parallel to its edges. This way if any energy is radiated from them, the chances are that it will interfere constructively with the antenna's radiation pattern [41].

Metallic bias lines will deteriorate the corresponding antenna's performance. An example of the performance deterioration is shown in [41]. A highly resistive but conducting lines are suggested to minimize the disturbance caused by the bias lines to the antenna's performance. After applying all the previously discussed constraints such as incorporating highly resistive materials for the bias lines and optimizing the directions and extensions of the bias lines, the layout of the antenna in [41] is shown in Fig.2.23.

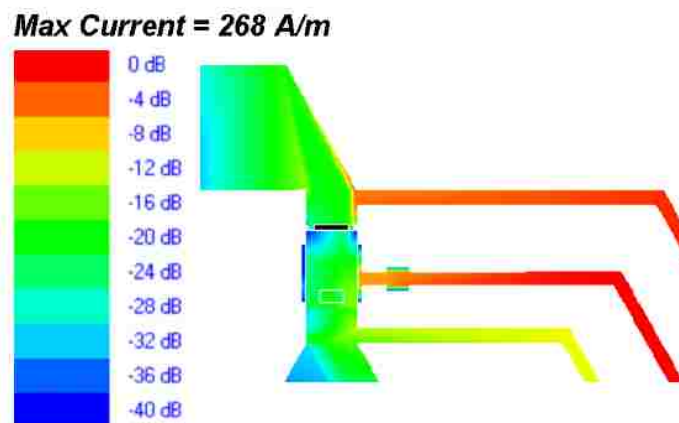


Fig. 2.22 The biasing lines and current distribution at 7 GHz as discussed in [41]

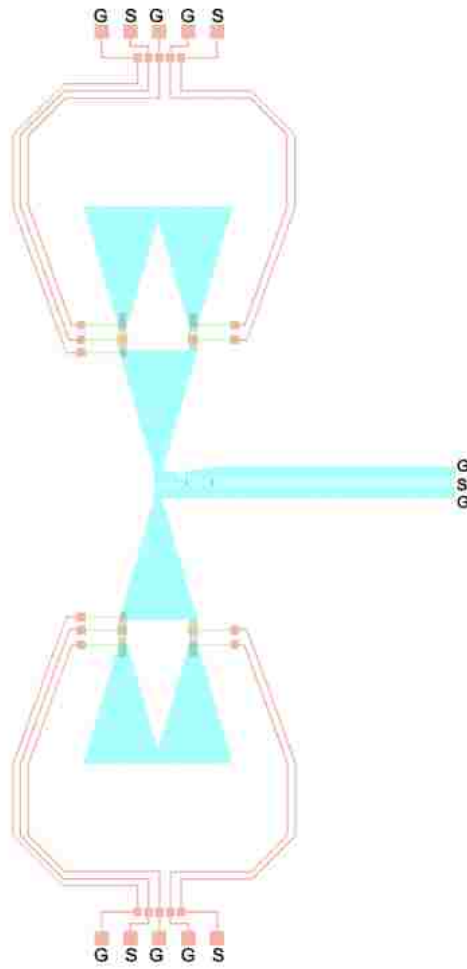


Fig. 2.23 The antenna layout with biasing lines and RF MEMS as in [41]

2.3.2 Biasing of p-i-n and Schotky diodes:

Most designers resort to p-i-n diodes [36] to achieve switching , however others resort to schotky diodes [42] or other types of diodes to achieve switching. There is usually a trade off between the p-i-n diodes and Schotky diodes. A Schotky diode has a high switching speed with an estimated insertion loss of 2 dB,

while a p-i-n diode has a slower switching speed with a lower insertion loss (typically 1 dB).

The biasing of such diodes has to be achieved by connecting one endpoint of each diode to ground when the other endpoint is connected to a DC voltage. The voltage value depends on the diode used. The connection to ground or VCC has to be achieved using quarter wave transformers and radial stubs at the end for better matching.

In [42] the authors specified that they combined the RF signal feeding the antenna with 1.5 V/0V using a bias network. The authors also isolated the DC feed by cutting a slot across the patch as shown in Fig.2.24 .

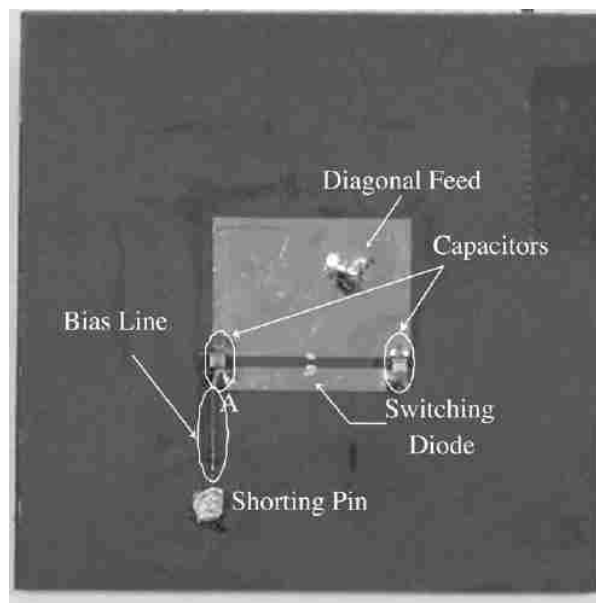


Fig. 2.24 Antenna in [42] with biased Schottky diodes

Two 47 pF capacitors are soldered at the ends of the slot to maintain the RF connection. The lower part of the patch is dc grounded by a shorting pin using a $\lambda/4$ bias line [42]. Fig.2.24 shows the antenna structure with biased Schottky diodes.

In [36] p-i-n diodes were used to control the length of a microstrip line feeding an antenna. Fig. 2.25 shows the antenna with the microstrip line reconfigured by p-i-n diodes with the corresponding biasing network.

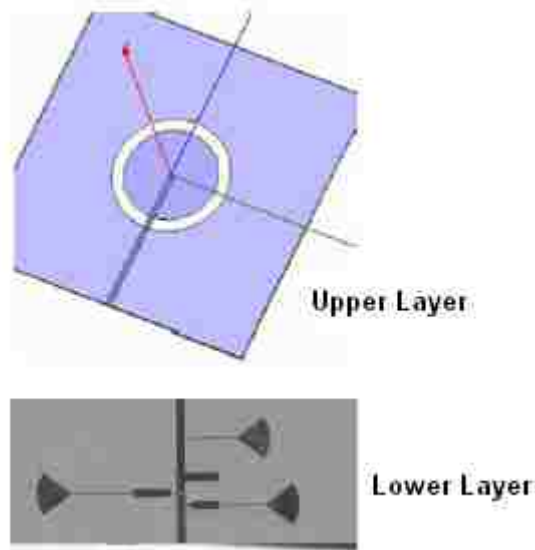


Fig. 2.25 The antenna in [36] with biasing lines for the corresponding p-i-n diodes

2.4 Comparison Between Different Reconfiguration Techniques:

All the techniques used in the designs presented in the previous sections have

advantages and disadvantages. Investigating all these designs, one notices *a shift in use from RF-MEMS to p-i-n diodes* to achieve switching. While p-i-n or Schottky diodes require less biasing lines, the difficulties encountered with biasing RF-MEMS are not greatly alleviated by the use of p-i-n or Schottky diodes. The use of variable capacitors is considered an efficient reconfiguration method however many issues appear in terms of achieving voltage variations or biasing varactors.

Mechanical and physical alterations of an antenna structure is generally difficult to implement and designers are still looking for an easy way to implement mechanical reconfiguration. Reconfiguring the feeding network and the excitation of different antenna elements in reconfigurable antenna arrays as well as biasing different antenna parts at different times still present a great challenge.

Some researchers are still looking for *new techniques* they can use with the least amount of losses, interferences and difficulties; while others are trying to *optimize the existing methods* and improve their implementation. In the following chapters , new reconfiguration techniques as well as new design and optimization techniques are presented to reduce the cost and losses that are present in currently existing designs.

CHAPTER 3

NEW RECONFIGURABLE ANTENNA DESIGNS

3.1 Introduction:

In this chapter *new reconfigurable antenna designs* as well as *a new reconfiguration technique based on slot rotation* are introduced. The mechanization of reconfigurable antennas such as the automation of the slot rotation process gives it more precision and accuracy. The use of algorithms defined in other areas such as computer science, control systems and neural networks is beneficial to program a Field Programmable Gate Array (FPGA) to achieve a better control of any reconfiguration process. In the case where p-i-n diodes are used to reconfigure an antenna, the activation of diodes and control of their OFF/ON states can be also achieved through an FPGA.

3.2 A New Reconfigurable Antenna Based on a Rotating Feed:

3.2.1 Antenna Structure and Properties:

The antenna we propose here is the one in [22, 43]. The basic structure [44-45] of this antenna, shown in Fig. 3.1, consists of three different layers. The lower layer, which constitutes the ground plane, covers the entire substrate (width 3cm and length 7.5 cm). The middle substrate has a dielectric constant of $\epsilon_r=3.9$ and a height of 0.16cm. The upper layer, which is the patch, consists of a rectangle

of $1.5\text{cm} \times 2\text{cm}$ joined with an isosceles triangle (base= 1.5 cm and height $h=4\text{ cm}$). Inside the rectangular patch, ten rectangular slots that follow a Chebychev distribution around a center rectangular slot, were inserted. Furthermore, inside the triangular patch a triangular slot of base $=0.75\text{ cm}$ and of height 0.6062 cm is inserted. The antenna is fed through a $50\ \Omega$ SMA connector where the feeding position is optimized for the original slot position.

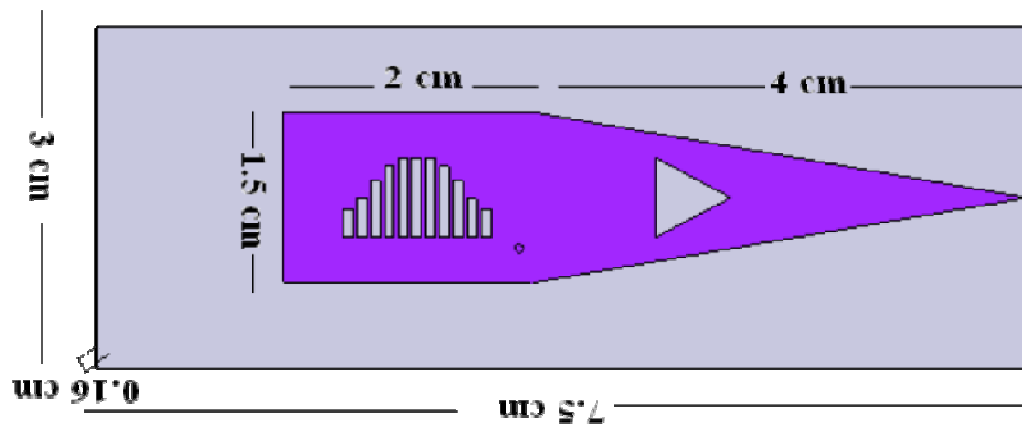


Fig. 3.1 Antenna structure in [44-45] with initial slot position

The patch is composed of a rectangular part joined with a triangular part. The resultant shape with the Chebychev slots improves the multi-band property of the entire antenna and the triangular slot fine-tunes these resonances to some desired frequencies as detailed in [44-45].

A comparison between the surface current distribution on the antenna structure with and without the slots is shown in Fig.3.2. The multi- resonance operation of this antenna is shown in the return loss plot of Fig.3.3 and in the zero-reactance crossing of the antenna input impedance in Fig.3.4. Fig. 3.5 shows the three-dimensional radiation pattern of the antenna at 4.6 GHz. The simulations were done using Ansoft's HFSS V11.

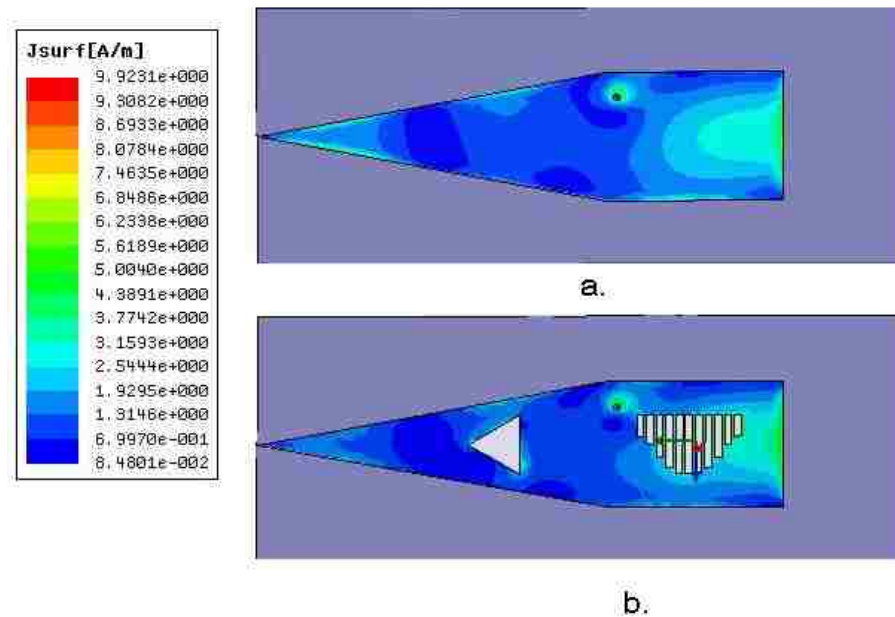


Fig. 3.2 Surface current distribution at 4.66 GHz on the antenna structure. a.

Without Slots b. With Slots

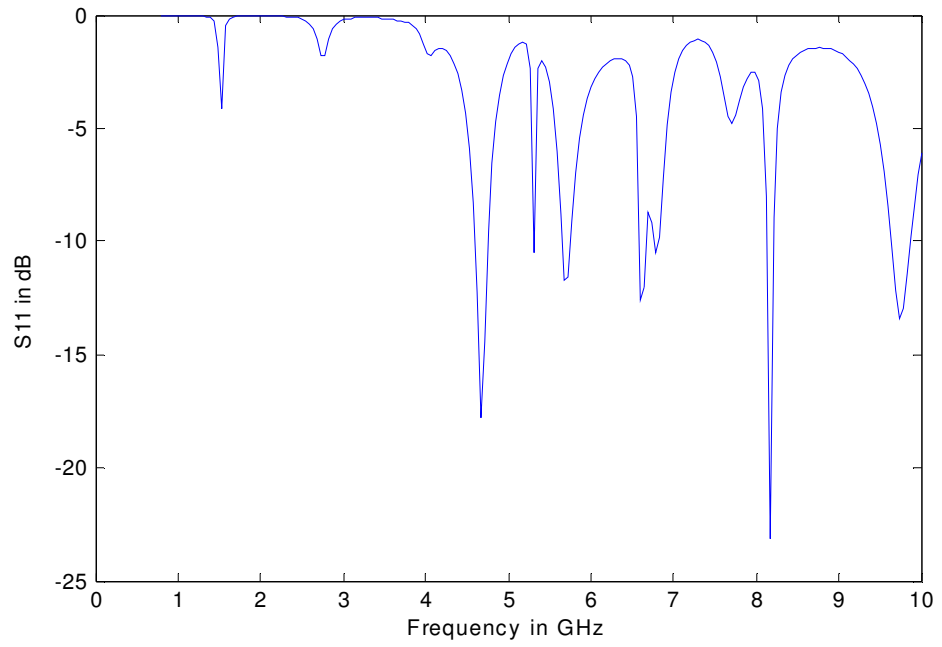


Fig. 3.3 Antenna return loss in dB at initial slot position

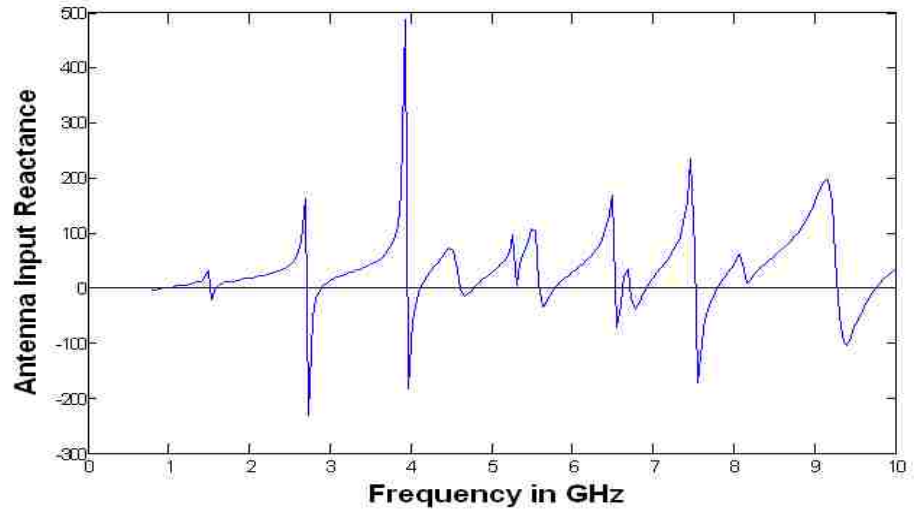


Fig. 3.4 Antenna input reactance as a function of frequency at the initial slot position

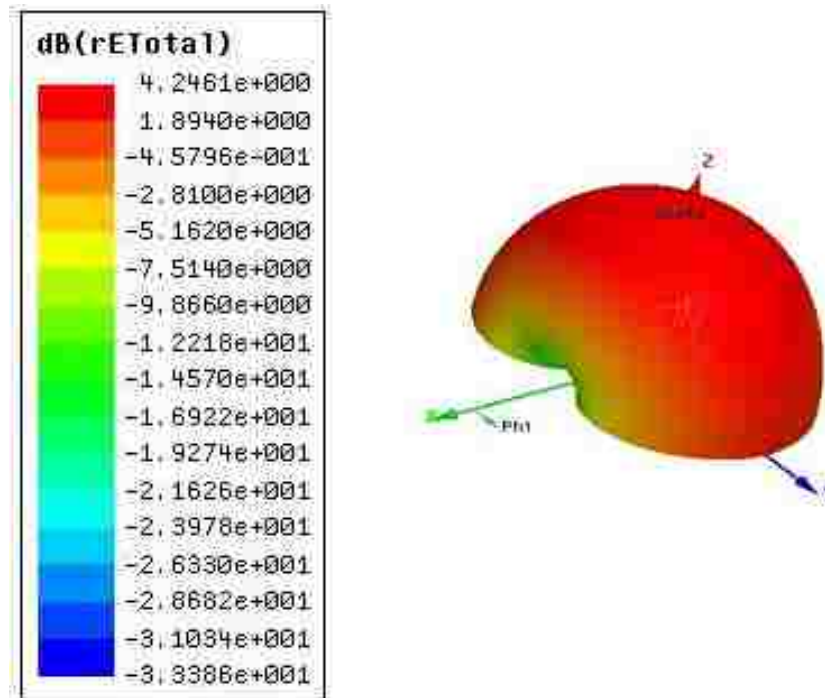


Fig. 3.5 Antenna 3-D radiation pattern at 4.6 GHz when slot is at the initial slot position

3.2.2 Reconfigurable Antenna Design:

We want to achieve an antenna with reconfigurable resonant frequencies and without the use of switches. For each surface current distribution the antenna exhibits a set of resonant frequencies. The alteration of the surface current distribution will result in a reconfigurable resonance antenna. The reconfiguration technique investigated here makes use of a slot rotation. Since the Chebychev slots boost the antenna's multi band property, their rotation will change the surface current distribution on the patch of the antenna and will constitute an indirect feed

rotation.

The slot rotation changes the reactive loading imposed by the presence of the slots in the structure. Fig. 3.6 shows the simulated VSWR (Voltage Standing Wave Ratio) for 3 different slot positions illustrating the structure's resonance tuning. Fig. 3.6 shows that this resonance tuning is clearer for frequencies higher than 4 GHz. New resonances are created as well as shifts in bandwidths and changes in amplitudes.

The fabricated antenna is shown in Fig. 3.7 and represents the last prototype fabricated. A small cylinder was removed from the body of the antenna and then reattached with a manual handle. The removal of the cylinder has to start from the bottom of the antenna (ground plane) reaching to the top (the patch), leaving a small copper extension from the body of the patch around the cavity, constantly touching the circle holding the slots at all time, as shown in Fig. 3.8. It is important to keep the connection between the circle holding the slots and the rest of the patch at all slots position so that the surface currents have a continuous flow. The knob is manually rotated in the fabricated prototype. Fig. 3.9 shows the matching between the return loss for the fabricated and the simulated antenna when the Chebychev slots are at 90 degrees. Fig. 3.10 shows the simulated radiation patterns for different slot positions and different plane cuts at 1.6 GHz

and 4.29 GHz. The measured return loss tuning for different slot positions is shown in Fig. 3.11. We note that the rotation from 0 to 90 degrees shifts the resonances to higher frequencies while the rotation from 90 to 180 degrees shifts these resonances back to lower frequencies as shown in Fig.3.11.

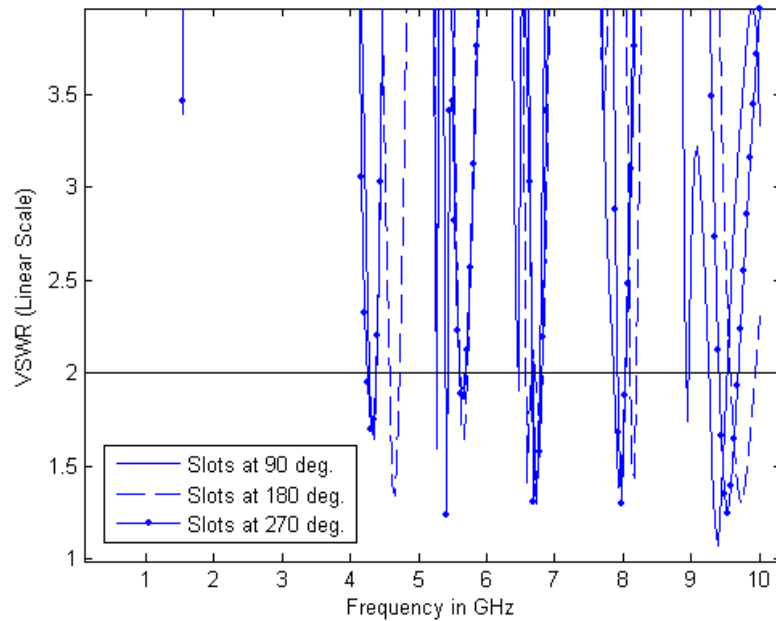


Fig. 3.6 VSWR for 3 different slot positions



Fig. 3.7 Front and back view of the fabricated prototype

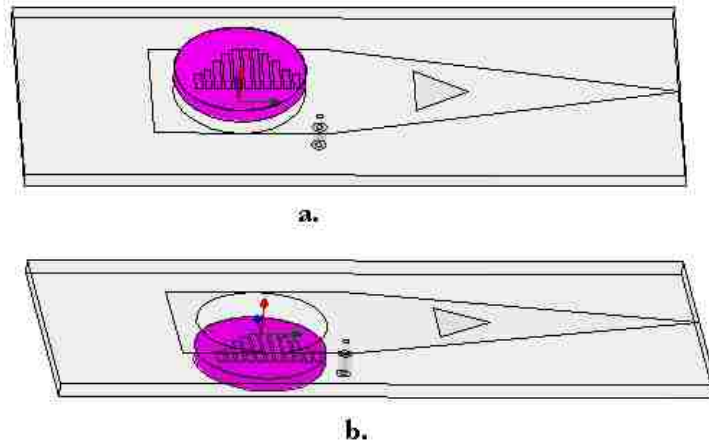


Fig. 3.8 a. The removal of the cylinder holding the Chebyshev slots. b. The re-insertion of the cylinder holding the Chebyshev slots through the cavity to the extended copper

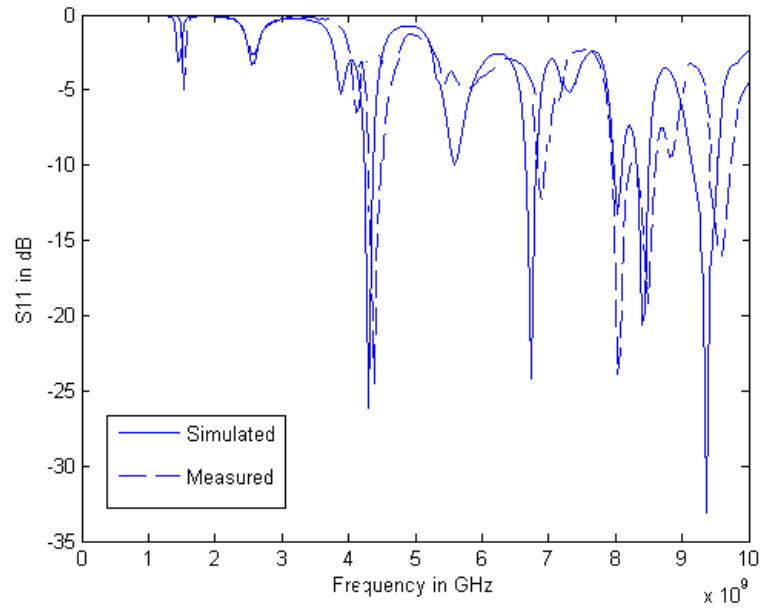


Fig. 3.9 Comparison between simulated and measured S11 for slot at 90 deg.

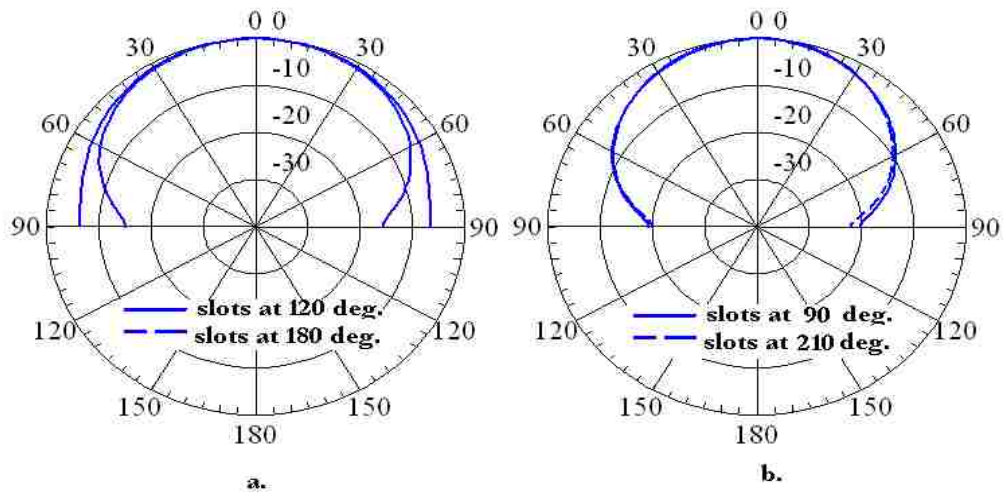


Fig. 3.10 Radiation pattern for different slot positions. a. $\Phi = 90^\circ$ cut at 1.6 GHz. b. $\Phi = 0^\circ$ cut at 4.29 GHz

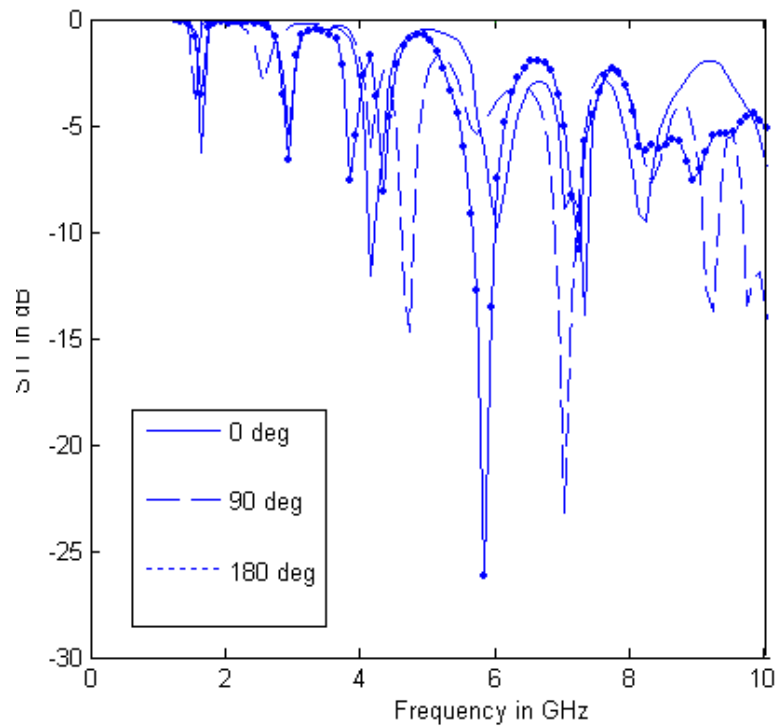


Fig. 3.11 Comparison between measured results for different slot positions

3.2.3 Rotation Process Control:

Several commercial rotary switches can be used to automatically rotate the slot. Rotary switches can also be customized for this design and implemented through an FPGA to control the rotation of the slots on the antenna. In the next chapter an algorithm based on graph models is proposed to be implemented on the FPGA to control the slot rotation.

The slot rotation technique was also used to reconfigure an antenna designed based on cellular automata “Game of Life” rules [46]. Different resonant frequencies are obtained for different slot positions. The transition between cellular automata stages is done via rotation.

3.3 A Star Shaped Reconfigurable Antenna:

3.3.1 Antenna Structure:

Two different prototypes [23, 47] were investigated with the same basic structure. The differences between the two prototypes are the substrate used and the switches arrangement. This example takes into consideration the last prototype presented in [47]. The basic structure of the proposed antenna is shown in Fig. 3.12. The antenna consists of 3 layers. The lower layer, which constitutes the ground plane, covers the entire hexagon shaped substrate which has a side of 2.915 cm. The middle substrate is Isola Gigaver 210 [47]. The substrate’s

dielectric constant ϵ_r is 3.75 and the height is 0.235 cm. The upper layer, which is the patch, completely covers the hexagonal top surface. Six triangle slots of sides 1.2 cm and 1.4 cm and a base of 0.73 cm are cut out of the patch giving it the shape of a six armed star. In the star patch six rectangular slots of length 1.4 cm and width 0.2 cm are cut on each branch of the star, as shown in Fig. 3.12. The antenna is fed with a coaxial probe of 50 Ω impedance. The feeding position was optimized using Ansoft HFSS V11. The optimization process took into consideration the antenna reconfigurable functioning and its radiation properties.

3.3.2 Antenna Reconfiguration:

The antenna was at first simulated without any added component. It was then fabricated and measured and a comparison between simulation and measurements results is shown in Fig. 3.13, where good agreement between them can be observed. The fabricated prototype is shown in Fig. 3.14.

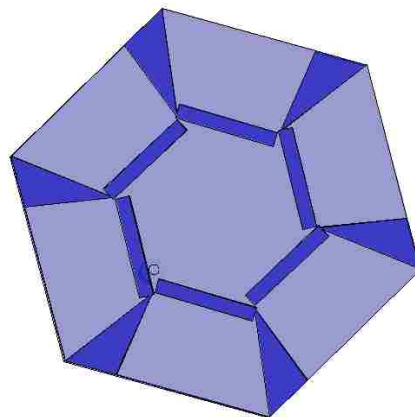


Fig. 3.12 Antenna structure [47]

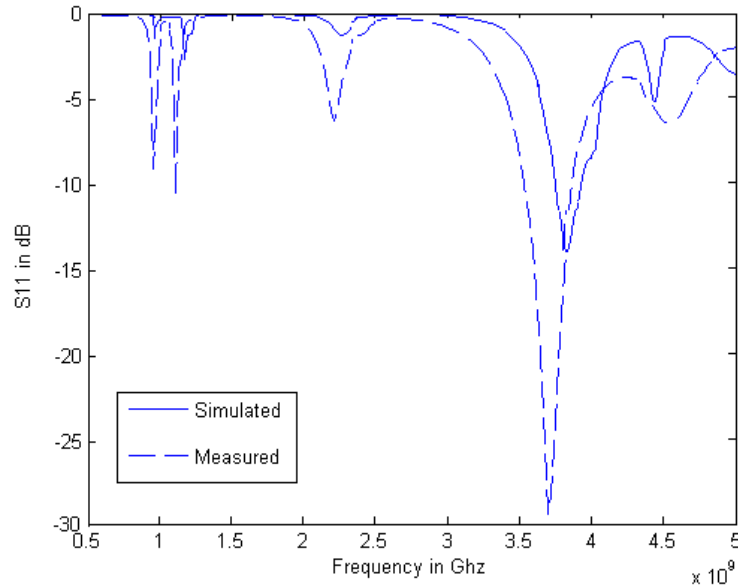
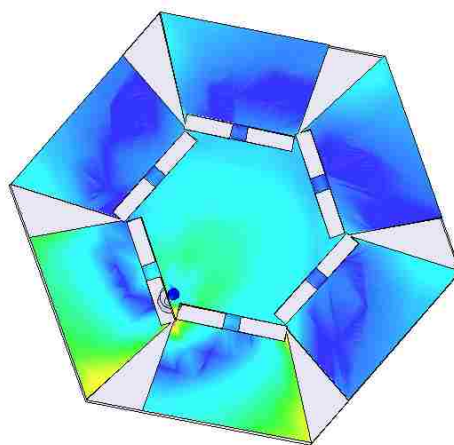


Fig. 3.13 Comparison between simulated and measured return loss for all open switches

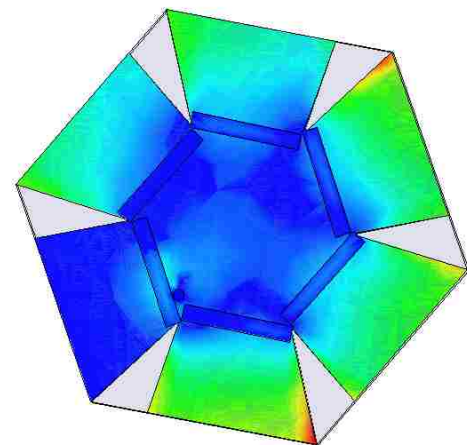
The reconfiguration of the antenna is investigated in [23] by using six square switches of side 0.2 cm that were mounted at the center of the rectangular slots, as shown in Fig. 3.15.a. These switches can be replaced in reality by p-i-n diodes. Using these switches, a reconfigurable return loss is achieved as shown in [23]. However the radiation pattern did not exhibit significant changes. Replacing the square switches by switches covering the whole slots is proposed. The electric field distribution (Fig. 3.15.b) becomes completely different from the electric field distribution of the structure using the small square switches (Fig. 3.15.a), exhibiting now higher intensities.



Fig. 3.14 The fabricated antenna



a) Small Square Switches



b) Whole Slots Switches

Fig. 3.15 Electric field distribution for the antenna for the two different switches propositions

The radiation pattern reconfiguration is shown in Fig. 3.16 and 3.17, where the patterns for the antenna with all deactivated and activated switches are shown, respectively. The change in the radiation pattern is significant when all switches are activated simultaneously. The changes for other antenna configurations are not as remarkable. The radiation patterns obtained at the frequency 2.8 GHz for the E and H planes are shown in Fig. 3.16 and 3.17. The antenna also exhibits frequency tuning as can be seen in Fig. 3.18.

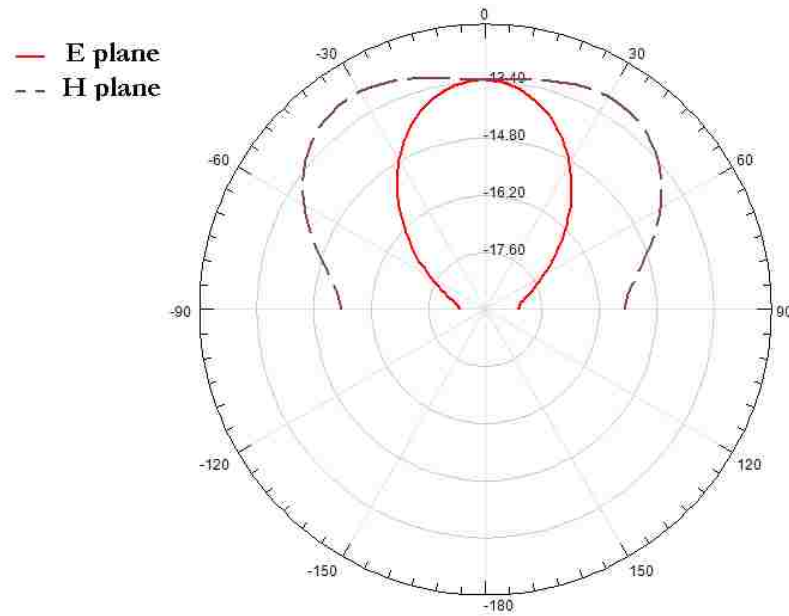


Fig. 3.16 E and H plane electric field simulated radiation pattern in dB when no switch is activated at 2.8 GHz

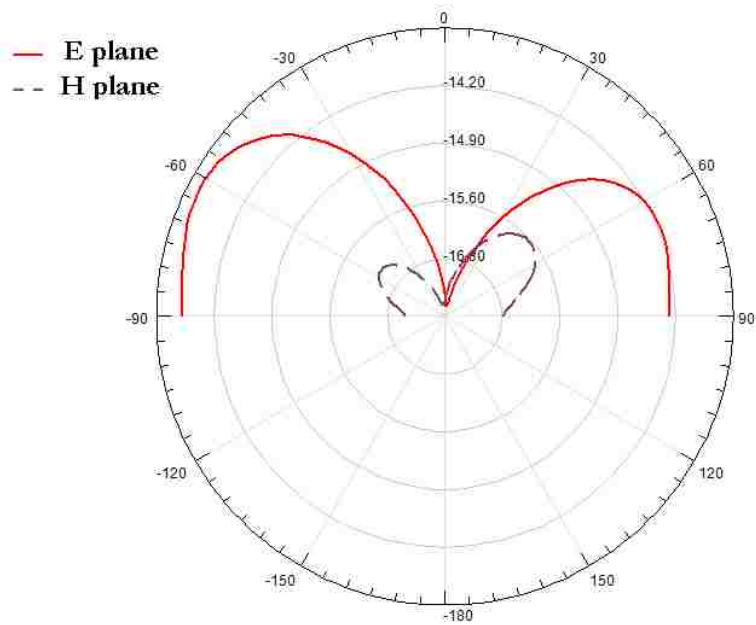


Fig. 3.17 E and H plane electric field simulated radiation pattern in dB when all switches are activated at 2.8 GHz

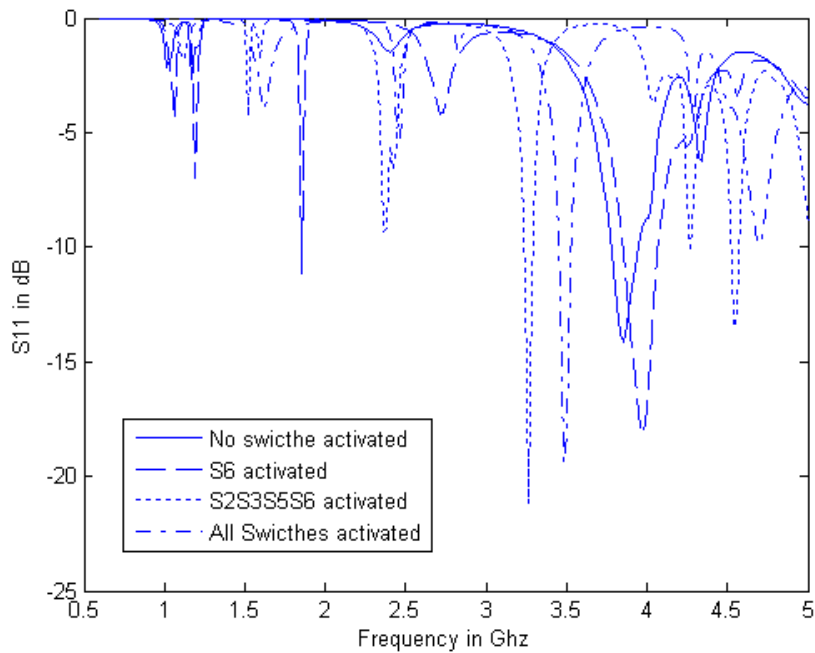


Fig. 3.18 S11 comparison for different antenna configurations

3.4 A Reconfigurable Multi-Band Microstrip Antenna based on open ended microstrip

lines :

3.4.1 Antenna Design Procedure:

Another new concept proposed [48] is to build an antenna with many open ended microstrip lines. These lines intersect together to achieve the structure of the suggested antenna. The different microstrip lines are used to achieve a multi-resonant antenna.

When adding microstrip lines side by side the spacing between the lines has to be taken into consideration. The spacing has to be optimized with respect to the desired antenna resonance and the length of the microstrip lines. The microstrip lines suggested have a length of 45 mm corresponding to $\lambda/2$ for 3.34 GHz. This frequency is chosen because it is the center frequency of the spectrum of interest (1 GHz-5.68 GHz). The width of each stub is 3mm equivalent to a 50Ω transmission line on an Isola Gigaver 410 substrate of dielectric constant equal to 3.9 and a 0.16 cm thickness. The patch formed by these two lines connected together, as shown in Fig. 3.19, is fed by a 50Ω SMA connector. The spacing between the lines is varied from 2 mm to 5 mm. A comparison between the S11 parameter for S=2mm and S=5 mm is shown in Fig. 3.20.

Fig. 3.21 shows 4 mcirostrip lines connected together by one line. These

placed side by side with a 2 mm spacing. These lines introduce 4 resonances as shown in the return loss plot in Fig. 3.22. Our objective though is to design a reconfigurable multi-band antenna. The reconfigurability has to be achieved in multiple frequency tuning and radiation pattern changes. The structure of the proposed antenna has to be altered accordingly.

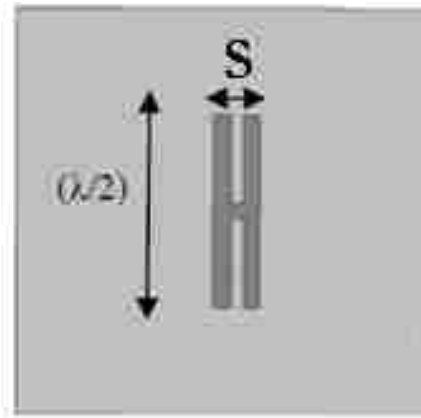


Fig. 3.19 Two stubs with spacing S and length $\lambda/2$ [48]

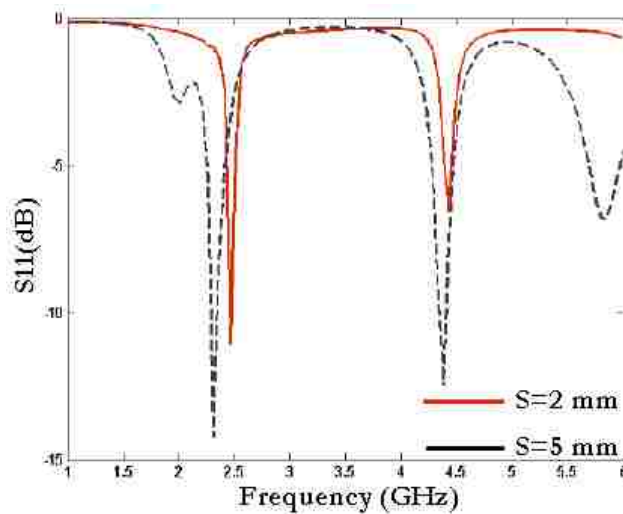


Fig. 3.20 The S_{11} parameter for the 2 stubs patch with $S=2$ mm and $S = 5$ mm [48]

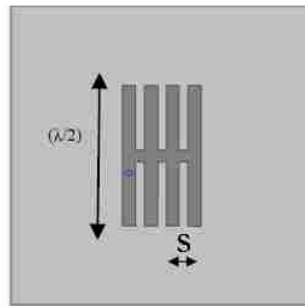


Fig. 3.21 The 4 stubs patch [48]

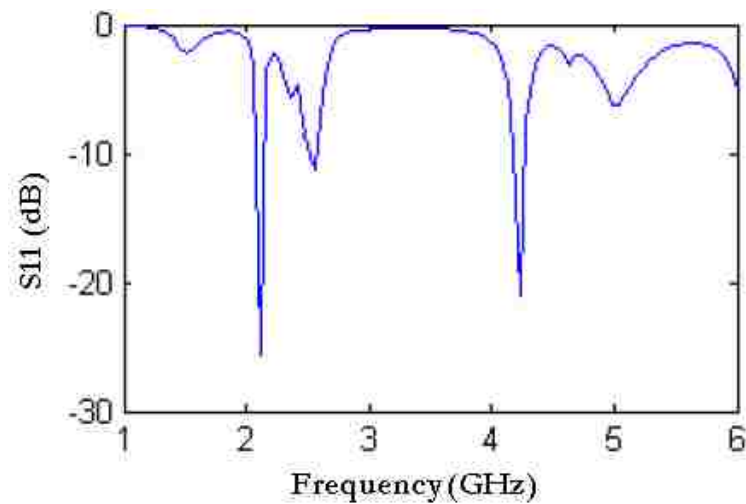


Fig. 3.22 The S11 results for the 4 lines patch with $S=2$ mm

3.4.2 Antenna Structure:

The structure of the antenna [48] designed to achieve multi resonance is shown in Fig. 3.23. The proposed antenna consists of 3 layers. The lower layer which constitutes the square ground plane covers the entire substrate and has a side length of 7 cm. The middle substrate has a dielectric constant $\epsilon_r=3.9$ and a height 0.16 cm. The upper layer is composed of 4 microstrip lines intersecting with

each other. The length of the microstrip lines are optimized to correspond to $\lambda/2$ at 3.34 GHz (45 mm). Other lengths can be considered if the desired applications were different [48].

Changing the length of the microstrip lines shifts the resonant frequencies. Increasing the length will shift the frequency lower since the surface current path will become longer. A comparison between the S11 parameters for different lengths is shown in Fig. 3.24.

The width of the microstrip line is taken as 3 mm to correspond to a characteristic impedance of 50 Ω . The optimized spacing between the lines is 2mm. The choice of 4 microstrip lines with optimal spacing intersecting each other on the upper layer of the antenna is to achieve a multi-band antenna with a considerable bandwidth.

The antenna was simulated using HFSS V11. The feeding position was optimized to minimize attenuation and obtain the best radiation properties. The fabricated prototype is shown in Fig. 3.25. The simulated and tested return loss results are compared in Fig. 3.26. A good agreement is noticed between the measured and simulated data. The antenna exhibits a lot of resonances between 2 GHz and 4 GHz. This antenna can be used for many applications like WiFi and GPS.

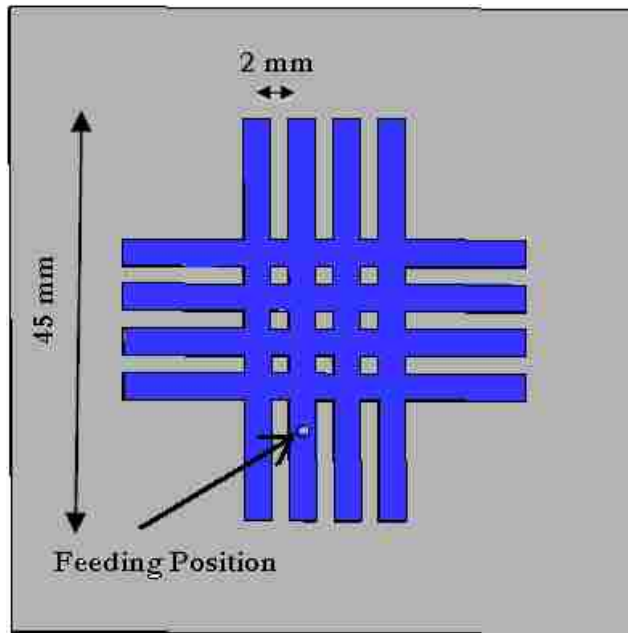


Fig. 3.23 The proposed antenna structure

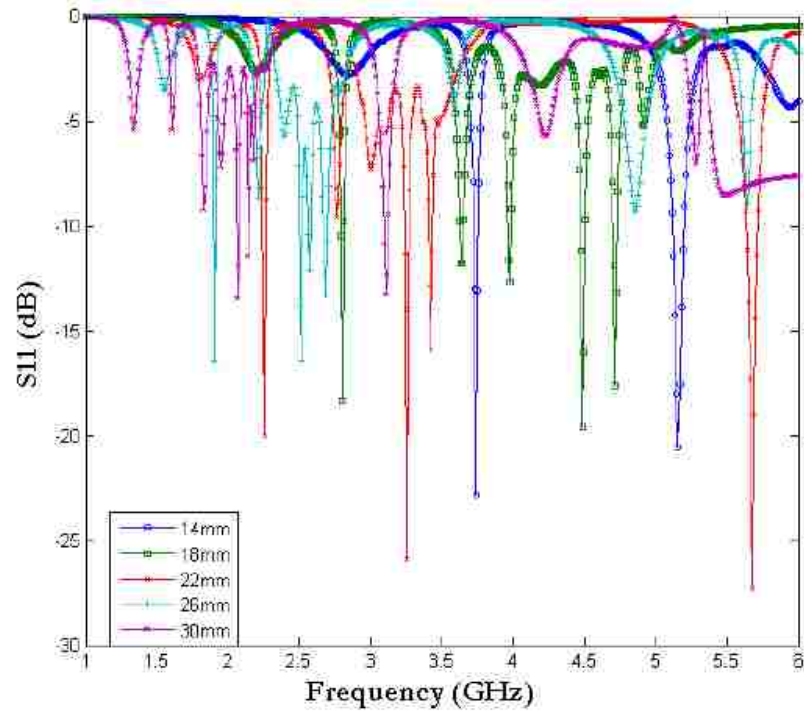


Fig. 3.24 Different S11 for different stubs lengths [48]



Fig. 3.25 The fabricated prototype

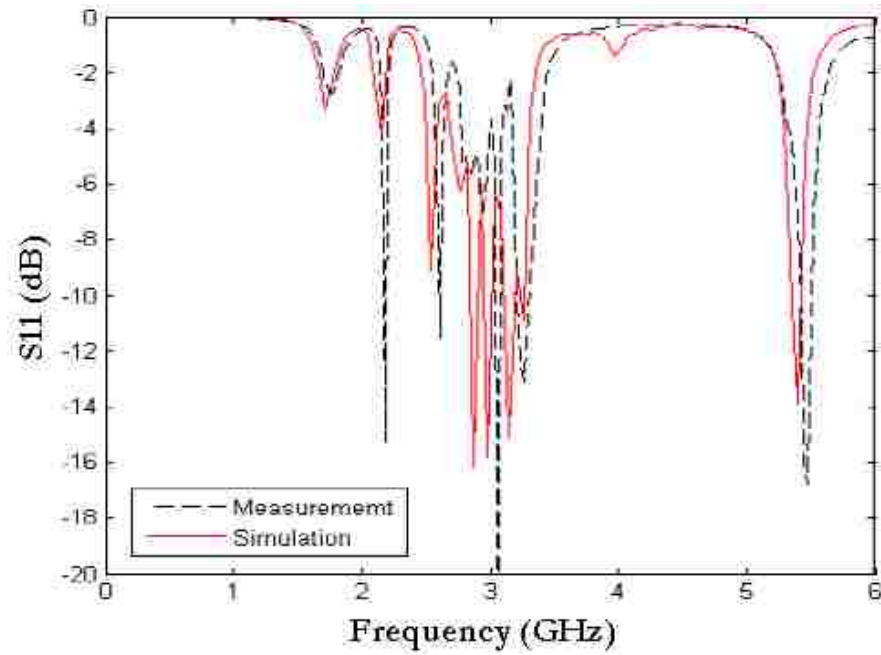


Fig. 3.26 A comparison between the measured and simulated return loss [48]

3.4.3 Antenna Reconfiguration:

In order to achieve resonance tuning the surface current distribution has to be altered. This alteration can be physical or electrical; however this antenna is also required to show radiation pattern reconfigurability. Achieving frequency and radiation pattern reconfigurability requires the changes to be physical in order to change the antenna structure drastically.

Keeping the feeding position fixed, switches are used to connect different microstrip lines to the body of the antenna as shown in Fig.3.27. The reconfigurability of the antenna is achieved using these switches that will control the length of the stubs. The antenna has to present both a reconfigurable return loss and a reconfigurable radiation pattern since the attachment or detachment of the different stubs will change the antenna structure completely.

The length alteration of the microstrip lines will tune the resonances of the antenna. As shown in Fig. 3.28 when the switches are off most of the resonances between 2.5 GHz and 3.5 GHz disappear and 2 new resonances appear between 2 GHz and 2.5 GHz, giving the antenna a new application (Bluetooth at 2.4 GHz). The radiation pattern will also be affected by this action due to the change in the radiating elements. When the switches are activated, the maximum radiation in the E plane is at 320° and for the H plane it is at 40° . The pattern totally changes when

the switches are turned off. The radiation pattern reconfigurability is clearly illustrated in Fig.3.29 for the E plane and Fig. 3.30 for the H plane.

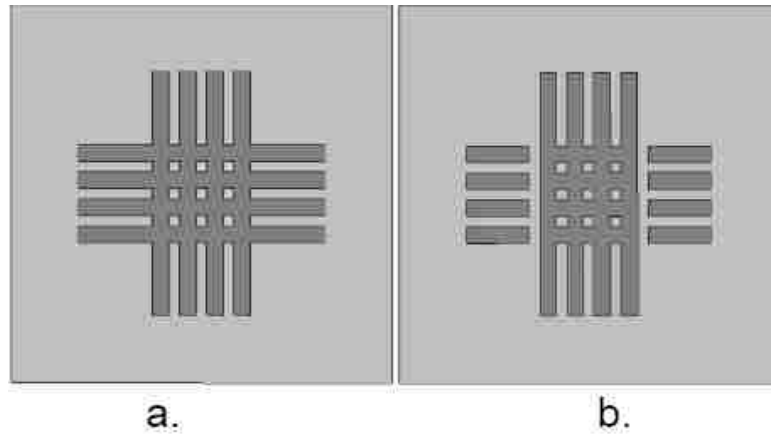


Fig. 3.27 The antenna structure. a) Switches ON. b) Switches OFF

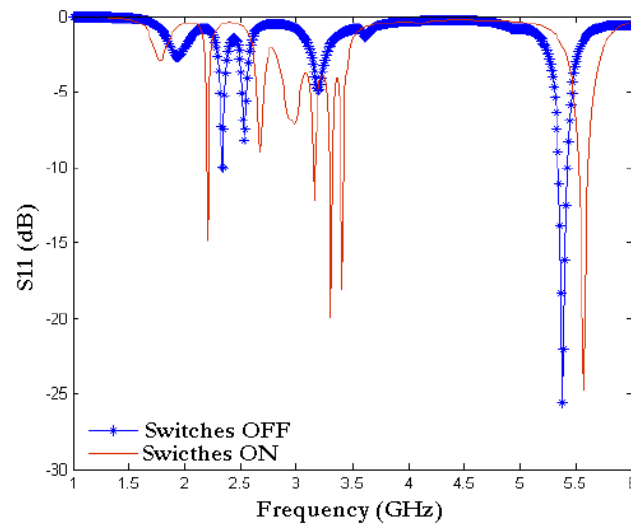


Fig. 3.28 S11 resonance tuning for different configurations [48]

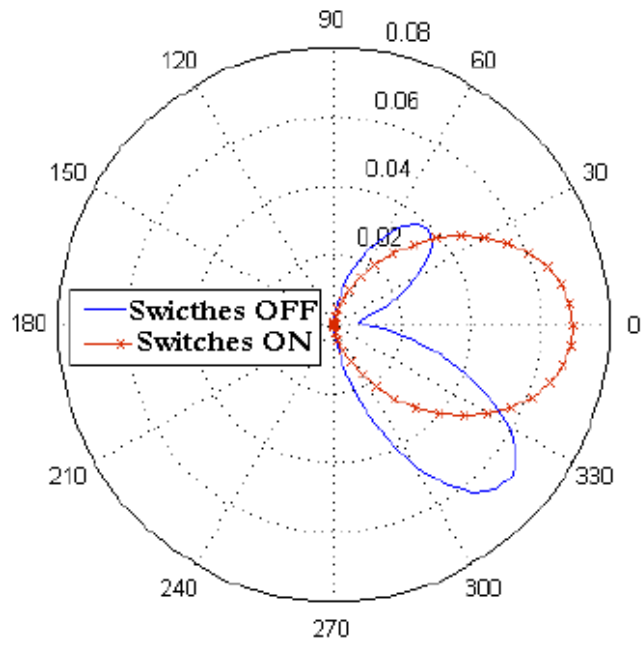


Fig. 3.29 E plane radiation pattern reconfigurability [48]

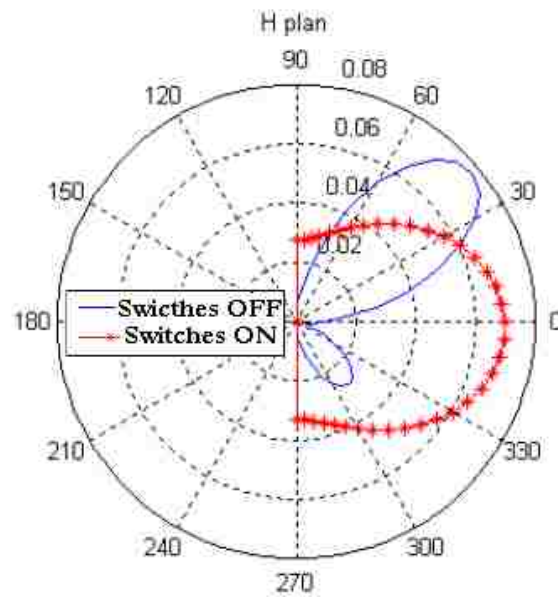


Fig. 3.30 H plane radiation pattern reconfigurability [48]

3.5 The Use of FPGAs to Control Reconfigurable Antennas:

3.5.1 Field Programmable Gate Arrays :

FPGAs are constructed using one basic “logic-cell”, duplicated thousands of times [49]. A logic-cell is simply a small lookup table (LUT), a D flip flop, and a two to one multiplexer for bypassing the flip flop. The LUT is just a small Random Access Memory (RAM) cell and usually has four inputs, so it can in effect become any logic gate with up to four inputs.

Every logic cell can be connected to other logic cells using interconnect resources. These resources are wires and multiplexers that are placed around logic cells. The FPGA's interconnect wires extend to the boundary of the device where Input Output cells are used to connect to the pins of the FPGA. FPGAs contain fast dedicated lines connecting neighboring logic cells. These lines can be implemented in order to create arithmetic functions like counters and adders efficiently.

Voltages are asserted on four output lines from the FPGA by way of the Joint Test Access Group 1149.1 standard [50]. The standard's main function is the boundary scan; however it is used here to assert signals. A major advantage of using JTAG is that it will not interfere with circuit functions when not in testing

mode. A TAP controller module is a finite state machine that is programmed in VHSIC Hardware Description Language (VHDL) onto the FPGA.

3.5.2 Reconfigurable Antenna Structure, Design and Tuning :

The antenna structure consists of 3 layers. The bottom layer constitutes the square ground plane that covers the entire substrate. The middle substrate has a dielectric constant $\epsilon_r=4.2$ and a height of 0.235 cm. The patch on the upper layer is composed of a main mid-section and four surrounding smaller sections as shown in Fig.3.31. This antenna is fed through a 50 Ω coaxial cable. The feeding position and the antenna dimensions are shown in Table 3.1.

Microsemi's GC 4712 GaAs p-i-n diodes are used to connect the small section to the main section as shown in Fig.3.31. These p-i-n diodes operate up to 18 GHz and are oriented in the X direction.

47 pF capacitors are connecting the p-i-n diodes to the main section of the antenna; these capacitors are oriented in the Y direction. The capacitors are used to prevent the DC current from crossing into the main section while passing the RF current. Quarter wave length transmission lines designed at 7.7 GHz are used to bias the p-i-n diodes. These $\lambda/4$ lines are terminated by $\lambda/4$ radial stubs in order to eliminate interference of the DC biasing network with the radiating structure. Biasing these p-i-n diodes separately can connect the corresponding side sections to the mid-section respectively.

To reduce fabrication costs, the biasing lines are etched on copper. These copper lines will resonate at a frequency where the length of the bias lines is approximately $0.45\lambda_{\text{eff}}$ and at its odd multiples; λ_{eff} being the effective wavelength at the frequency of operation [8]. In this case these lines radiate around 9 GHz and its odd multiples which are outside the desired operating band (1-6GHz) of this antenna. The directions of the biasing lines are also optimized to contribute constructively to the radiation pattern of the antenna that is reconfigured.

The antenna achieves multi-frequency resonance tuning which is shown in Fig.3.32. The 4 configurations shown represent an example of the 16 possible configurations achieving frequency change. This shift is noticed at frequencies lower than 3.5 GHz where a lot of wireless communications applications can be found; which improves the practicality of the design. In Fig. 3.32 “0” represents the OFF state of a diode and 1 represents the ON state.

The 3-D simulated radiation pattern for the 0010 configuration as well as the E and H plane cuts at 4.875 GHz are shown in Figs. 3.33 and 3.34 respectively. This radiation pattern is plotted at a resonance frequency common to all the antenna configurations.

3.5.3 Reconfigurable Antenna Fabrication, Measurement and FPGA control:

The fabricated prototype is shown in Fig.3.35. Shorting pins were inserted into 0.75 mm diameter holes drilled at the point of intersection between the p-i-n

diodes and the 47 pF capacitors. These shorting pins are used to connect the Microsemi's GC 4712 GaAs p-i-n diodes to ground. The VCC is connected to the through pins across holes drilled in the radial stubs. The FPGA's output lines feed these pins to activate and de-activate the p-i-n diodes.

In order for the FPGA to control the diodes, activation, voltages are asserted on four output lines from the FPGA by way of the Joint Test Access Group 1149.1 standard [9]. A Digilent Spartan 3E board with a Xilinx Spartan XC3S500E FPGA is programmed with the TAP Controller module. A Xilinx Parallel III cable is connected from a parallel port on a Linux PC to the JTAG interface pins on the Spartan 3E board [10].

Four pins on the Spartan 3E board serve as the outputs for driving signals to the diode biasing network. The parallel III cable as well as the board is shown in Fig.3.36.

The antenna reconfiguration is achieved through the following setup: A Linux computer runs the JTAG software, issuing instructions to a Spartan 3E Xilinx FPGA over a Parallel III cable. The TAP controller programmed on the FPGA translates these instructions and asserts the associated signals to bias the p-i-n diodes on the antenna. The VHDL code used to program the FPGA was assembled from [11]. With one of the p-i-n diodes biased, the RF signal passes from the main patch through the capacitor and that diode to the outer patch.

Since there are four diodes, sixteen antenna configurations are possible. The measurement and reconfiguration setup is shown in Fig.3.37. Two comparisons between the simulated and fabricated S11 results are shown in Fig.3.38 and 3.39 respectively where analogy can be noticed. A diagram showing the whole system is shown in Fig.3.40.

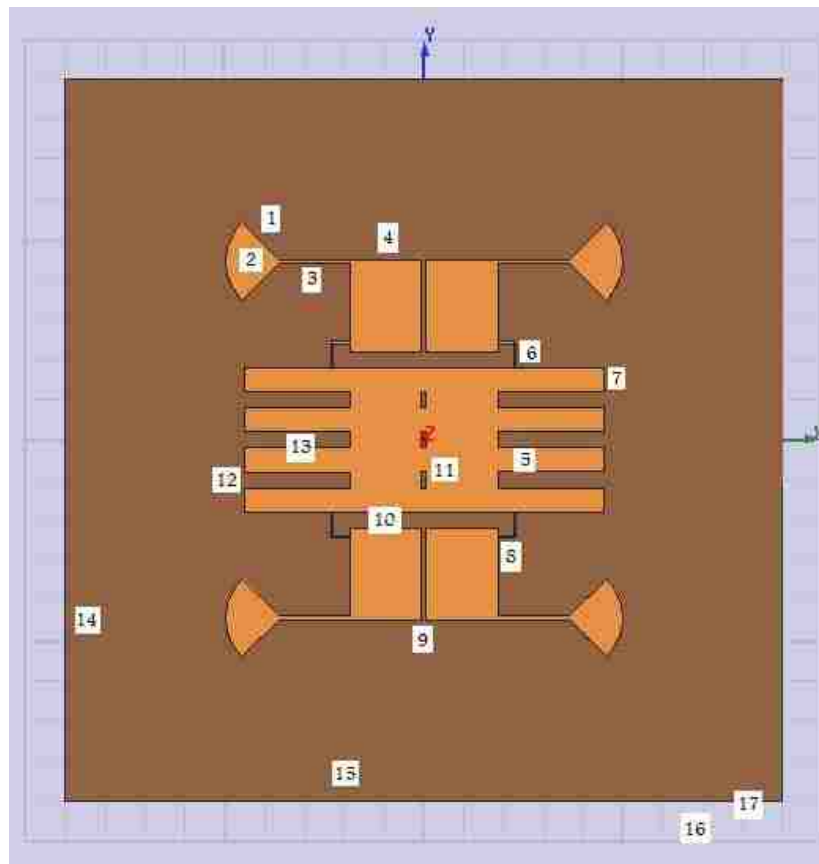


Fig. 3.31 Schematic representation of the reconfigurable antenna

Part	Description	Length
1	Radial Stub	6.921mm
2	Radial Stub Angle	90
3	Quarter Wave TLine	X: 8.959mm, Y: 0.5mm
4	Outer Patch Width	9mm
5	Feed Position	X: 12.5mm, Y: -2.5mm
6	Capacitor	X: 0.25mm, Y: 3mm
7	Main Arm Y	3mm
8	Diode	X: 2mm, Y: 0.25mm
9	Outer Patch X Gap	0.6mm
10	Outer Patch Y Gap	2mm
11	Main Patch Hole	X: 0.6mm, Y: 2mm
12	Main Patch Arm Gap	Y: 2mm
13	Main Patch Arm X	X: 13.2mm
14	Substrate Y	90mm
15	Substrate X	90mm
16	Substrate Dielectric	4.2ε0
17	Substrate Height	H: 2.35mm

Table 3.1 Antenna dimensions

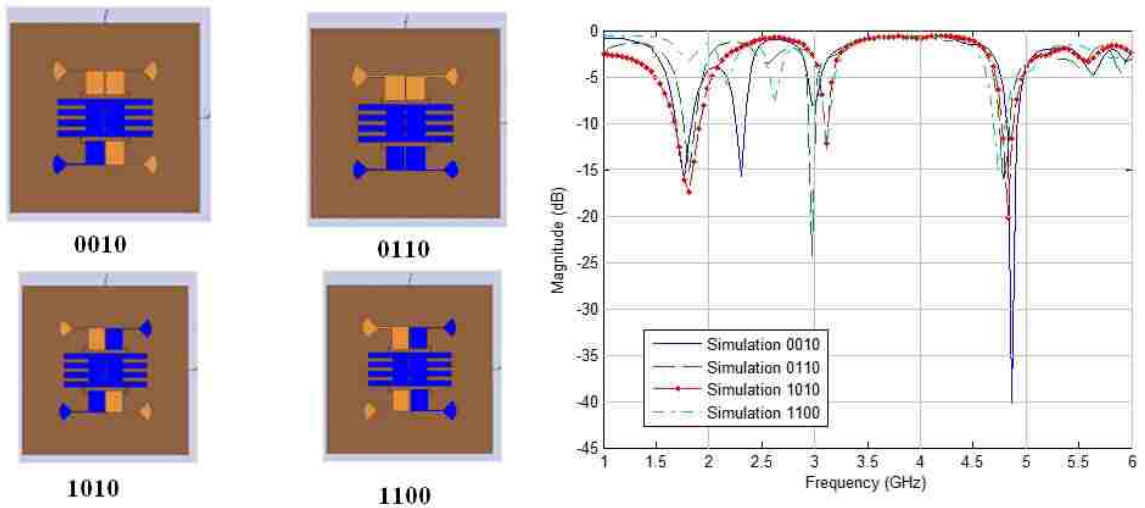


Fig. 3.32 Antenna resonance for different diodes states 0- Diode OFF, 1 Diode ON

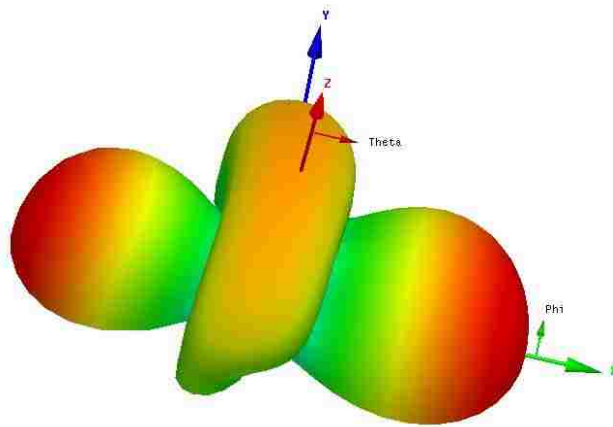


Fig. 3.33 Simulated 3-D radiation pattern at 4.875 GHz

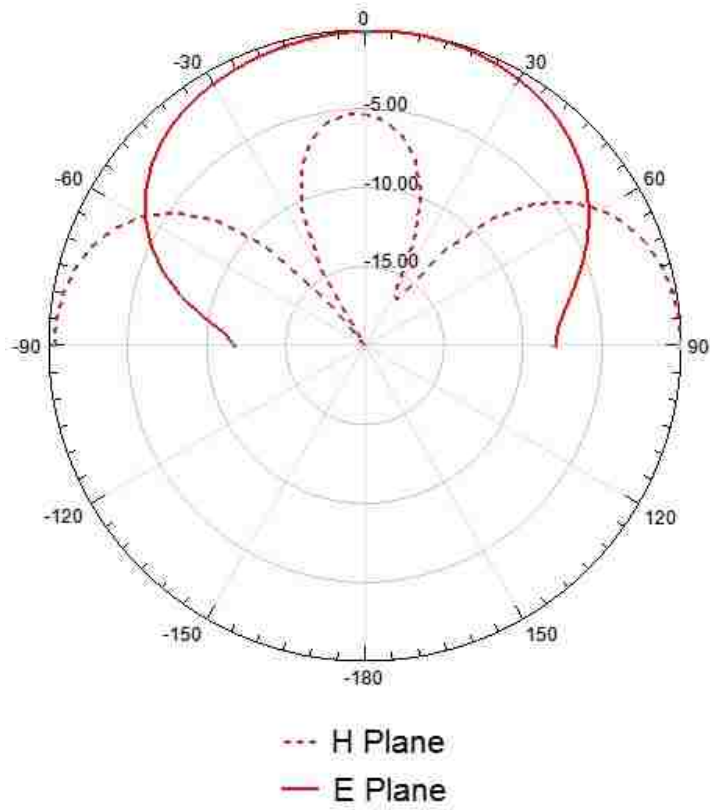


Fig. 3.34 E and H plane cuts at 4.875 GHz

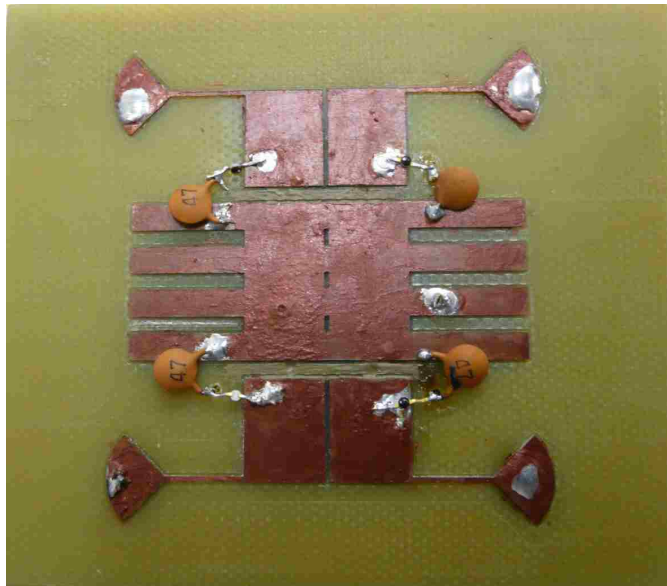


Fig. 3.35 The fabricated prototype

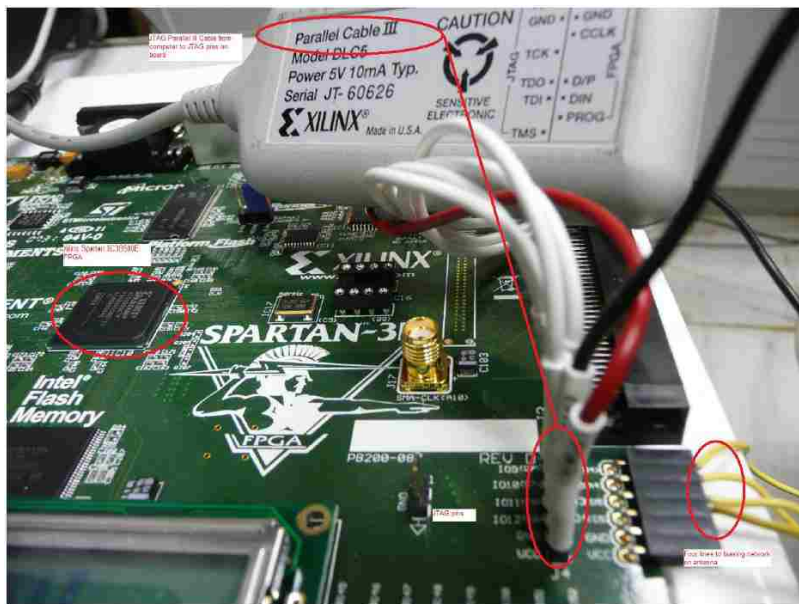


Fig. 3.36 The parallel III cable with FPGA board

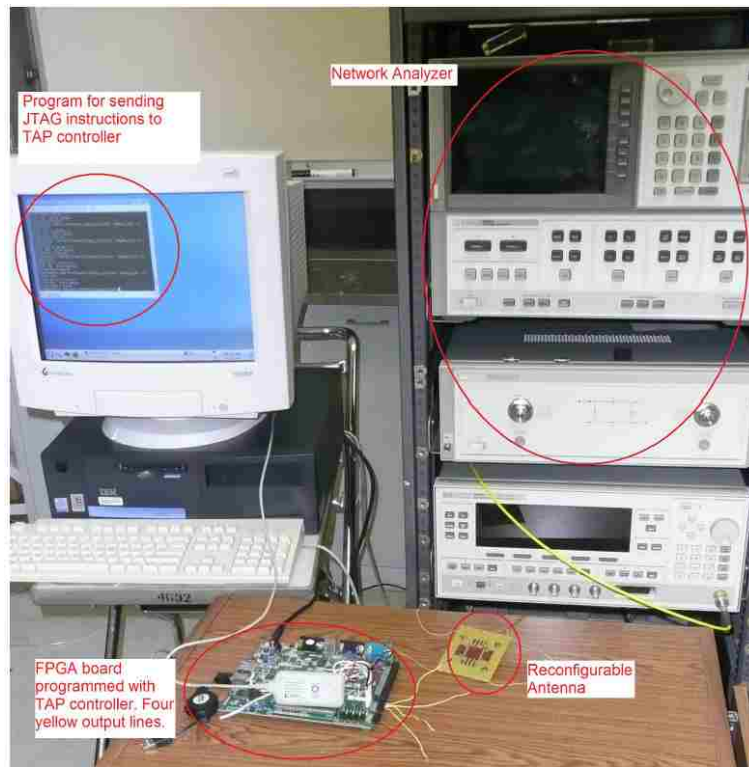


Fig. 3.37 The S11 measurement setup

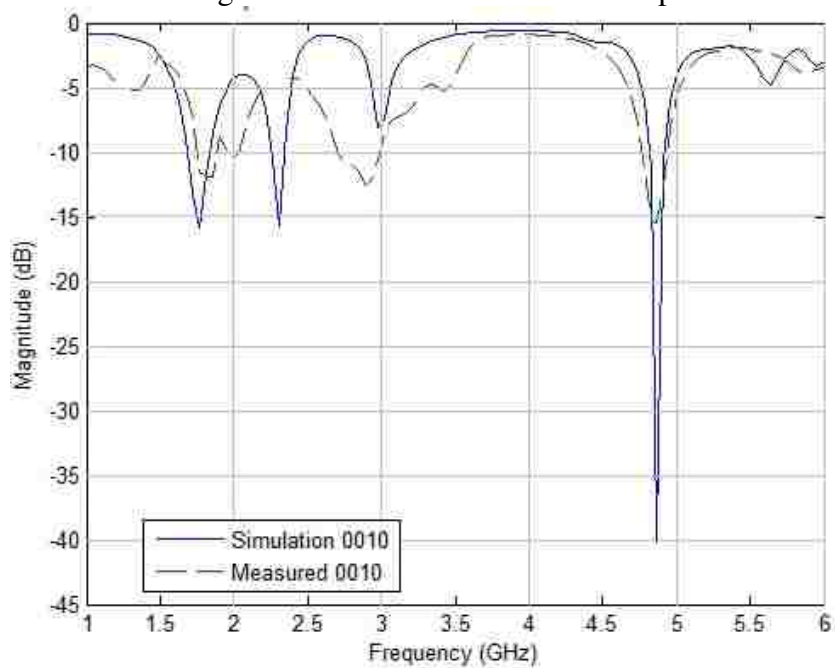


Fig. 3.38 A comparison between actual measurements and simulation for an antenna state

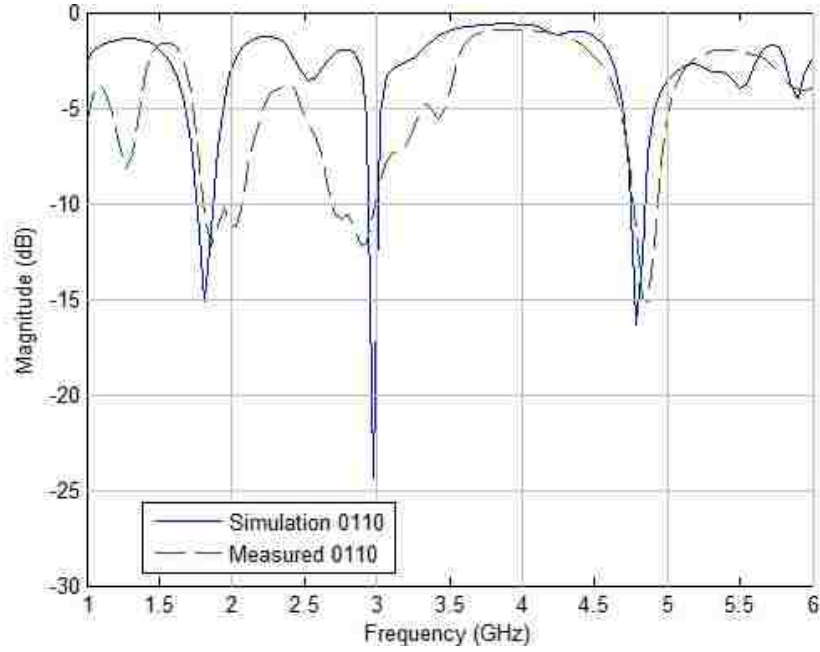


Fig. 3.39 A comparison between actual measurements and simulations for an antenna state

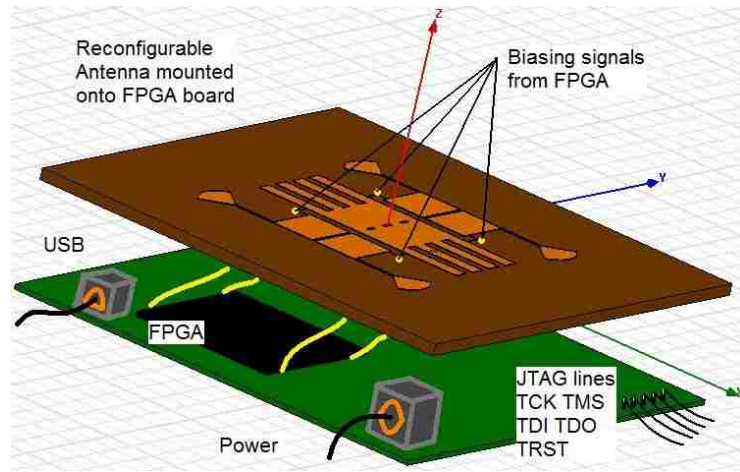


Fig. 3.40 Whole system diagram

3.5.4 Applying Neural Networks on FPGA:

While the application of neural networks on FPGA is beyond the work done in this dissertation, it is important to note that FPGA architectures can be

easily reconfigured to adapt the weights and topologies of a neural network. After training the neural networks with the desired behavior specifications of a certain reconfigurable antenna or environment, the fully trained weights coefficients and network topologies are then configured on the FPGA. This technology can find applications in antenna arrays or reconfigurable antenna systems. In the case of an element failing in an antenna array, the reconfiguration of the whole system can be achieved and controlled through a neural network programmed FPGA.

Neural networks on FPGAs can also find application in cognitive radio. The emphasis of using neural networks for cognitive radio applications resides on the level of learning and cognition. A certain level of “intelligence” can be built into the radio device using neural networks, in order to develop the next generation of responsive circuits. The aim is to have a device with “intelligent” antennas that can recognize their environment, collaborate between themselves during sensing and communication, reconfigure their radiation, polarization, or frequency and even self-tune themselves based on changes in their environment or operational mission.

3.6 Discussion:

In this chapter new reconfigurable antenna designs were presented. A new reconfiguration technique based on slot rotation was introduced. The fabrication and

measurement issues of antennas using this reconfiguration technique were addressed. Rotary switches are proposed to control the slot rotation process.

The activation and deactivation of p-i-n diode switches installed on antennas were discussed to be achieved through FPGA. The platform as well as the programming procedure was presented and tested.

In the next chapter Graph models are introduced and reconfigurable antenna graph modeling guidelines are presented. Graph algorithms can be used to facilitate the design and automation of reconfigurable antennas.

CHAPTER 4

GRAPH MODELING RECONFIGURABLE ANTENNAS

4.1 Introduction:

Graphs are *symbolic representations of relationships* between different points in a system. They are *mathematical tools* used to model real life situations, in order to organize them and improve their status. They are widely used in computer science, control systems and in the development of algorithms for working with them, is fundamental to these fields [52]. Graphs also find applications in self assembly robotics where they are used to model the physics of the particles by describing the outcomes of interactions among them [53]. A graph may also be a description of a communication protocol; in particular, a suitably designed graph can precisely describe and direct the changing network topology of a self-organizing system [53].

Since reconfigurable antennas can be seen as a collection of self-organizing parts; the authors in [54] used graphs to model this type of antennas. *Graph rules can be introduced to relate each possible topology to a corresponding electromagnetic performance in terms of achieving a characteristic frequency of operation, impedance and polarization.* These rules can help designers understand reconfigurable antenna structures and their operation. Various algorithms can be incorporated such as search algorithms and shortest path algorithms which facilitate the design, automation and optimization process of reconfigurable antennas.

In this chapter graph models and their terminologies are introduced. Guidelines for the modeling of reconfigurable antennas are set and different algorithms are presented for possible incorporation on FPGA to automate reconfiguration mechanisms.

4.2 Graph Outlines:

4.2.1 The Definition of a Graph:

A graph can be defined as the collection of *vertices* that may be connected together with lines called *edges*. A graph $G=(V(G),E(G))$ consists of two finite sets [55]:

- $V (G)$, the vertex set of the graph, often denoted by just V , which is a nonempty set of elements called Vertices.
- $E (G)$, the edge set of the graph, often denoted by just E , which is a possibly empty set called Edges. Each edge e in E is assigned an unordered pair of vertices (u, v) , called the end vertices of e [55].

Vertices are also sometimes called points, nodes or just dots. If e is an edge with end vertices u and v then e is said to join u and v . It is important to note that the definition of a graph allows the possibility of the edge e having identical end vertices, i.e. it is possible to have a vertex u joined to itself by an edge; such an edge is called a loop [55].

Example 4.1 [55]:

Let $G=(V,E)$ where $V=\{a,b,c,d,e\}$, $E=\{e1,e2,e3,e4,e5,e6,e7,e8\}$ and the ends of

the edges are given by : $e_1 \leftrightarrow (a,b)$, $e_2 \leftrightarrow (b,c)$, $e_3 \leftrightarrow (c,c)$, $e_4 \leftrightarrow (c,d)$,
 $e_5 \leftrightarrow (b,d)$, $e_6 \leftrightarrow (e,d)$, $e_7 \leftrightarrow (b,e)$, $e_8 \leftrightarrow (e,b)$.

We can represent G diagrammatically as in Fig. 4.1

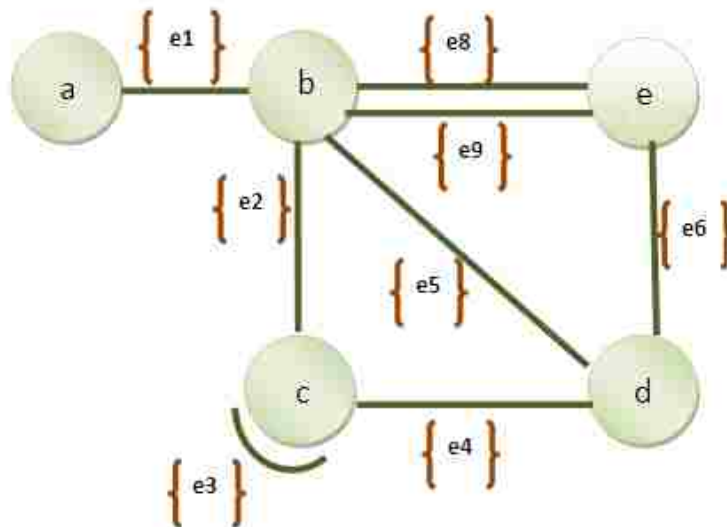


Fig. 4.1 A graph G with five vertices and eight edges [55]

4.2.2 The Properties of a Graph:

A graph can be either *directed or undirected*. A directed graph (often called digraph) is a finite vertex set V together with a non reflexive relation R on V [56]. The edges in a directed graph have a certain determined direction while this is not the case in an undirected graph.

If two or more edges of a graph G have the same end vertices then these edges are called parallel. A vertex of G which is not the end of any edge is called isolated. Two vertices joined by an edge are said to be adjacent or neighbors. The

set of all neighbors of a fixed vertex v of G is called the neighborhood set of v and is denoted by $N(v)$ [55].

Vertices may represent physical entities and edges between them in the graph represent the presence of a function resulting from connecting these entities. If one is proposing a set of guidelines for antenna design, then a possible modeling rule may be to create an edge between two vertices whenever their physical connection results in a meaningful antenna function.

Edges may have weights associated with them to represent costs or benefits that are to be minimized or maximized. For example if a capacitor is connecting two end points of a system and these end points are represented by two vertices in a graph, then the edge connecting these two vertices has a weight equal to the capacitance of that capacitor. Fig. 4.2 shows an example of an undirected as well as a weighted directed graph.

An empty graph is a graph with no edges. An edge e of a graph G is said to be incident with the vertex v if v is an end vertex of e . In this case we also say that v is incident with e . Two edges e and f which are incident with a common vertex v are said to be adjacent. The degree d of a vertex v , $d(v)$, is the number of edges of G incident with v , counting each loop twice, i.e. it is the number of times v is an end vertex of an edge. A vertex is called odd or even depending on whether its degree is odd or even.

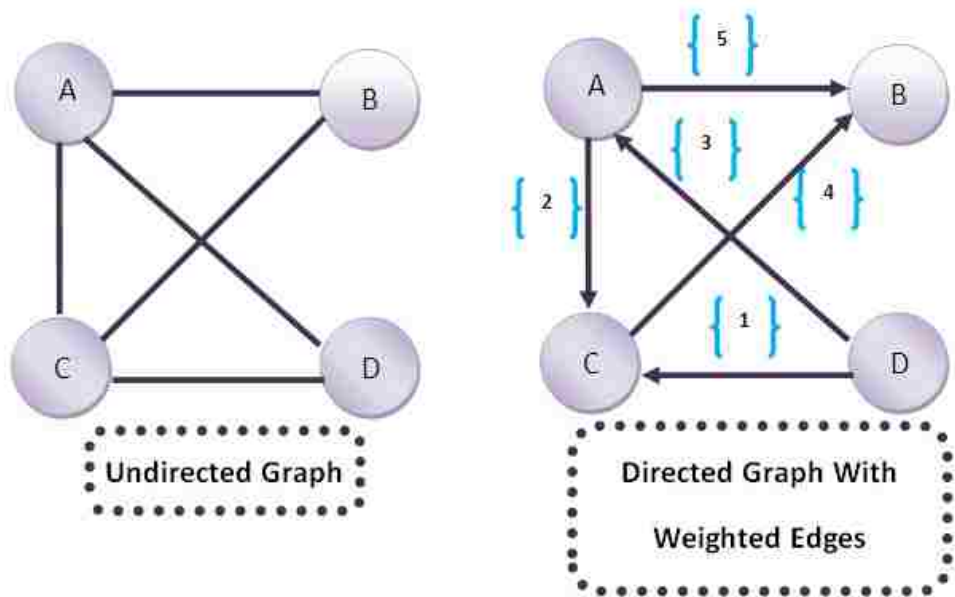


Fig. 4.2 An example of an undirected as well as directed graph with weighted edges

Example 4.2 [55]:

In the graph of Fig.4.3 we have $d(v_1)=3, d(v_2)=4, d(v_3)=3, d(v_4)=3, d(v_5)=1$.

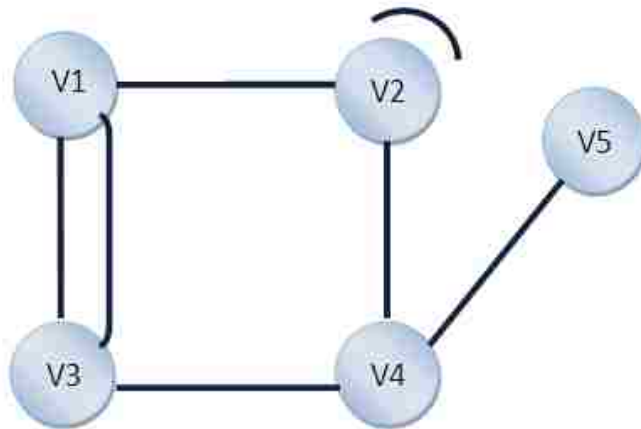


Fig. 4.3 A graph with 5 vertices [55]

4.2.3 The Adjacency Matrix Representation of a Graph:

The adjacency-matrix representation of a graph G , assuming that the vertices are numbered $1, 2, \dots, |V|$ in some arbitrary manner, consists of a $|V| \times |V|$ matrix $A = (a_{ij})$ such that [52]:

$$a_{ij} = \begin{cases} 1 & \text{if } (i, j) \in E \\ 0 & \text{Otherwise} \end{cases} \quad (4.1)$$

Example 4.3 :

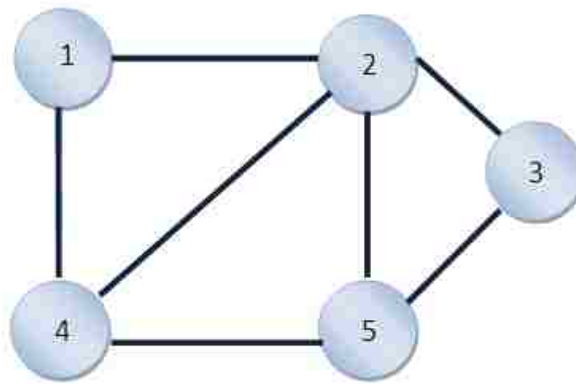


Fig. 4.4 A graph representation with 6 vertices

The adjacency matrix of the graph shown in Fig.4.4 is presented in the matrix A below:

$$A = \begin{bmatrix} 0 & 1 & 0 & 0 & 1 \\ 1 & 0 & 1 & 1 & 1 \\ 0 & 1 & 0 & 1 & 0 \\ 0 & 1 & 1 & 0 & 1 \\ 1 & 1 & 0 & 1 & 0 \end{bmatrix} \quad (4.2)$$

The adjacency-matrix representation can also be used for weighted graphs. *The corresponding weights in a graph are grouped into the adjacency matrix.* For example, if $G = (V, E)$ is a weighted graph with edge-weight function $w(u, v)$ of the edge (u, v) . W is simply stored as the entry in row u and column v of the adjacency matrix. If an edge does not exist, a NIL value can be stored as its corresponding matrix entry, though for many problems it is convenient to use a value such as 0 or ∞ [52]. Moreover, if the graph is un-weighted, there is an additional advantage in storage for the adjacency-matrix representation. Rather than using one word of computer memory for each matrix entry, the adjacency matrix uses only one bit per entry [52].

4.2.4 Paths and Cycles of a Graph:

A walk in a graph G is a finite sequence :

$$W = v_0 e_1 v_1 e_2 v_2 \dots v_{k-1} e_k v_k \quad (4.3)$$

Whose terms are alternatively vertices and edges such that, for $1 \leq i \leq k$, the edges e_i has ends v_{i-1} and v_i . Thus each edge e_i is immediately preceded and succeeded by the two vertices with which it is incident. The vertex v_0 in the above walk is called the origin of the walk W , while v_k is called the terminus of W . Note that v_0 and v_k need not be distinct. A trivial walk is one containing no edges [55].

If the vertices v_0, v_1, \dots, v_k of the walk W are distinct then W is called a

Path. Any two paths with the same number of vertices are isomorphic [55]. *The weight of a path is defined as the sum of the weights of its constituent edges.* In some cases it is useful to find the *shortest path* connecting two vertices. This notion is used in graph algorithms in order to optimize a certain function. The shortest path distance in a non weighted graph is defined as the minimum number of edges in any path from vertex s to vertex v ; otherwise if the graph is weighted then the shortest path corresponds to the least sum of weights in a particular path.

4.3 Review of Graph applications in control systems such as robotics:

The work [57-60] facilitated understanding the use of graphs to model the topologies of self assembled systems such as reconfigurable antennas and organize their communication protocols. Different parts [57-60] self organize and group, they unit and disperse based on different rules and different conditions. Achieving this self-assembly robots resorted to graph grammar [57-60]. Graph grammar was defined and algorithms were introduced to achieve the desired performance.

In [58] a class of graph grammar was defined. It can be used to model and direct distributed robotic assembly or forming processes. A grammar was synthesized [58] so that it generates a given pre-specified assembly. A graph grammar program for robotic self-assembly was also described [59], together with measurements of kinetic rate data, yield a Markov process model of the dynamics of programmed self-assembly. Graph grammar was also shown usable to describe or direct the changing connection topology of

a collection of self-organizing robots. Productions in a graph grammar described the legal local interactions in which the robots may engage, and the resulting global structures and processes that form can be analyzed by looking at the set of reachable graphs generated by the grammar.

4.4 Rules and Guidelines for Graph Modeling Reconfigurable Antennas:

In this section, we set some rules to graph model reconfigurable antennas. These *rules are not unique*; however they are required for our reconfigurable antenna design steps; i.e. a designer following our design steps with the proposed graph modeling rules should end up with an optimal reconfigurable antenna.

The graph modeling of a certain antenna is governed by its structure and the reconfiguration techniques used in that particular structure. *Each rule is valid for a certain reconfigurable antenna group*. These groups were defined in section 1.2 of chapter 1 of this work. We set constraints for each rule in order to facilitate the graph modeling process.

Rule 1.a: The graph modeling of a multi-part antenna whose parts are connected by switches is undirected with weighted edges connecting the vertices that represent the different parts.

Valid for:

This rule is valid for multi-part group 1 antennas.

Constraints:

The connection between each two parts has a distinctive angular direction. The designer defines a reference axis that represents the direction that the majority of parts have with each other or with a main part. The connections between the parts are represented by the edges. The edges' weights represent the angles that the connections make with the reference axis. A weight $W=1$ is assigned to an edge representing a connection that has an angle 0° or 180° with the reference axis, otherwise a weight $W=2$ is assigned to the edge as shown in Eq. (4.4).

$$W_{ij} = P_{ij} \tag{4.4}$$

$$\text{Where } P_{ij} = \begin{cases} 1 & A_{ij} = 0^\circ \text{ or } 180^\circ \\ 2 & \text{Otherwise} \end{cases}$$

Where A_{ij} represents the angle that the connection i,j form with the reference axis.

Example 4.4:

As an example we will take the antenna shown in Fig.4.5 [7-10] and model it into a graph following rule 1.a. The basic antenna is a 130° balanced bowtie. A portion of the antenna corresponds to a two-iteration fractal Sierpinski dipole. The remaining elements are added (three on each side) to make the antenna a more generalized reconfigurable structure.

Following rule 1.a, the different adjacent triangular parts of the antenna (triangles

added) are interconnected by MEMS switches as shown in Fig. 4.5. The vertices in the graph model represent the triangles added. The edges connecting these vertices represent the connection of the corresponding triangles by MEMS switches. If a switch is activated to connect triangle T1 to triangle T'1 shown in Fig. 4.5 then an edge appears between the vertex T1 and the vertex T'1 as shown in the 1st state of the graph model in Fig. 4.6. In this design the connection between T1 and T2 , T2 and T4, T'1 and T'3 , T'3 and T'6 are collinear with the reference axis and as a result the edges representing these connections are weighted with $W=1$ and $W=2$ for the other connections. The cost of connecting parts at the same direction is less ($w=1$) than connecting parts at a deviated direction ($w=2$).

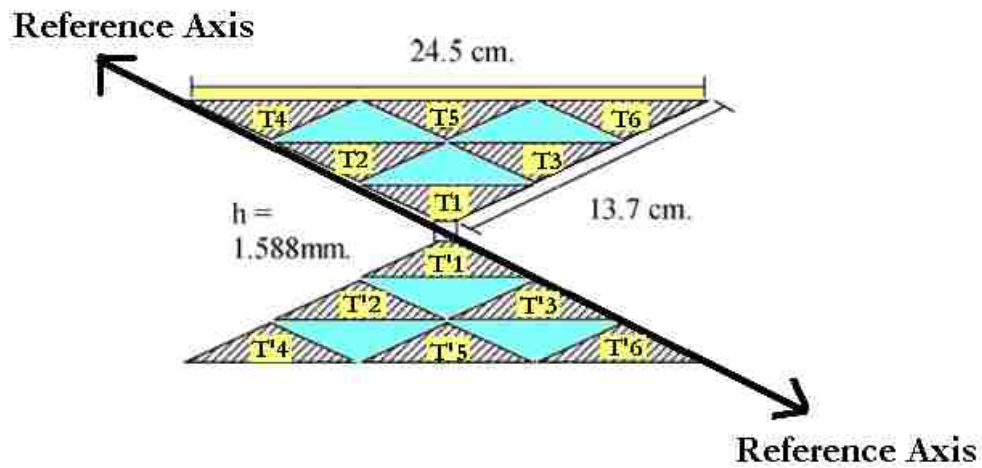


Fig. 4.5 The antenna structure in [7-10]

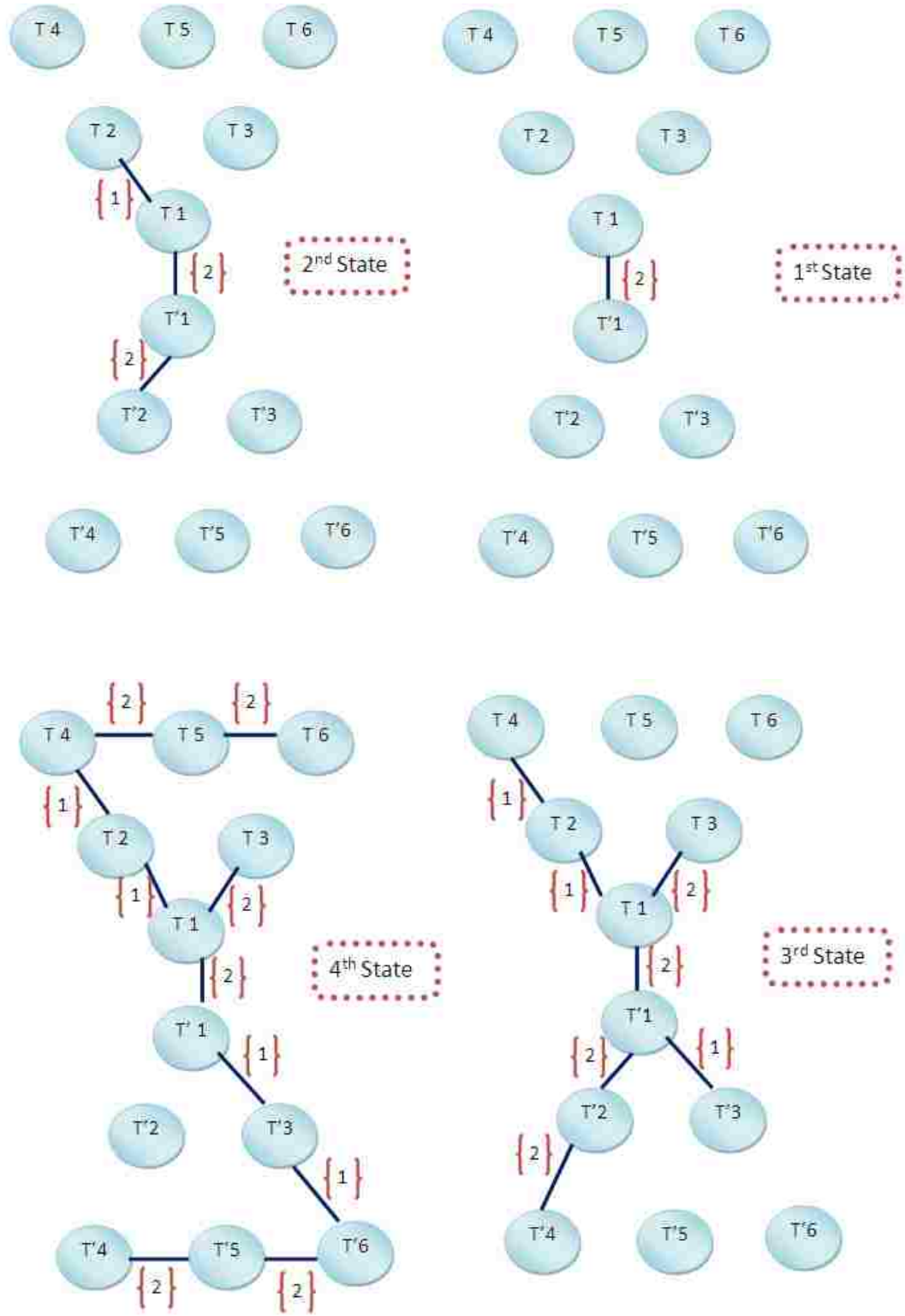


Fig. 4.6 Graph model for different configurations of the antenna in [8]

Rule 1.b: The graph modeling of a single part antenna with switches bridging over slots is undirected with non-weighted edges connecting vertices that represent the end points of each switch.

Valid for:

This rule is valid for single part group 1 antennas.

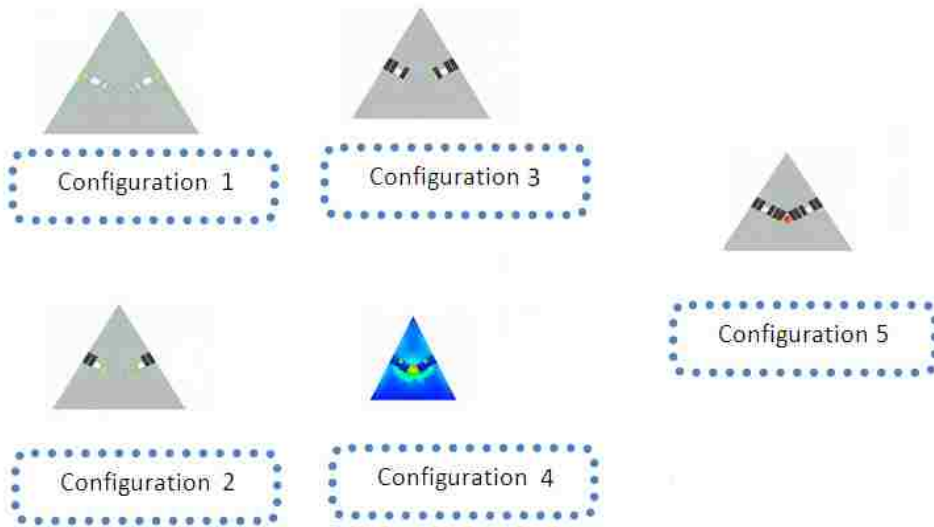
Constraints:

In the case of switches bridging over multiple slots in one antenna structure the graph model takes into consideration one slot at a time.

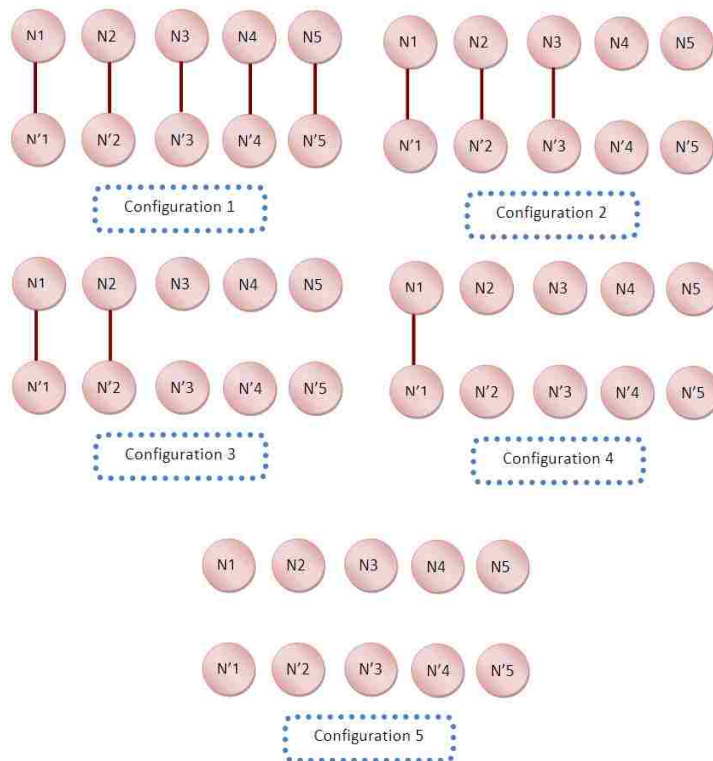
Example 4.5:

As an example we will take the antenna shown in Fig. 4.7.a [5]. This antenna is a triangular patch antenna with 2 slots incorporated in it. The authors suggested 5 switches to bridge over each slot in order to achieve the desired required functions.

The graph modeling of this antenna following rule 1.b is shown in Fig. 4.7.b where vertices represent the end points of each switch and edges represent the connections between these end points. When switch 1 is activated an edge appears between N1 and N'1 representing the 2 end-points of switch 1. The graph model of Fig. 4.7.b represents each slot at a time. For example N1 represent end-point 1 for switch 1 in slot 1 and end-point 1 for switch 1 in slot 2.



a.



b.

Fig. 4.7 a. Antenna structure in [5] with different configurations. b. Graph modeling

Rule 2.a: The graph modeling of a multi-part antenna with parts connected by capacitors or varactors is undirected with weighted edges connecting vertices that represent the different parts connected.

Valid for:

This rule is valid for multi-part group 2 antennas.

Constraints:

The edges' weights in this case are calculated according to Eq. 4.5. All the capacitances of the different capacitors connecting the parts should be transformed to the same unit and then they should be normalized with respect to the largest capacitance. The weights represent the addition of the normalized capacitances values with the values of P_{ij} as shown in Eq. 4.5. P_{ij} was discussed in rule 1.a.

$$W_{ij} = P_{ij} + C_{ij_{normalized}} \quad (4.5)$$

$$\text{Where } P_{ij} = \begin{cases} 1 & A_{ij} = 0^\circ \text{ or } 180^\circ \\ 2 & \text{Otherwise} \end{cases}$$

Where A_{ij} represents the angle that the connection i,j form with the reference axis. C_{ij} represents the normalized capacitance of the capacitor connecting parts i and j .

In Fig.4.8, a graph with 3 edges connecting 4 vertices is presented. The weights of

the edges are calculated according to Eq. 4.5 as detailed in Eq. 4.6 (a,b,c) and assuming that the capacitors have the same unit:

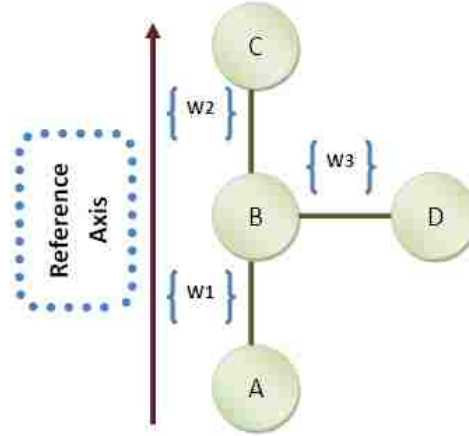


Fig. 4.8 Illustration of Rule 2.a

$$W_1 = \frac{C1}{\text{Max}(C1, C2, C3)} + P_{AB} = \frac{C1}{\text{Max}(C1, C2, C3)} + 1 \quad (4.6.a)$$

$$W_2 = \frac{C2}{\text{Max}(C1, C2, C3)} + P_{BC} = \frac{C2}{\text{Max}(C1, C2, C3)} + 1 \quad (4.6.b)$$

$$W_3 = \frac{C3}{\text{Max}(C1, C2, C3)} + P_{BD} = \frac{C3}{\text{Max}(C1, C2, C3)} + 2 \quad (4.6.c)$$

Example 4.6:

In this case we take the antenna shown in Fig. 4.9 [12]. The antenna is a 2x2 reconfigurable planar wire grid antenna designed to operate in free space. Variable capacitors were placed in the centers of 11 of the 12 wire segments that comprise the grid. The values of the variable capacitors were constrained to lie between 0.1pF and 1 pF. The

graph modeling of this antenna follows rule 2.a and is shown in Fig. 4.10. The vertices in this graph model represent the different parts of the lines that are connected together via a capacitor.



Fig. 4.9 Antenna structure in [12]

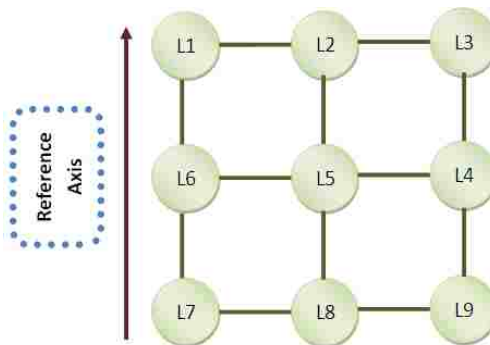


Fig. 4.10 Graph model of the antenna in [12]

The values of the capacitors were not specified in [12]. The weights governing the edges are defined according to Eq. 4.5 and are shown in the adjacency matrix

$$A = \begin{bmatrix} 0 & W_{12} & 0 & 0 & 0 & W_{16} & 0 & 0 & 0 \\ W_{21} & 0 & W_{23} & 0 & W_{25} & 0 & 0 & 0 & 0 \\ 0 & W_{32} & 0 & W_{34} & 0 & 0 & 0 & 0 & 0 \\ 0 & 0 & W_{43} & 0 & W_{45} & 0 & 0 & 0 & W_{49} \\ 0 & W_{52} & 0 & W_{54} & 0 & W_{56} & 0 & W_{58} & 0 \\ W_{61} & 0 & 0 & 0 & W_{65} & 0 & W_{67} & 0 & 0 \\ 0 & 0 & 0 & 0 & 0 & W_{76} & 0 & 0 & 0 \\ 0 & 0 & 0 & 0 & W_{85} & 0 & 0 & 0 & W_{89} \\ 0 & 0 & 0 & W_{94} & 0 & 0 & 0 & W_{98} & 0 \end{bmatrix} \quad (4.7)$$

Where

$$W_{12} = \frac{C1}{\text{Max}(C1, \dots, C11)} + 2$$

$$W_{23} = \frac{C2}{\text{Max}(C1, \dots, C11)} + 2$$

$$W_{34} = \frac{C2}{\text{Max}(C1, \dots, C11)} + 1$$

$$W_{49} = \frac{C4}{\text{Max}(C1, \dots, C11)} + 1$$

$$W_{45} = \frac{C5}{\text{Max}(C1, \dots, C11)} + 2$$

$$W_{56} = \frac{C6}{\text{Max}(C1, \dots, C11)} + 2$$

$$W_{98} = \frac{C8}{\text{Max}(C1, \dots, C11)} + 2$$

$$W_{85} = \frac{C10}{\text{Max}(C1, \dots, C11)} + 1$$

$$W_{52} = \frac{C11}{\text{Max}(C1, \dots, C11)} + 1$$

$$W_{76} = \frac{C7}{\text{Max}(C1, \dots, C11)} + 1$$

$$W_{61} = \frac{C9}{\text{Max}(C1, \dots, C11)} + 1$$

Rule 2.b: *The graph modeling of a single part antenna where capacitors or varactors are bridging over slots is undirected with weighted edges connecting vertices that represent the end points of each capacitor.*

Valid for:

This rule is valid for single part antennas of group 2.

Constraints:

The graph should be undirected and weighted where the weights are defined in Eq. 4.8.

$$W_{ij} = C_{ijnormalized} \quad (4.8)$$

Where C_{ij} represents the normalized capacitance of the capacitor connecting end-points i and j . The capacitances values are calculated as discussed in rule 2.a. In the case of multiple slots, rule 1.b applies with the addition of Eq. 4.8.

Example 4.7:

As an example we take the antenna shown in Fig. 4.11 [6]. Different variable capacitance diodes (varactors) values are used, and these varactor values are obtained by changing the biasing voltages. The graph modeling of this antenna follows rule 2.b. where the vertices represent the end points of the different varactors. The undirected edges are weighted with different varactor values. The graph model is shown in Fig. 4.12.

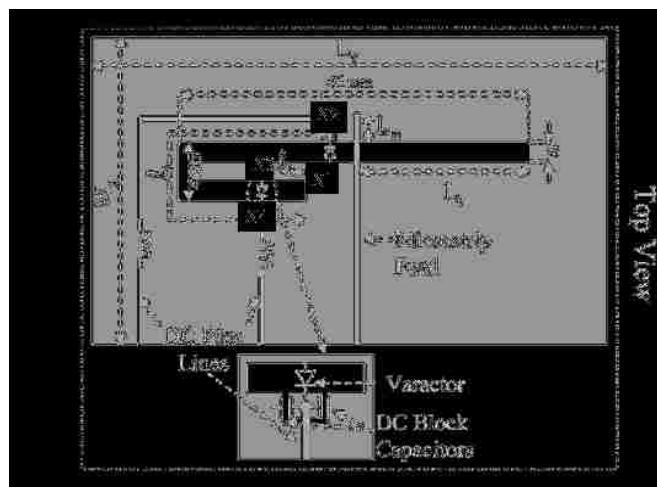


Fig. 4.11 Antenna structure in [6]

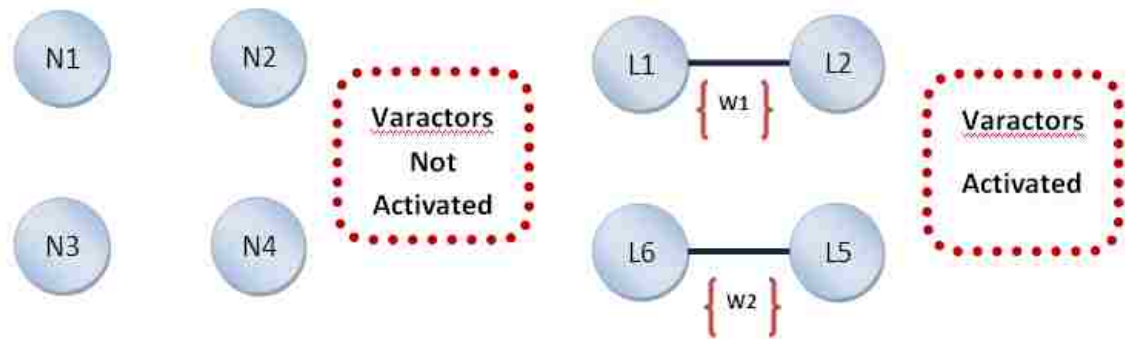


Fig. 4.12 Graph modeling for the antenna in [6]

Rule 3: The graph modeling of an antenna using angular change in its structure is undirected with weighted edges connecting vertices that represent the different angles of the physical action.

Valid for:

This rule is valid for antennas of group 3.

Constraints:

The graph modeling of this type of antennas is undirected since the angular change (bending or rotation) is reversible. The vertices represent the angles of this physical action. The weighted edges connecting the vertices represent the rotation or the bending process that is the state change from one angle to another. The weights represent constraints related to the system controlling the angular change like the rotation or the bending process i.e. time of rotation...

Example 4.8:

As an example we take the antenna shown in Fig. 4.13 [3]. This antenna exhibited a return loss tuning and a reconfigurable radiation pattern [3]. The graph modeling follows rule 3 where the bending angles are considered as vertices. The physical bending is occurring as a response to an external field applied then removed when the antenna reaches a rest angle. The time it takes for an antenna to reach that rest angle is very important in the antenna's applications. The edges' weights which are the costs that a designer must pay may represent in this case the time of bending. The different weights can be evaluated as in Eq. 4.9:

$$w_{ij} = T(A_i \rightarrow A_j) \quad (4.9)$$

The weight W_{ij} in this case represents the time it takes to bend the antenna from position i into position j . The adjacency matrix A shown below can be evaluated numerically however the exact numerical values depend on the fabricated system.

$$A = \begin{bmatrix} 0 & T(A_1 \rightarrow A_2) & T(A_1 \rightarrow A_3) & T(A_1 \rightarrow A_4) \\ T(A_2 \rightarrow A_1) & 0 & T(A_2 \rightarrow A_3) & T(A_2 \rightarrow A_4) \\ T(A_3 \rightarrow A_1) & T(A_3 \rightarrow A_2) & 0 & T(A_3 \rightarrow A_4) \\ T(A_4 \rightarrow A_1) & T(A_4 \rightarrow A_2) & T(A_4 \rightarrow A_3) & 0 \end{bmatrix} \quad (4.10)$$

This antenna is shown in Fig. 4.13 and the graph modeling is shown in Fig. 4.14.



Fig. 4.13 Antenna structure in [3]

In the graph model of Fig.4.14 A1 represents 0°, A2 represents 15°, A3 represent 45° and A4 represents 90°. Bending from 0° to 45° has to pass by 15° then the path from A1 to A3 has to pass by A2 as shown in Fig.4.14.

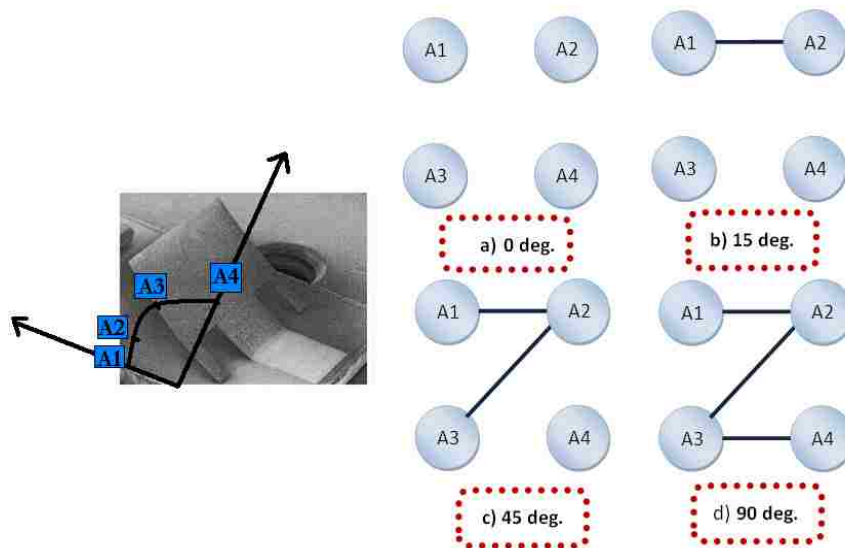


Fig. 4.14 Graph modeling of the antenna in [3]

Rule 4: *The graph modeling of an antenna using biasing networks to attach additional parts to each other is undirected with weighted edges connecting vertices that represent the parts of the whole antenna system.*

Valid for:

This rule is valid for antennas of group 4.

Constraints:

The same constraints as rule 1.a apply.

Example 4.9:

As an example we take the antenna shown in Fig. 4.15 [4]. Reconfiguration is achieved by turning ON or OFF various sections, to change the active length of the assembled monopole structure. The graph modeling of this antenna follows rule 4 where the different parts are the vertices and the edges represent the connection of these parts by the activation of the different biasing networks. The antenna's graph model is shown in Fig. 4.16.

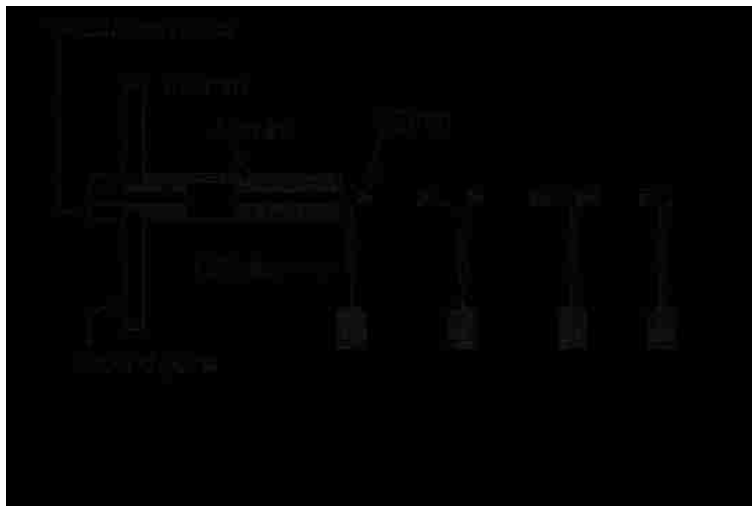


Fig. 4.15 The antenna structure in [4]

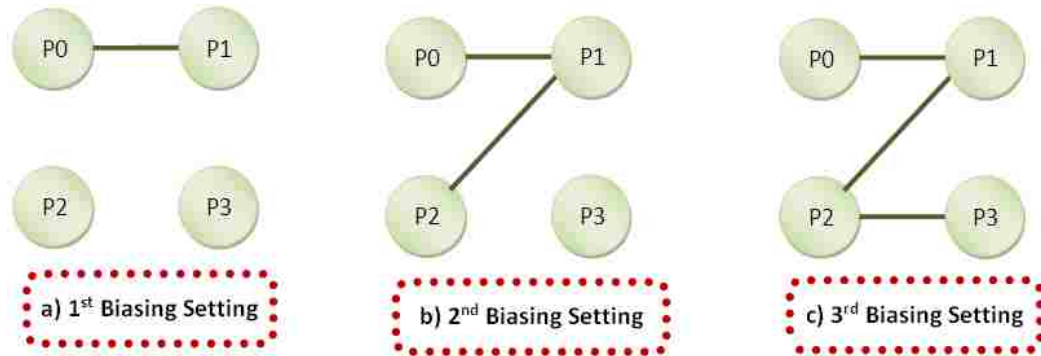


Fig. 4.16 Antenna graph model

Rule 5: The graph modeling of an antenna array where different antennas are excited at different times is undirected with weighted edges connecting vertices that represent the different antennas forming the array.

Valid for:

This rule is valid for antenna of group 5.

Constraints:

In the case where different antennas in an array system are excited at different times, the vertices in the modeling graph represent the different antennas. Undirected edges connecting different vertices represent the excitation presence of the corresponding different antennas at the same time. The angle that the antennas form with each other is of importance in the array function. The corresponding graph should be undirected with weighted edges where weights correspond to the antennas' positions relatively to each

other in addition to the absolute value of the mutual coupling in the case where mutual coupling is counted. M is the mutual coupling. All of the mutual coupling values should be expressed in the same unit and then they should be normalized with respect to the highest value. The weights are calculated according to Eq. 4.11:

$$W_{ij} = P_{ij} + |M_{ij_{normalized}}| \quad (4.11)$$

$$\text{Where } P_{ij} = \begin{cases} 1 & A_{ij} = 0^\circ \text{ or } 180^\circ \\ 2 & \text{Otherwise} \end{cases}$$

A_{ij} represents the angle that the antennas have with each other. M_{ij} represents the normalized mutual coupling amount between antennas i and j . If there isn't any mutual coupling between the antennas i and j then $M_{ij}=0$.

Example 4.10:

As an example we take the antenna shown in Fig. 4.17 [25]. This antenna is a 3-Dimensional model and it exhibits reconfigurable radiation pattern [25]. The graph modeling of this antenna follows rule 5 where the vertices are the different antennas on the different cube faces and the edges between them occur when the corresponding antennas are activated at the same time simulating their connection by the same feeding network and their radiated field coupling connection. The exact mutual coupling values between each 2 antennas were not specified in [25] however the weights are calculated according

to Eq. 4.11 and are shown in the adjacency matrix A below. The graph model is shown in Fig. 4.18.

$$A = \begin{bmatrix} 1 & 2 + |M_{12}| & 1 + |M_{13}| & 2 + |M_{14}| \\ 2 + |M_{21}| & 2 & 2 + |M_{23}| & 2 + |M_{24}| \\ 1 + |M_{31}| & 2 + |M_{32}| & 1 & 2 + |M_{34}| \\ 2 + |M_{41}| & 2 + |M_{42}| & 2 + |M_{43}| & 2 \end{bmatrix} \quad (4.12)$$

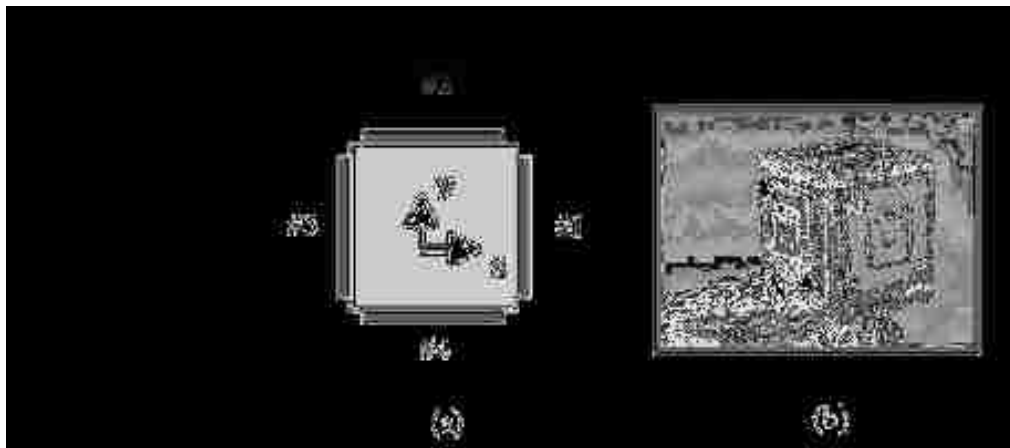


Fig. 4.17 The antenna array in [25]

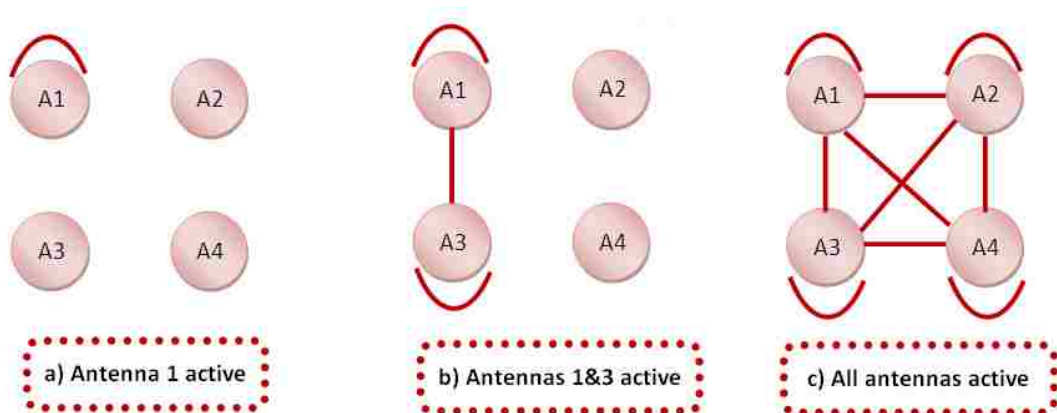


Fig. 4.18 Graph model of the array antenna in [25]

Rule 6: The rules defined previously in this section apply for the graph modeling of a reconfigurable feeding antenna where the reconfiguration is achieved in the feeding network.

Valid for:

This rule is valid for antennas of group 6.

Constraints:

The graph components in this case represent the feeding components. All the rules constraints defined previously apply correspondingly. For example if the feeding reconfiguration is through switches then rule 1.a applies and so on.

Example 4.11:

As an example we take the antenna in [24]. This antenna is based on the parasitic antenna concept and it realizes pattern diversity. To realize the pattern diversity, each of the slot pairs in the parasitic patches is loaded by a switchable stub. The stub lengths are adjusted by p-i-n diodes which allow four different patterns for one of the polarization state [24]. . By switching ON a diode while the other is OFF, the antenna can switch between horizontal or vertical polarization states with a single feeding port. Fig. 4.19 shows the feeding configuration connected by different diodes. The graph model according to rule 6 leads us to rule 1.a. where the vertices are the different lines in the feeding network connected together. The graph model is shown in Fig. 4.20 where the

edges weights are calculated according to Eq.4.4. We took into consideration 4 antenna states in the graph model shown in Fig. 4.20.

A summary of all the previous rules is shown in Table 4.1.

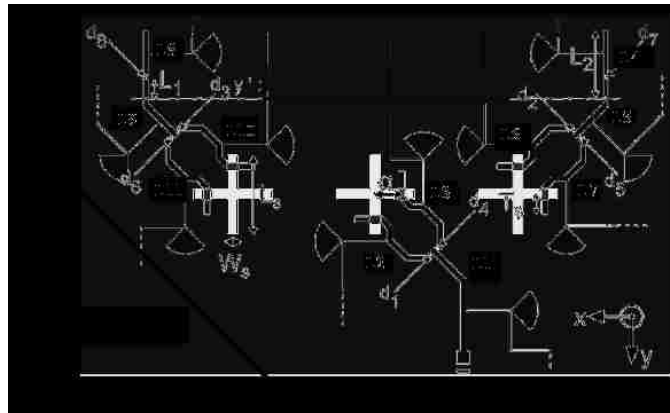
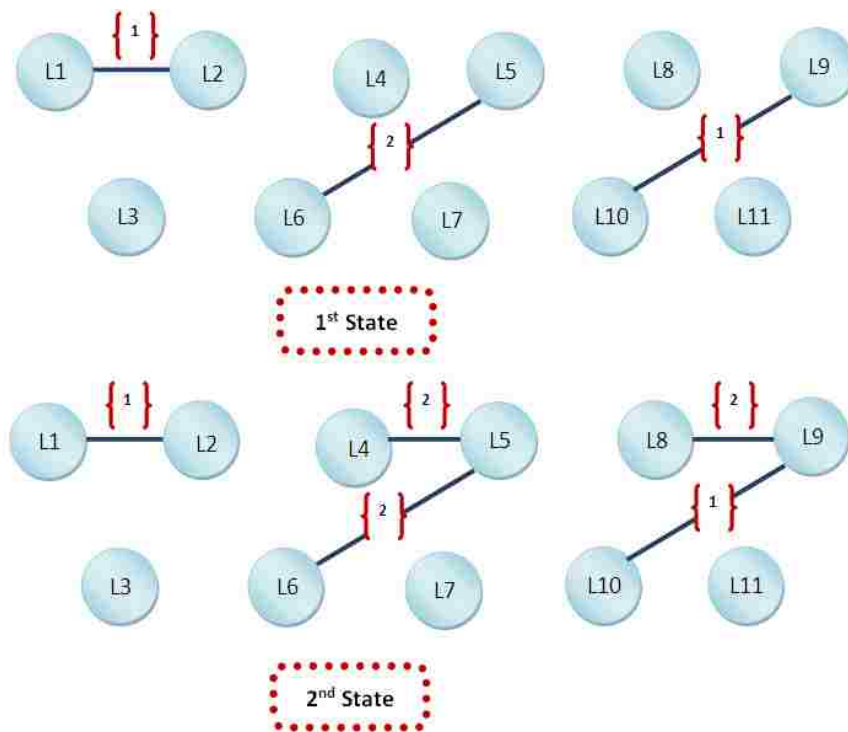


Fig. 4.19 The feeding network of the antenna in [24]



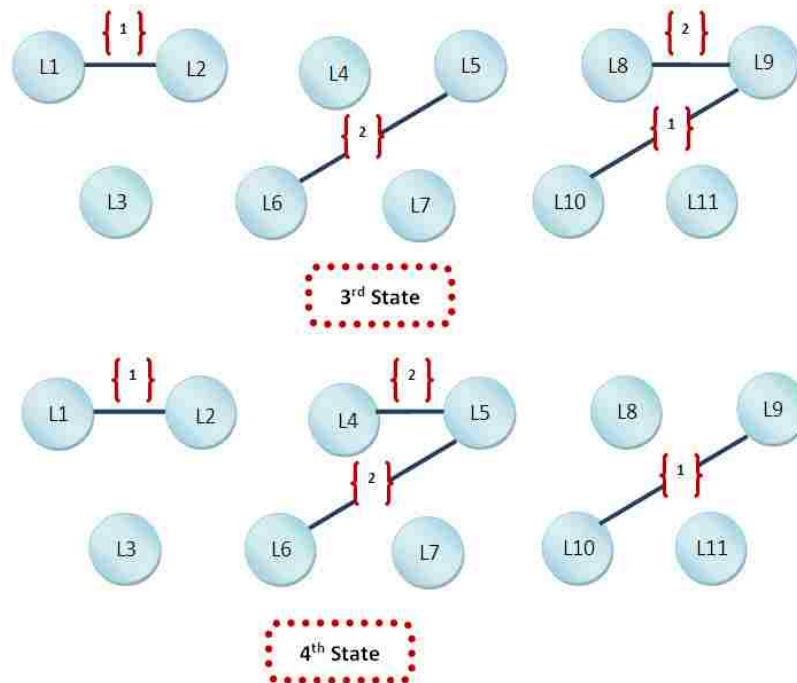


Fig. 4.20 The graph model for the antenna in [24]

4.5 Dijkstra's Shortest Path Algorithm:

4.5.1 Introduction to Dijkstra's algorithm:

Dijkstra's algorithm [52] solves the single source shortest-paths problem on a weighted, directed graph for the case in which all edge weights are nonnegative. The algorithm repeatedly selects the vertex with the minimum shortest-path estimate. For a given node in the graph, the algorithm finds the lowest cost path between that vertex and every other vertex. The algorithm can also be used to find the costs of shortest paths from one node to a certain destination node. The

algorithm needs to stop once the shortest path has been identified. A summary of Dijkstra's algorithm operating procedure is shown in Fig. 4.21

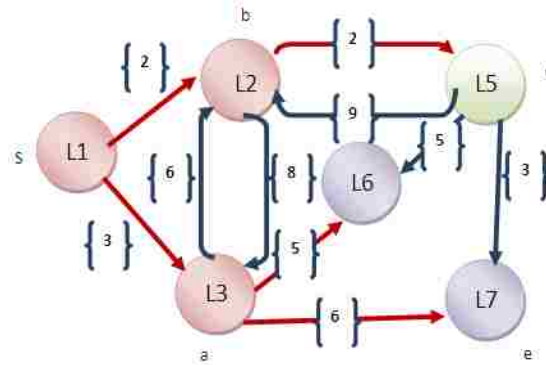


Fig. 4.21 The shortest path shown in red as calculated by Dijkstra's algorithm for a weighted graph

4.5.2 Dijkstra's Algorithm Mechanism:

Dijkstra's algorithm [52] starts at the source vertex, s , it grows a tree, T , that ultimately spans all vertices reachable from S . Vertices are added to T in order of distance i.e., first S , then the vertex closest to S , then the next closest, and so on. The distance between two vertices is affected by the edge weight connecting these two vertices.

Dijkstra's algorithm can be described in the following 8 steps [52]:

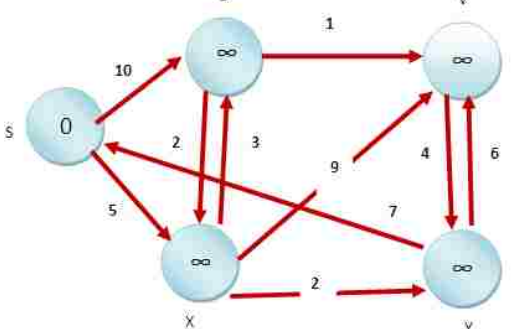
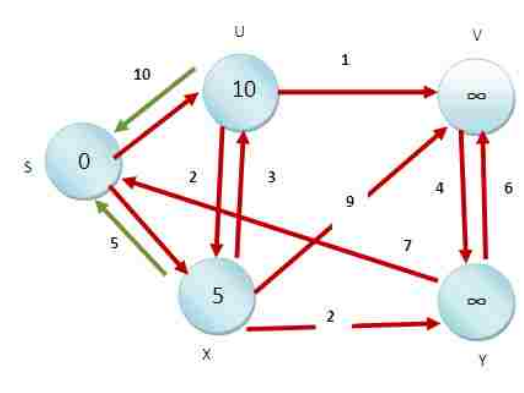
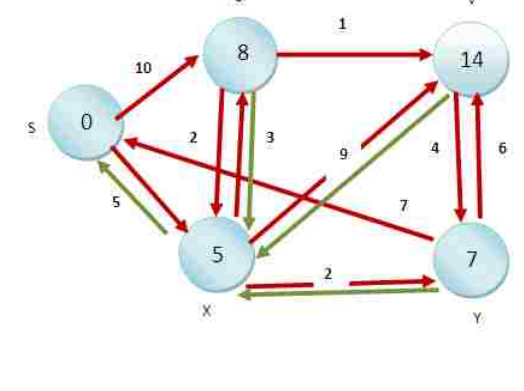
1. INITIALIZE SINGLE-SOURCE (G, s)
2. $S \leftarrow \{ \}$ // S will ultimately contains vertices of final shortest-path weights from s
3. Initialize priority queue Q i.e., $Q \leftarrow V[G]$

4. while priority queue Q is not empty do
5. $u \leftarrow \text{EXTRACT_MIN}(Q)$ // Pull out new vertex
6. $S \leftarrow S \dot{\cup} \{u\}$ // Perform relaxation for each vertex v adjacent to u
7. for each vertex v in $\text{Adj}[u]$ do
8. Relax (u, v, w)

	Multi-Part	Vertices	Directed	Weighted
Switches	YES	Parts	NO	YES
	NO	End-Points	NO	NO
Capacitors	YES	Parts	NO	YES
	NO	End-Points	NO	YES
Angular Change	N/A	Angles	NO	YES
Many Biasing Networks	YES	Parts	NO	YES
Antenna Arrays	N/A	Antennas	NO	YES
Reconfigurable Feeding	YES	Parts	NO	YES

Table 4.1 A summary of section 4.4 rules for the graph modeling of reconfigurable antennas

An illustration of the step by step operation of Dijkstra's algorithm is shown in Table 4.2

<p>Step 1: Given initial graph $G=(V, E)$. All nodes have infinite cost except the source node, s, which has 0 cost.</p>	
<p>Step 2: First we choose the node, which is closest to the source node, s. We initialize $d[s]$ to 0. Add it to S. Relax all nodes adjacent to source, s. Update predecessor for all nodes updated. (check green arrows)</p>	
<p>Step 3: Choose the closest node, x. Relax all nodes adjacent to node x. Update predecessors for nodes u, v and y. (check green arrows)</p>	

<p>Step 4: Now, node y is the closest node, so add it to S. Relax node v and adjust its predecessor. (green arrows)</p>	
<p>Step 5: Now we have node u that is closest. Choose this node and adjust its neighbor node v. (green arrows)</p>	
<p>Step 6: Finally, add node v. The predecessor list now defines the shortest path from each node to the source nodes. (green arrows)</p>	

Table 4.2 The illustration of the step by step operation of Dijkstra's algorithm

4.5.3 Applying Dijkstra's Algorithm to The Control Process of Reconfigurable

Antennas:

In certain reconfigurable antennas a shorter path may mean a shorter

current flow and thus a certain resonance associated with it. A longer path may denote a lower resonance frequency than the shorter path. In reconfigurable antennas resorting to physical and angular alterations a shorter path means a faster response and a swifter reconfiguration.

The antenna in [43] resorts to slot rotation to achieve reconfiguration. Several commercial rotary switches can be used to automatically rotate the slot. Rotary switches can also be customized for this design and implemented through an FPGA (Field Programmable Gate Array) to control the rotation of the slots on the antenna.

The graph model of this antenna follows rule 4 of section 4.4. Vertices correspond to the antenna's different angles of rotation as shown in Fig. 4.22. The edges connecting these vertices are undirected and they represent the rotation process between 2 angles.

The cyclic flow of the graph is due to the fact that the graph is modeling the rotation process controlled by rotary switches. The mode of operation of rotary switches ensures a sequential rotation. For example if A1 represents 0 degree, A2 represents 30 degrees and A3 represents 60 degrees. The rotation from 0 degree to 60 degrees is represented by edges connecting A1 (0 degree) to A2 (30 degrees) and A2 (30 degrees) to A3 (60 degrees). The edges in the graph are weighted. In this model the weights represent the time of rotation from one angle

into another and they are calculated according to Eq. 4.9. The graph modeling of this antenna with all possible edges is shown in Fig. 4.22.

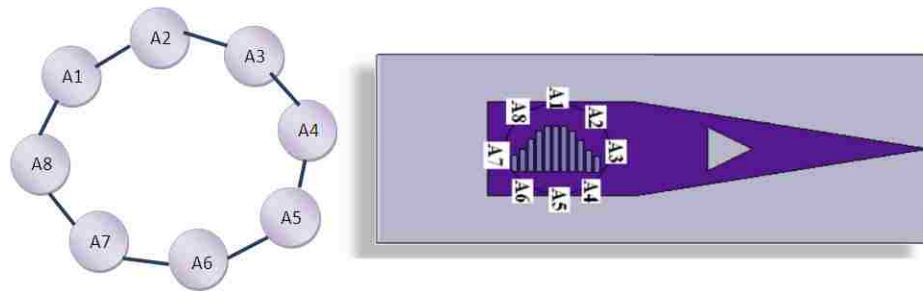


Fig. 4.22 All possible configurations represented by all possible edges [43]

In the case where this antenna is implemented on a time sensitive platform like a satellite, arriving at the desired position with the shortest time possible, regardless of the system constraints is very important. Finding the shortest path for each possible scenario is a major requirement.

The complication of the rotational slotted antenna may vary from one system into another. For example: In a particular system, going from 0 degree to 30 degrees might be more costly than going from 0 to 230 degrees and thus the importance of application of algorithms like Dijkstra's algorithms. This algorithm can be used to program an FPGA to control the rotation of the slots through a rotary switch. The direction of rotation of the slots will be chosen according to the direction of the shortest path to move from one position into another.

The adjacency matrix A showing all the graph weights calculated according to Eq. 4.9 is shown below. This matrix represents only four rotation processes. It can be evaluated numerically however the exact numerical values depend on the fabricated system and the rotary switch used.

$$A = \begin{bmatrix} 0 & T(A_1 \rightarrow A_2) & T(A_1 \rightarrow A_3) & T(A_1 \rightarrow A_4) \\ T(A_2 \rightarrow A_1) & 0 & T(A_2 \rightarrow A_3) & T(A_2 \rightarrow A_4) \\ T(A_3 \rightarrow A_1) & T(A_3 \rightarrow A_2) & 0 & T(A_3 \rightarrow A_4) \\ T(A_4 \rightarrow A_1) & T(A_4 \rightarrow A_2) & T(A_4 \rightarrow A_3) & 0 \end{bmatrix} \quad (4.13)$$

4.6 Discussion:

In this chapter guidelines for graph modeling the different groups of reconfigurable antennas were introduced. These guidelines will lead in the next chapters to new design and optimization techniques as discussed in Chapters 5 and 6. These models will be combined with information theory in Chapter 7 to analyze the reliability and complexity issues of reconfigurable antenna systems.

Dijkstra's shortest path algorithm was also introduced in this chapter. This algorithm is proposed to be applied to an FPGA to control the rotation process of slots in reconfigurable antennas. The application of this algorithm on reconfigurable antennas using mechanical alteration, achieves reconfiguration in the fastest and most efficient manner.

CHAPTER 5

A RECONFIGURABLE ANTENNA DESIGN APPROACH USING GRAPH MODELS

5.1 Introduction:

Despite some publications where genetic algorithms were used as a design methodology for reconfigurable frequency selective surfaces [61]; the design of reconfigurable antennas with all the available techniques today still lacks any clear tactic.

Reconfigurable antenna structure redundancy has never been previously investigated. Presently, efficient designs are desired in order to reduce costs and losses. In fact one might propose a design technique that will lead to a *constraint satisfying design* that lacks redundant elements and unnecessary electronic components.

Antenna designers are in need of an easy tool that is *not time consuming or modeling exhaustive*. In order to achieve this goal we resorted to graph models. In this chapter we present a new reconfigurable antenna designing technique that combines antenna theory, reconfiguration techniques and graph models. This technique consists of six steps that make use of concepts discussed in previous chapters. *Following the steps of this technique a designer ends up with an optimal design.*

5.2 Proposed Reconfigurable Antenna Design Steps

We set some steps to facilitate the reconfigurable antenna design. The designer can use these steps in a new designing project. These steps are concluded from patterns noticed in existing designs.

Step 1: Specify the reconfigurability property that needs to be obtained

First, the designer needs to define the reconfigurability property required from the antenna. These properties can be a reconfigurable frequency, reconfigurable radiation pattern, reconfigurable polarization or different combinations of these properties. Based on the desired property the designer can later on, in the following steps, decide on the type of antenna he/she needs to design, which reconfiguration technique to employ and fine tune its design accordingly.

Example on Design Step 1:

Resonance tuning and reconfigurable radiation pattern

Step 2: Specify the antenna structure while considering the design constraints

At this step the designer is required to have an idea of the general shape and structure of the design in question, considering all the imposed constraints and without determining the exact dimensions and specifications.

Example on Design Step 2:

The designer [48] is required to design a multi-band planar antenna (constraint 1). This antenna is also required to have 5 different configurations (constraint 2). In order to meet the requirements the designer decides to use intersecting microstrip lines. Four microstrip lines and a mid-section patch are required to satisfy the constraints. Fig. 5.1.a shows the structure in [48]

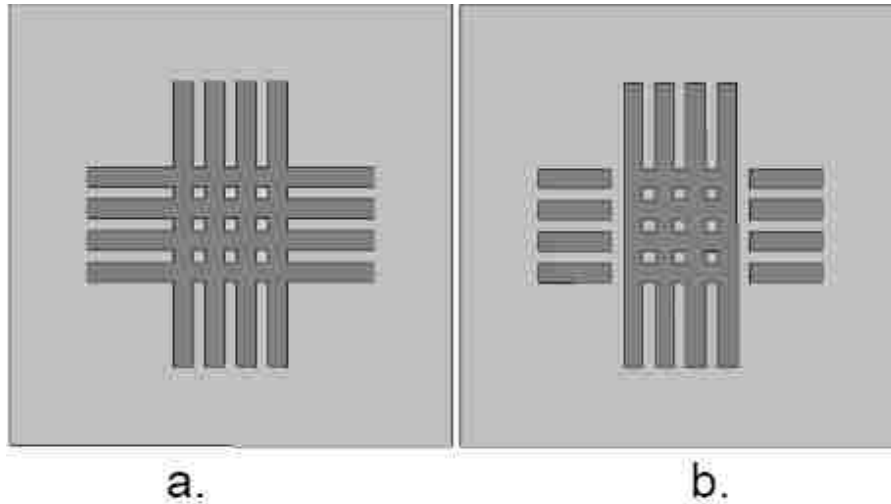


Fig. 5.1 The proposed structure a) Switches ON . b) Switches OFF

Step 3: Choose the reconfigurable technique by applying the statements in section 1.3 and considering the design constraints.

Based on all the statements defined in section 1.3 the designer can resort to many techniques. For frequency reconfigurable antennas, the application of statement 1 requires the usage of switches, capacitors or other techniques as in [7-23].

For antennas with reconfigurable radiation pattern, the application of statement 2 requires the incorporation of switches, a physical alteration or the reconfiguration of the feeding network as in [24-26]. For reconfigurable polarization the application of statement 3 requires the installation of switches, capacitors, incorporation of antenna arrays or the reconfiguration of the feeding network [27-28]. Finally, for an antenna with multiple reconfigurable properties the application of statement 4 requires the incorporation of the

principles mentioned in section 1.3 simultaneously [29-32].

Example on Design Step 3:

Since the antenna in Fig.5.1 needs to exhibit resonance tuning and a reconfigurable radiation pattern then statement 4 of section 1.3 applies which proposes a combination of statements 1 and 2. We need to execute a surface current distribution alteration and an alteration of the radiating edges.

By using switches to connect and disconnect the mid-section from the microstrip lines as shown in Fig.5.1, the whole antenna structure changes leading to a modification in the surface currents distribution and the radiating edges.

Step 4: Graph model the structure using proposed guidelines

Graph model the design based on the general shape of the structure initiated in step 2 and the graph modeling rules and guidelines of section 4.4 in chapter 4.

Example on Design Step 4:

Graph model the structure shown in Fig.5.1. In this case, rule 1.a of section 4.4 is applied. We have a mid section that other parts will be added to it. The vertices will represent the parts. Let's call the vertex representing the mid-section P0. The different parts will be added symmetrically and at the same time as shown in Fig.5.1. The edges connecting the vertices represent the connection of these parts to the mid-section. The graph model is shown in Fig. 5.2.

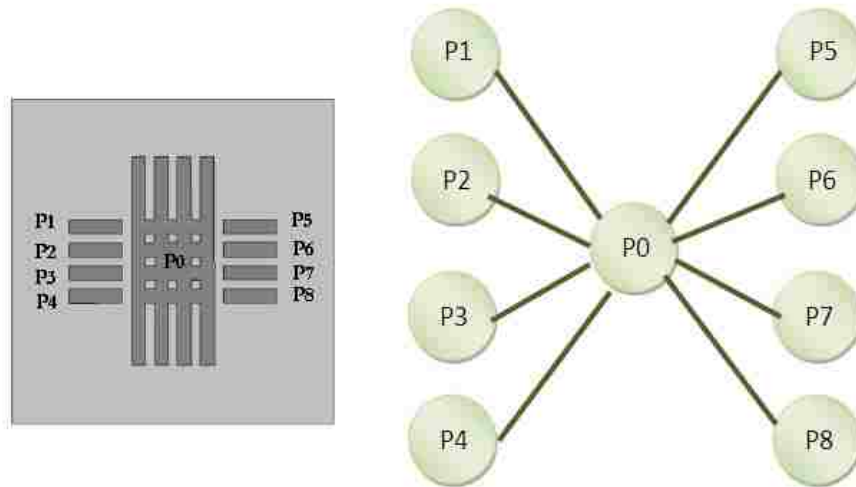


Fig. 5.2 The graph model showing all possible connections

Step 5: Fine tune the structure according to desired applications using simulations and testing.

Simulate the structure outlined in step 2 and fine tune it to satisfy the existing constraints. At this point the design is defined and specified with exact dimensions. The designer is required to check with measurements if necessary the accuracy of its design and the fidelity of its response.

Example on Design Step 5:

Simulate the structure shown in Fig.5.1 to satisfy the existing constraints. The structure of the proposed antenna [48] is discussed in section 3.4.2 of chapter 3. The S11 parameter of this antenna was measured between 1 Ghz and 6 Ghz. 5 resonances are clearly shown between 2.5 Ghz and 6 Ghz. The antenna presents both a reconfigurable

return loss and a reconfigurable radiation pattern as shown in Fig. 3.28, 3.29 and 3.30 of section 3.4.3 in chapter 3.

Step 6: In the case the designer is interested in finding an optimal solution for a configuration parameter such as redundancy. The designer should iteratively repeat steps 4 and 5 checking the feasibility of a solution as the constraints are tightened.

An iterative repetition of steps 4 and 5 with tightening the constraints results in a non-redundant structure. The designer needs to start by removing parts from his/her structure while preserving the topological symmetry and characteristics. If by repeating steps 4 and 5 the designer ends up with the same antenna performance then the parts removed were redundant. A constant tightening of constraints and repetition of steps 4 and 5 until the desired functions are not obtained results in an optimal design.

Example on Design Step 6:

Optimizing the design requires five different configurations, which is interpreted by attaching 2 lines from each side of the mid-section. Five total parts preserves the symmetry of the structure and conserves the radiation pattern properties.

The graph model of the optimized antenna is shown in Fig. 5.3. The antenna was simulated with 2 parts from each side as shown in Fig. 5.4. The optimization of the 2 parts with HFSS V.11 led to lines of width 0.9 cm and length 1.15 cm from each side of the mid-section. A comparison was made between the optimal antenna and the old redundant antenna and the return loss results are very similar as shown in Fig. 5.5 which

proves that the parts removed were redundant and 4 switches were spared. The radiation patterns of the non optimal and the optimal antennas are compared in Fig. 5.6 when the switches are not activated (OFF) which proves that the removal of the redundant parts did not affect the radiation pattern properties. The optimal antenna is now fabricated and tested and great analogy was shown between the tested and simulated S11 results as shown in Fig. 5.7. The optimized fabricated antenna and the original fabricated redundant antenna are shown in Fig. 5.9 for comparison.

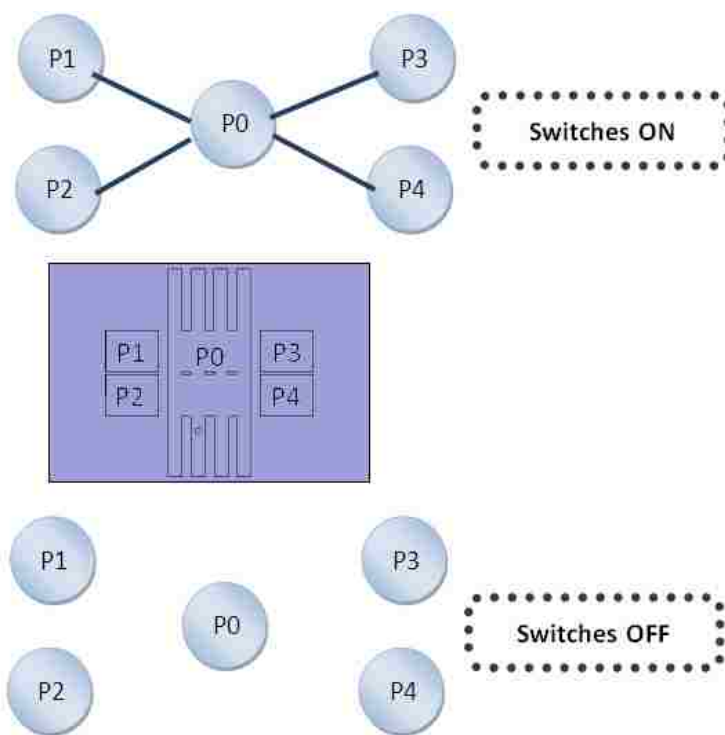


Fig. 5.3 The graph model of the iteratively optimized structure

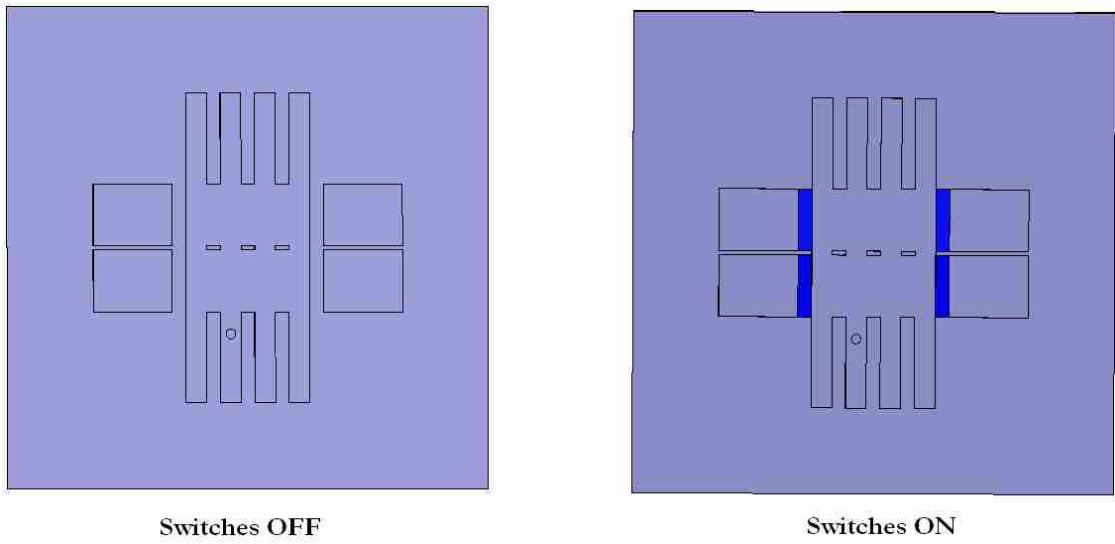


Fig. 5.4 The iteratively optimized antenna

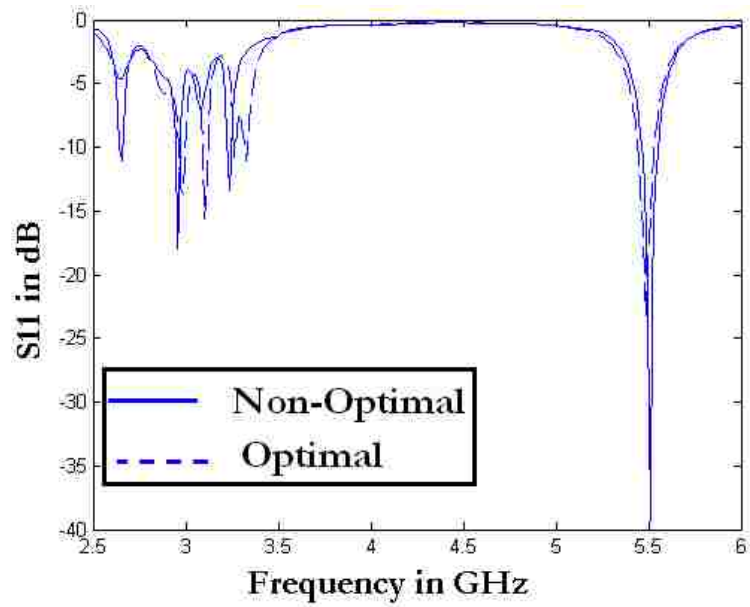


Fig. 5.5 Comparison between the S11 results for the non-optimal and the optimal antenna when the switches are activated

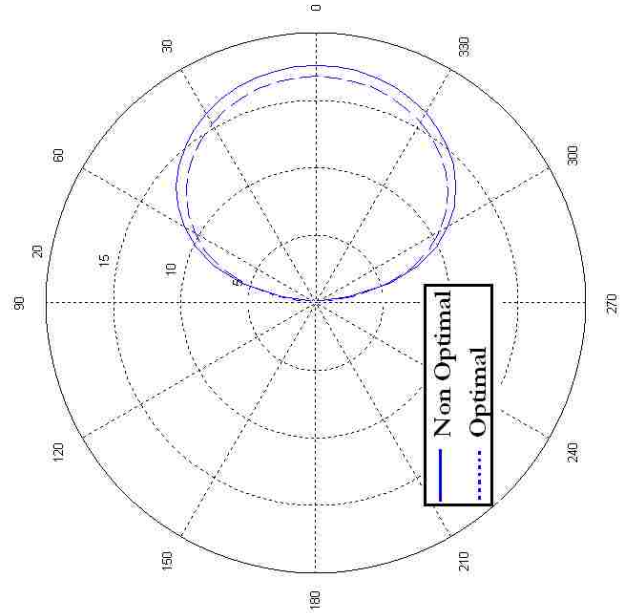


Fig. 5.6 The radiation pattern for the non optimal and the optimal antenna when the switches are open

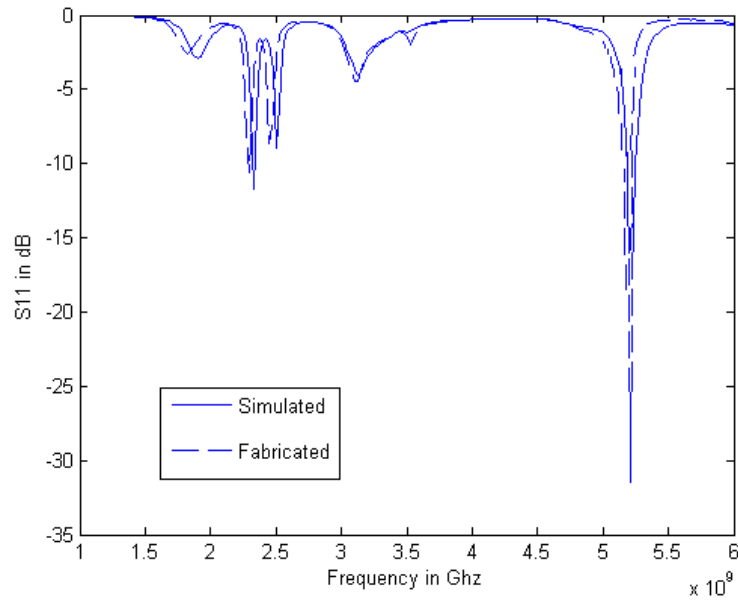


Fig. 5.7 A comparison between the simulated and tested S11 results for the optimal antenna

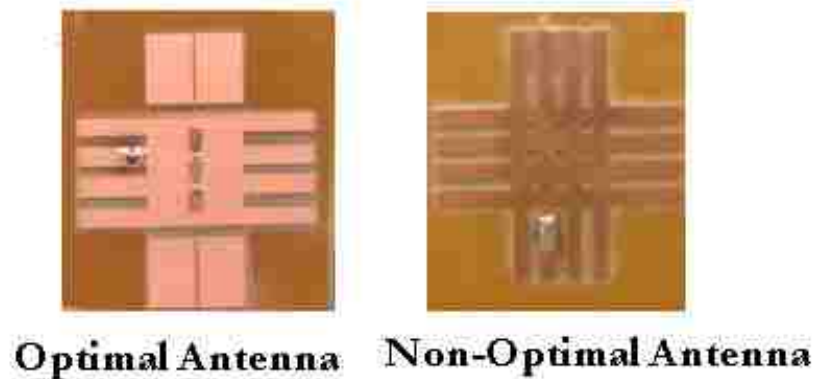


Fig. 5.8 The fabricated antennas

A Chart representing the proposed design technique is shown in Fig.5.9.

5.3 Designing Reconfigurable Antennas Using Proposed Design Steps

Example 5.1:

The objective of the design shown in Fig.5.10 [20] is to obtain a reconfigurable microstrip antenna that resonates at first at 1.85 GHz and 3.2 GHz, then at 1.85 GHz and 3.4 GHz and then at 1.85 GHz and 3.6 GHz. This antenna tunes the lower frequency from 1.85 GHz to 2.4 GHz, the higher frequencies remain unchanged. Four symmetrical parts are added for each length [20]. In this example the antenna is redesigned and the decision to add four symmetrical parts is re-examined. According to section 5.2:

Step1: A reconfigurable return loss.

Step2: The antenna required is a microstrip antenna. The material used is Rogers RO 3203 with 1.524 mm of height. The shape of the patch which is a monopole and having a coplanar ground plane is one of the constraints.

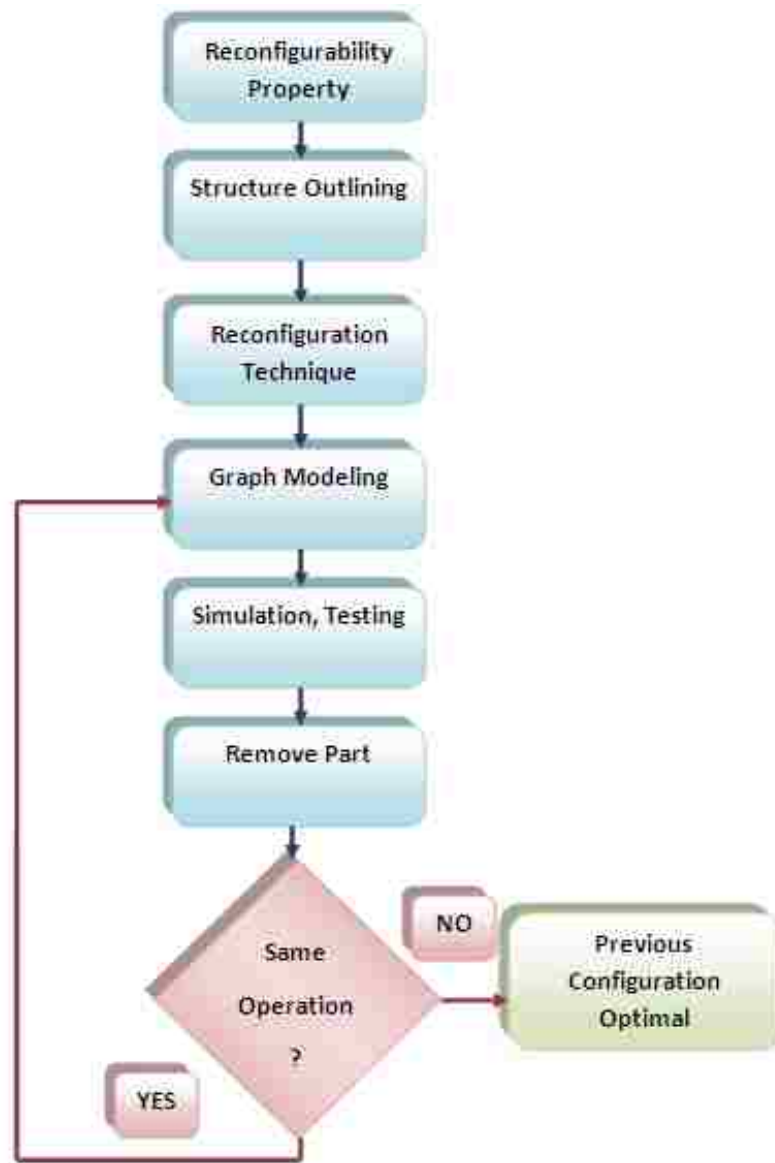


Fig. 5.9 A chart representation of the proposed design technique

Step3: Since this antenna is required to exhibit a reconfigurable return loss then statement 1 of section 1.3 applies. Switches are chosen to connect different parts to the monopole which satisfies a second designing constraint.

Step 4: Graph model the structure using section 4.4 rules. In this case rule 1.a of section 4.4 applies. We have a main monopole that other parts will be added to it. The vertices represent the different parts. Let's call the vertex representing the main monopole P0 and the added monopole P1. Three frequency changes are required for each length of the monopole; this means 3 antenna configurations are required for each monopole length.

The 4 symmetrical parts added in [20] are represented by P2, P3, P4 and P5. The edges between the vertices represent the connection of the different parts. These edges will be weighted and the weights are calculated according to Eq. 4.4. The main monopole's direction is considered as the reference axis. The graph modeling of this antenna with all possible connections is shown in Fig. 5.11. The adjacency matrix A representing all the weights for the antenna with a total of 6 parts is shown below.

$$A = \begin{bmatrix} W00 & W01 & W02 & W03 & W04 & W05 \\ W10 & W11 & W12 & W13 & W14 & W15 \\ W20 & W21 & W22 & W23 & W24 & W25 \\ W30 & W31 & W32 & W33 & W34 & W35 \\ W40 & W41 & W42 & W43 & W44 & W45 \\ W50 & W51 & W52 & W53 & W54 & W55 \end{bmatrix} = \begin{bmatrix} 0 & 1 & 0 & 2 & 2 & 0 \\ 1 & 0 & 0 & 0 & 0 & 0 \\ 0 & 0 & 0 & 1 & 0 & 0 \\ 2 & 0 & 1 & 0 & 0 & 0 \\ 2 & 0 & 0 & 0 & 0 & 1 \\ 0 & 0 & 0 & 0 & 1 & 0 \end{bmatrix} \quad (5.1)$$

Step 5: The design is simulated. The dimensions of the parts are optimized so that if the switch is off, 1.85 GHz is obtained and if the switch is on, 2.4 GHz is obtained.

Step 6: The designer's decision is not optimal since by comparison between the number of antenna configurations and the number of resonances obtained we find that 2 parts can be

easily omitted. An iterative repetition of steps 4 and 5 would result in removing the antenna redundancies. The desired optimal structure is graph modeled in Fig.5.12. The same functional behavior should be obtained from the optimized antenna. The optimized antenna structure has 4 parts instead of 6 and two switches should be eliminated. The optimized antenna resembles the original one in Fig. 5.10, except that it has only 4 total parts instead of 6. The adjacency matrix of the graph represented the optimized structure is shown below:

$$A_{opt} = \begin{bmatrix} 0 & 1 & 2 & 2 \\ 1 & 0 & 0 & 0 \\ 2 & 0 & 0 & 0 \\ 2 & 0 & 0 & 0 \end{bmatrix} \quad (5.2)$$

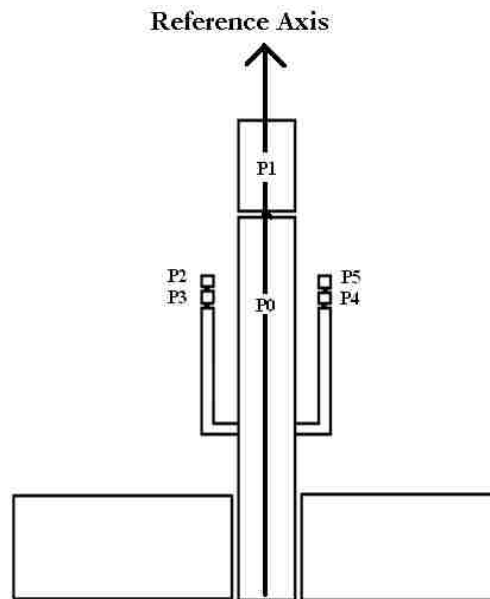


Fig. 5.10 Antenna structure in [20] with parts numbered

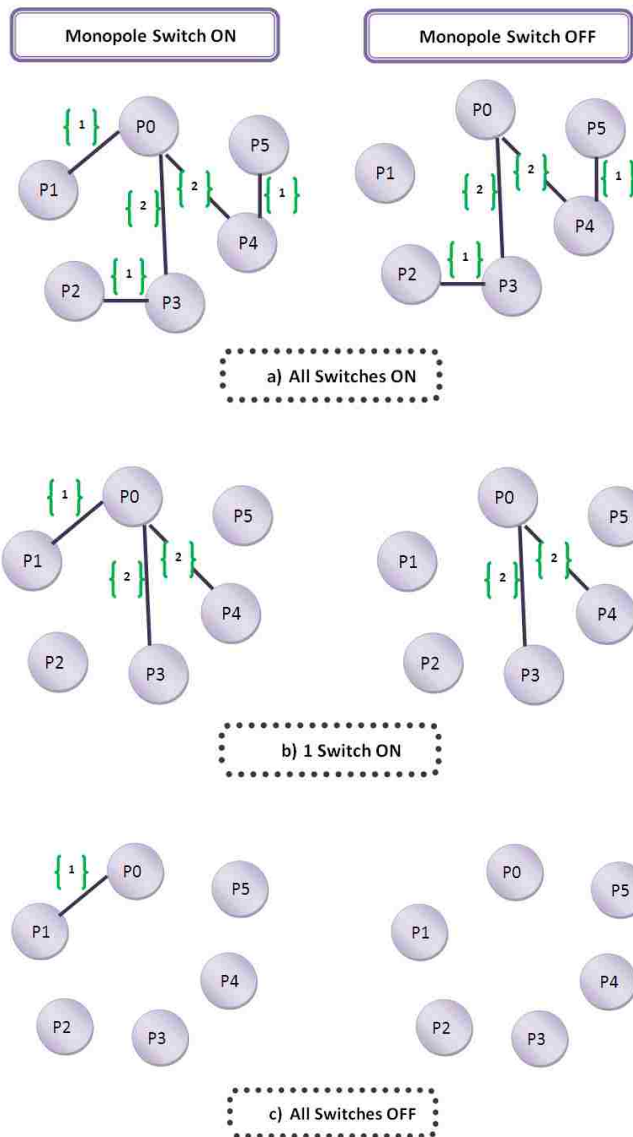


Fig. 5.11 Graph modeling before designing the antenna showing the different antenna configurations

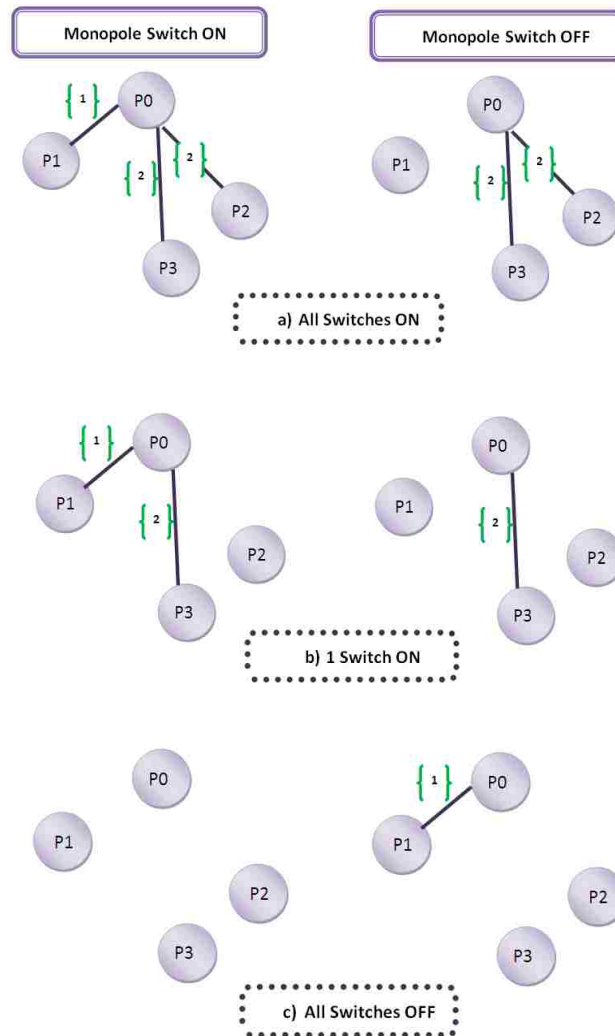


Fig. 5.12 Graph modeling for the optimal antenna design

Example 5.2:

Step1: Frequency reconfigurable antenna

Step2: The antenna type required is a microstrip antenna [5]. The substrate is a quartz substrate which satisfies one of the constraints [5]. This antenna is shown in Fig.5.13 where the choice of a triangular patch constitutes a second constraint.

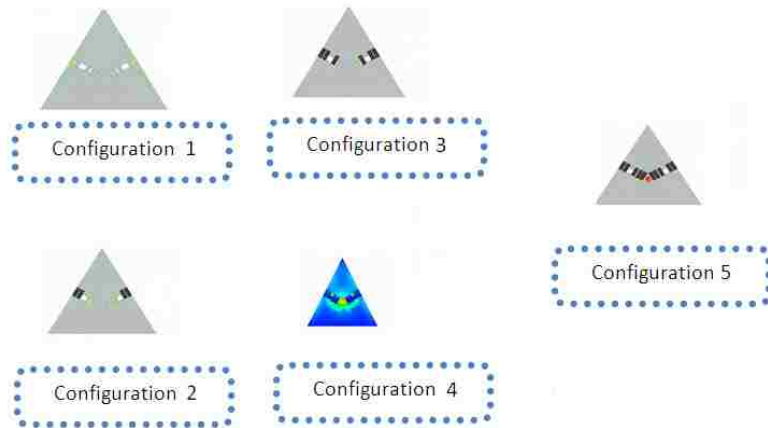
Step 3: Since this antenna is required to be frequency reconfigurable, then statement 1 of section 1.3 applies. RF MEMS are chosen to achieve reconfiguration (constraint 3) and this antenna is also required to operate at a specific mode (constraint 4). Slots with RF MEMS bridging over are incorporated into the triangular patch to achieve the specific mode [5].

Step 4: Graph model the structure using section 4.4 rules. In this case rule 1.b should be used. We have slots where switches are bridging over to achieve five different current paths. The vertices represent the end-points of the switches and the edge connecting 2 vertices represent a physical connection between the corresponding end-points. So each set of connections will represent a distinctive antenna configuration. The graph model is shown in Fig.5.13 where each vertex represents 2 end-points corresponding to 2 different switches at a symmetric position in the 2 slots. For example N1 represent end-point 1 for switch 1 in slot 1 and end-point 1 for switch 1 in slot 2.

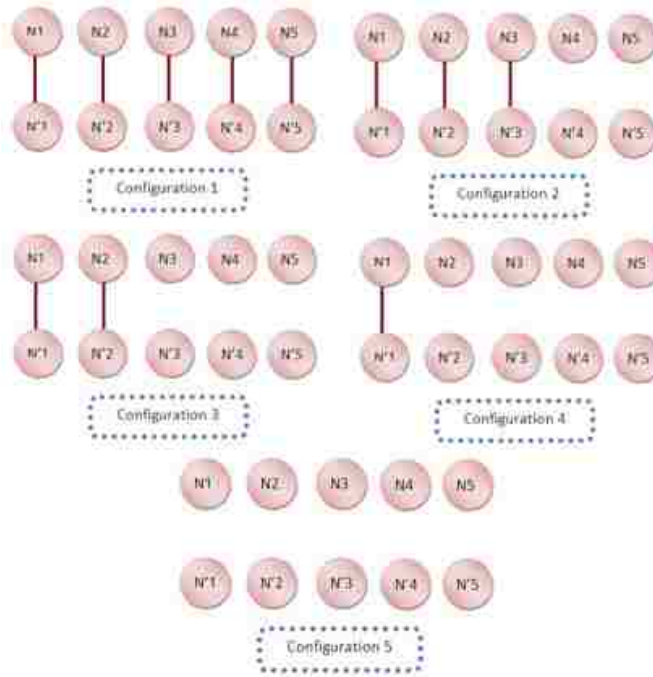
Step 5: The last step is simulation. The position of the slots is optimized and the length and width of the slots are specified [5].

Step 6: The use of 10 switches is not optimal and 4 switches are sufficient to achieve 5 different antenna configurations. All design constraints must be met including maintaining the same radiation characteristics. Two slots are preserved at the same position and in the same direction, however instead of having 10 switches, 4 switches accomplish the same job efficiently. An iterative repetition of steps 4 and 5 should be executed. The graph

model representing the optimized antenna is shown in Fig. 5.14 where each vertex represents an end-point of one switch in the slots.



a.



b.

Fig. 5.13 a. Different antenna configurations. b. Corresponding graph models

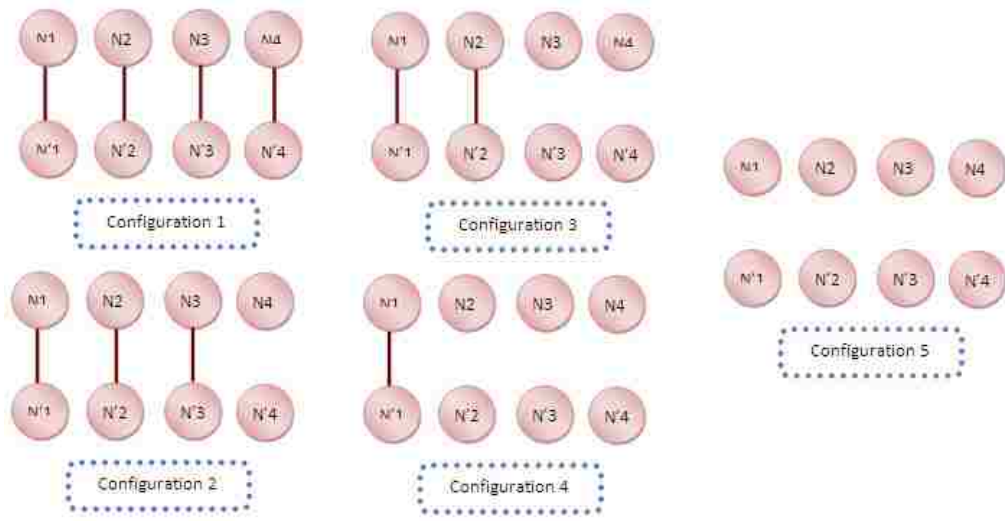


Fig. 5.14 The graph model of the proposed optimized topology

Example 5.3:

Step 1: Frequency reconfigurable antenna

Step 2: The basic structure of the antenna is discussed in section 3.2 of chapter 3.

Step 3: The technique here is the slot rotation [22,40].

Step 4: Graph modeling the structure. In this case rule 4 in section 4.4 applies. The vertices represent the angles of rotation and the edges connecting these vertices are undirected and they represent the rotation process between 2 angles as discussed in section 4.5.3. The graph model of this antenna is shown in Fig.5.15 and Table 5.1 shows graph models for different configurations of the antenna in question.

Step 5: Simulating the actual design and testing it. The simulation and measurement results are discussed in section 3.2 of chapter 3.

Step6: Since for each slot position the antenna exhibits a different resonance then this antenna does not have any redundancies unless the number of configurations required was limited. Such reconfiguration techniques make the iterative process unnecessary in case all possible configurations were accepted.

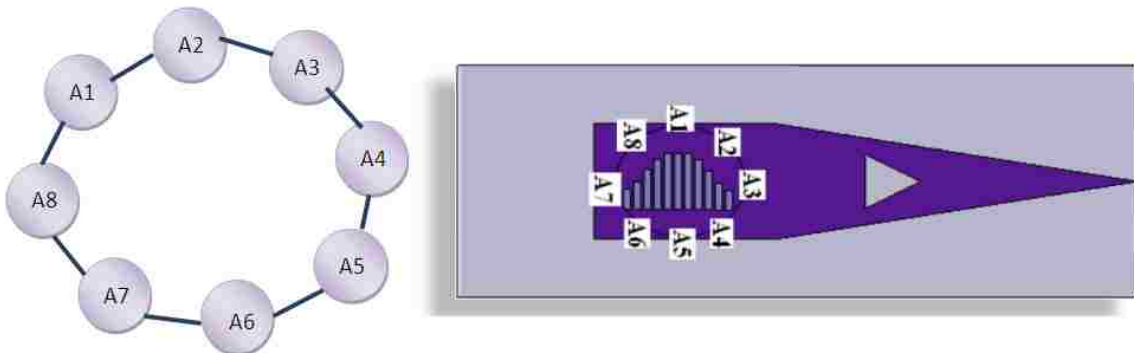
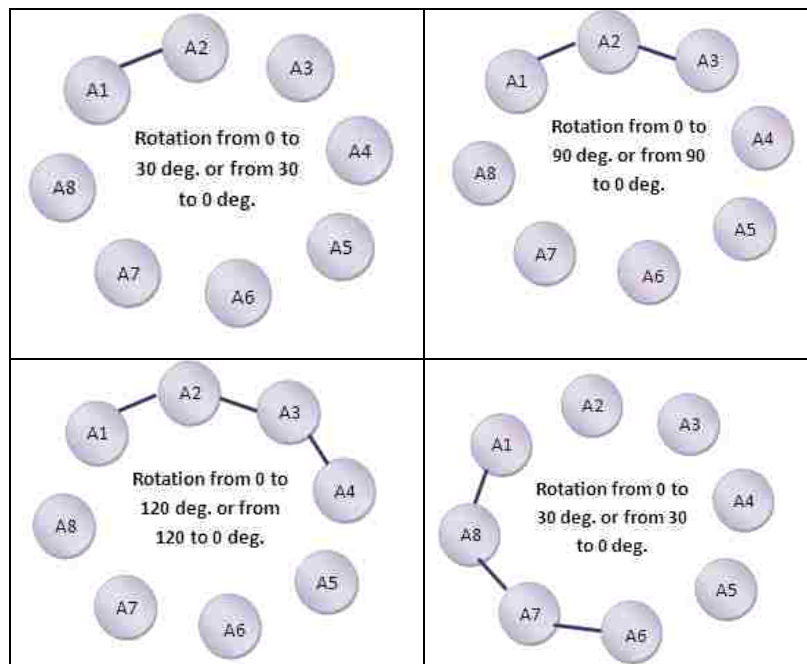


Fig. 5.15 Graph model for all possible configurations



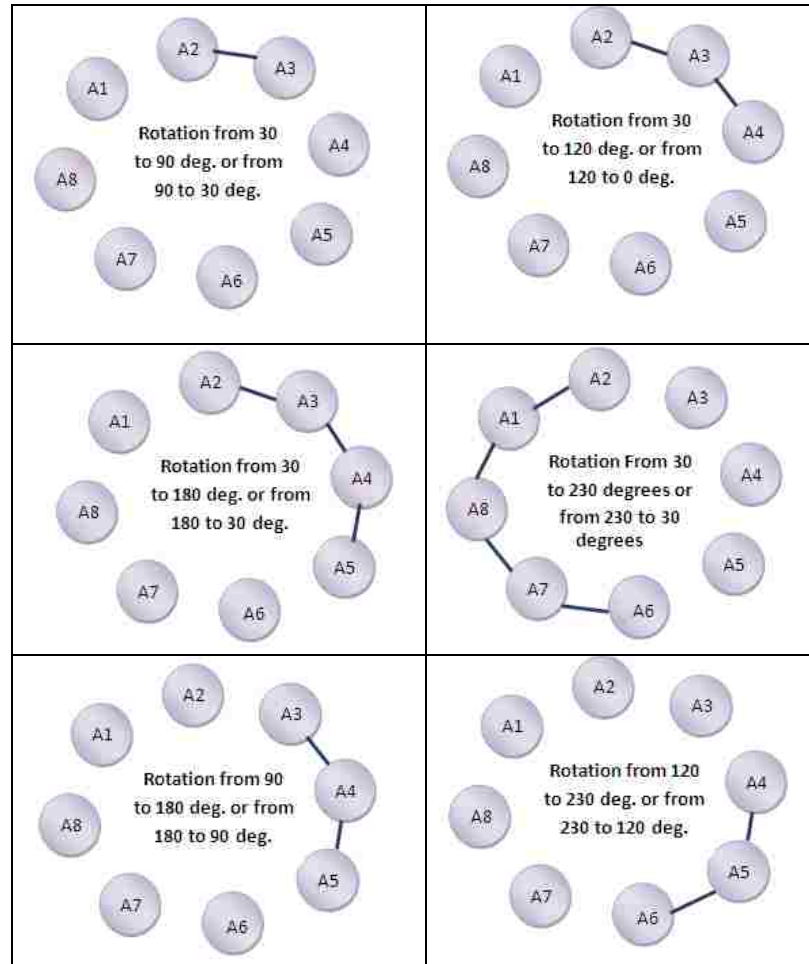


Table 5.1 Graph models for possible antenna configurations

5.4 Discussion:

In this chapter a new design technique was presented. This technique was tested with many examples and proven to facilitate the design process and iteratively optimize the final prototype. It helps researchers design reconfigurable antennas in a structured and organized manner. It also gives them a redundancy reduction methodology. However this technique is iterative and may be computationally exhaustive in large cases. In the next chapter we will present a mathematical optimization technique based on graph models.

CHAPTER 6

OPTIMIZING RECONFIGURABLE ANTENNAS USING GRAPH MODELS

6.1 Introduction and Optimization Techniques Review:

Different optimization algorithms are used to achieve the designers' objective of smoothing state transition in a reconfigurable antenna. In [61] the flexibility of a grid of metallic patches interconnected by a matrix of switches is exploited by optimizing the switch settings using a genetic algorithm to produce a desired frequency response. Genetic algorithms are also used in [62] to search the patterns that the antenna might produce for a given frequency.

Neural networks are used to select which switching devices should be activated for each reconfiguration state [9]. Each group of selected switches allows the antenna to resonate at a certain band. This task is handled as a classification type of problem and is accomplished by a self-organizing map neural network (SOM NN) [63].

A method based on the clonal selection algorithm (CLONALG) is used to design a reconfigurable dual-beam linear antenna array with excitation distributions differing only in phase [64]. The CLONALG is a relatively novel population-based evolutionary algorithm inspired by the clonal selection principle of the human immune system.

In order to decide which optimization method is the most convenient for a specific design, different algorithms are compared together [65]. The use of genetic algorithms,

simulated annealing, and ant-colony optimization applied to reconfigurable antennas is investigated in [65]. All these algorithms are compared to the random search method. The work shows that each optimization algorithm outperforms the random search method [65]. A comparison between genetic algorithms and particle swarm optimization, versus the cross-entropy method is shown in [66]. Results show that the cross-entropy method has a fast convergence speed, but it needs large population sizes to function [66]. A particular optimization algorithm cannot be separated from the rest as the best fit before selecting a specific reconfigurable scheme [67].

In this chapter a new optimization technique based on graph models is presented.

This technique discussed briefly in [68-69] resorts to the graph modeling guidelines previously defined in Section 4.4. Based on these guidelines a set of equations is formulated. These equations will indicate the presence or lack of redundancy in an antenna structure and in the number of reconfiguring elements used. *This approach proposes a way of reducing the antenna structure's complexity and thus can't be compared to the techniques discussed previously due to the difference in objective.*

6.2 Structure Redundancy Optimization:

A part is defined as redundant if its presence gives the antenna more functions than *required and its removal does not affect the antenna's desired performance*. The removal of a part from the antenna structure may require a change in the dimensions of the remaining parts in order to preserve the antenna's original characteristics i.e. a redundant

part can be removed as long as its removal will not affect the polarization status of the antenna in a reconfigurable return loss and reconfigurable polarization antenna.

Every path in every graph model representing the reconfigurable antenna should correspond to a different configuration. If the number of unique paths in the graph model is larger than the number of configurations, then redundancy might exist in the antenna structure. An example of counting the total number of unique paths in a graph model is shown in Fig. 6.1. If redundant parts were removed from the antenna structure their corresponding vertices and edges should be removed from the graph model.

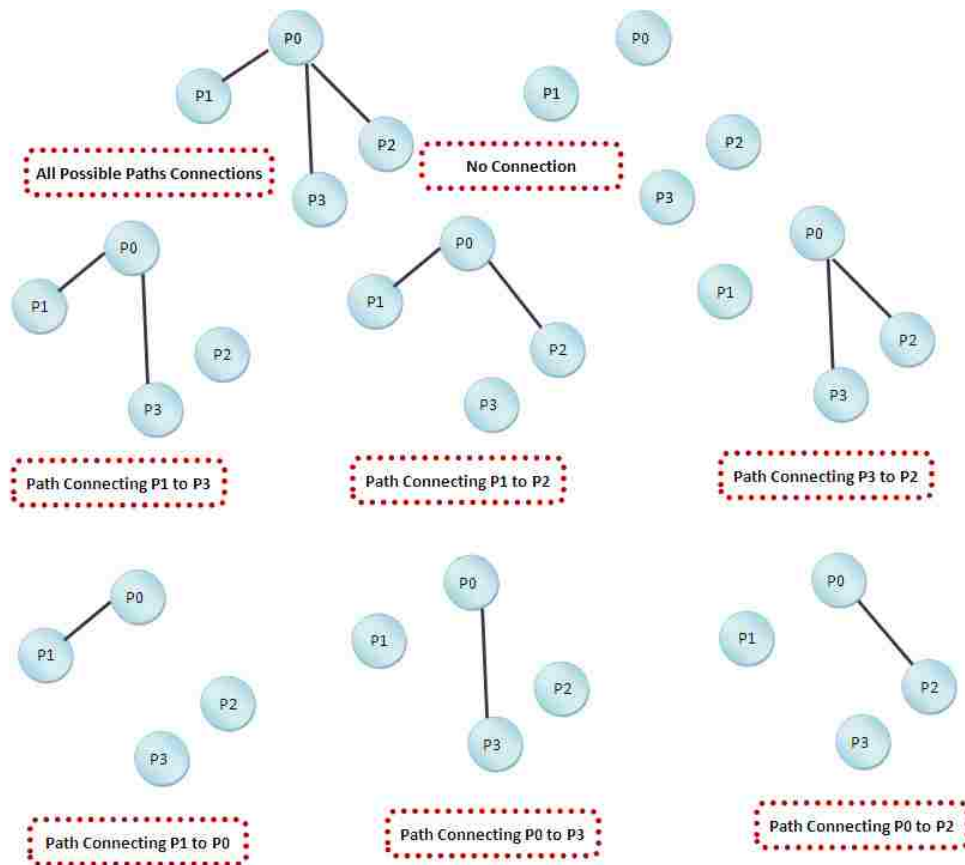


Fig. 6.1 An example of possible unique paths in a given graph

Since each unique path represents a unique antenna function, it is important to identify the number of possible unique paths. In our optimization approach reconfigurable antennas using one reconfiguration technique are investigated. If an antenna uses more than one reconfiguration technique then each technique is investigated separately.

6.2.1 The Total Number of Edges In a Complete Graph:

A complete graph is a simple graph in which every pair of distinct vertices is connected by an edge. Suppose the set of vertices in a complete graph model is $V = \{1, 2, \dots, N\}$. A vertex i can be selected in n ways, i.e. There are exactly $(N-1)$ edges between a selected vertex i and the remaining $(N-1)$ vertices [70]. In Fig. 6.2 a complete graph with 3 vertices is shown. Each vertex has $(N-1)=2$ edges with the remaining 2 vertices as shown in Fig. 6.2.

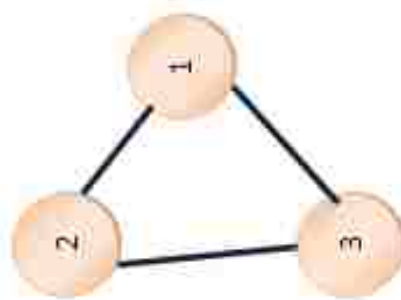


Fig. 6.2 A complete graph with 3 vertices

The edge joining i and another vertex j is the same as the edge joining j and i . Thus the total number of edges in the complete graph is $N(N-1)/2$, where N is the number of vertices. This is shown in Eq. 6.1 below:

$$K_N = \frac{N(N-1)}{2} \quad (6.1)$$

Where:

N = number of vertices

K_n = Total number of edges in a complete graph

Example 6.1:

A complete graph with 7 vertices is shown in Fig. 6.3. The total number of edges in this graph is calculated according to Eq. 6.1. as follows:

$$K_7 = \frac{7(7-1)}{2} = \frac{7 \times 6}{2} = 21$$

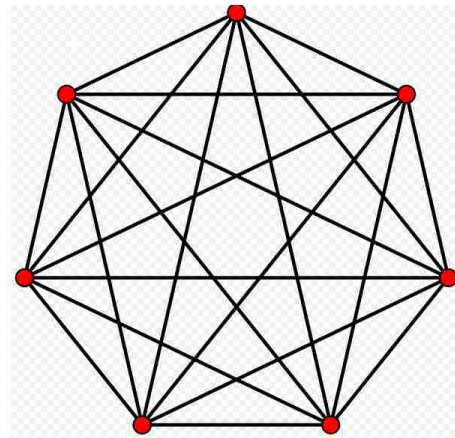


Fig. 6.3 A complete graph with 7 vertices

6.2.2 Deriving Equations For Redundancy Reduction in Multipart Antennas of Groups (1,2,4,5,6):

In order to set some equations for reducing redundancy in a multipart

antenna structure, and based on the fact that each unique path corresponds to a unique function, the number of unique paths in a graph has to be minimized. Formulating the total number of unique paths in any graph model has not been solved yet. According to the graph modeling rules defined in Section 4.4 for multi-part antennas of groups (1,2,4,5,6), graphs representing these antennas are arbitrary and depend on the antenna topology which is not generalized and may be considered random. *Thus the number of unique paths cannot be formulated and a minimum bound needs to be estimated in order to minimize the number of RF components used and reduce redundancies.*

The estimate of the necessary number of unique paths is NUP and it is formulated in Eq.6.3a, where N represents the number of vertices in the corresponding graph. Eq. 6.3 is based on the following point:

The minimum number of edges present in any graph model according to the rules of Section 4.4 is equal to (N-1). The Maximum number is equal to K_n from Eq. 6.1. Eq. 6.2 shows the bounds of the number of edges NE in a graph model of this category:

$$(N - 1) \leq NE \leq \frac{N(N - 1)}{2} \quad (6.2)$$

The number of unique paths in such a graph model (NUP) is always $\geq K_n$

or else idle vertices are present in that graph model. Then, the total number of edges in a complete graph as defined in Eq. 6.1 is sufficient to be considered as the necessary number of unique paths in order to minimize redundancies. By decreasing the number of unique paths, the number of possible configurations is reduced which results in reducing the number of vertices and redundant parts are removed.

Eq.6.3 b discusses the necessary number of available configurations where the case of no connection is added. Eq.6.3.c is a direct derivation of Eq. 6.3 a and b and represents the number of necessary vertices to achieve a certain number of configurations The reconfigurable antenna may have more possible configurations than NAC for a given set of vertices however NAC represents the minimum bound of configurations that are necessary to achieve a reliable antenna.

$$NUP = \frac{N(N-1)}{2} \quad (6.3.a)$$

$$NAC = NUP + 1 \quad (6.3.b)$$

$$N^2 - N - 2 \times (NAC - 1) = 0 \Rightarrow$$

$$N = \left\lceil \frac{1 + \sqrt{1 + 8 \times (NAC - 1)}}{2} \right\rceil \quad (6.3.c)$$

6.2.3 Deriving Equations For Redundancy Reduction in Single-Part Antennas of Groups (1,2,4,5,6):

In single part antennas, each vertex represents an end point of an RF element bridging over a slot and each edge represents the connection between these two end points as defined in Section 4.4. Thus the number of vertices N is double the number of all possible edges. In this case the number of possible unique paths is equal to the number of possible edges in the graph due to the rules of Section 4.4. Eq.6.4.a represents the minimum number necessary of available antenna configurations to achieve a reliable design. It is the number of possible edges in addition to the case where no connection exists. As in Eq.6.3, the reconfigurable antenna might have more possible configurations than NAC for a given set of vertices. Eq. 6.4.b is a direct derivation of Eq. 6.4.a and represents the number of vertices necessary to achieve a certain number of configurations.

$$NAC = \frac{N}{2} + 1 \quad (6.4.a)$$

$$N = 2 \times (NAC - 1) \quad (6.4.b)$$

6.2.4 Deriving Equations For Redundancy Reduction in Antennas of Group 3:

Eq.6.5 is valid for reconfigurable antennas of group 3. This equation represents the number of available configurations for antenna using angular

physical change as a reconfiguration technique. In this case for each angle a different configuration is possible. NAC represents the number of available configurations in a graph model, while N represents the number of vertices.

$$NAC = N \tag{6.5}$$

6.3 Examples:

Example 6. 2:

In this section, the antenna discussed in [48] is considered. The antenna is required to have resonance tuning and radiation pattern reconfigurability. The design as well as the graph model is presented in Fig.6.4. This antenna is required to have 5 different configurations.

Since this is a multi-part switch-reconfigured antenna Eq.6.3 must be applied. Eq. 6.3a,b reveal that the antenna has a minimum of 29 possible configurations.

$$NUP = \frac{N(N-1)}{2} = \frac{9(9-1)}{2} = 36$$

$$NAC = NUP + 1 = 37$$

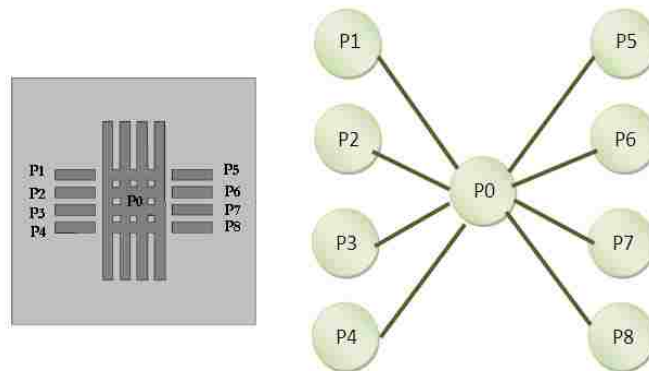


Fig. 6.4 Antenna structure in [48] and its graph model

Since the total number of possible configurations is larger than the required antenna configurations, redundancy exists. In order for the antenna to present only 5 configurations without compromising its originally required performance, 4 vertices are needed according to Eq.6.3.c as shown below:

$$NAC = 5$$

$$N = \left\lceil \frac{1 + \sqrt{1 + 8 \times (NAC - 1)}}{2} \right\rceil = \left\lceil \frac{1 + \sqrt{1 + 8 \times (5 - 1)}}{2} \right\rceil = 4$$

The graph model with 4 vertices is shown in Fig.6.5. It is composed of 3 vertices (P1, P2, P3) connected to a main vertex (P0). This graph model will be translated by reversing rule 1.a of section 4.4 into an antenna with 3 parts attached to a main part. This process doesn't preserve the structure symmetry. The optimization technique allows the removal of redundant parts as long as their removal does not affect the antenna characteristics such as symmetry. Therefore 4 total parts as represented by the 4 vertices is not a good solution for this antenna and in such a case, $N > 4$ is required. Taking $N=5$ leads to a minimum bound of $NAC = 11$ according to Eq. 6.3. a,b.

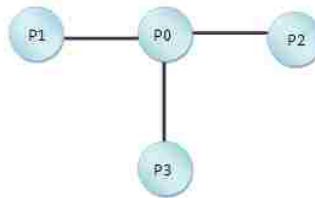


Fig. 6.5 Graph model with 4 vertices

$$NUP = \frac{N(N-1)}{2} = \frac{5(5-1)}{2} = 10$$

$$NAC = NUP + 1 = 11$$

The resulting antenna is shown in Fig.6.6 and is seen to preserve the symmetry of the structure. To verify the validity of our approach, the original and the optimized antennas were simulated using HFSS V11. *This approach matches the iterative optimization procedure of Section 5.2.* The new dimensions of the optimized antenna as well all the antenna's characteristics were discussed in Section 5.2.

The radiation patterns of the original and the optimized antennas were compared in Fig.6.7 while the switches are in the non- activated state (OFF). *The similarity between the patterns confirms that the removal of the redundant parts did not drastically affect the radiation characteristics.* The different S11 results for 4 different configurations with actual p-i-n diodes installed on the optimized antenna is shown in Fig.6.8.

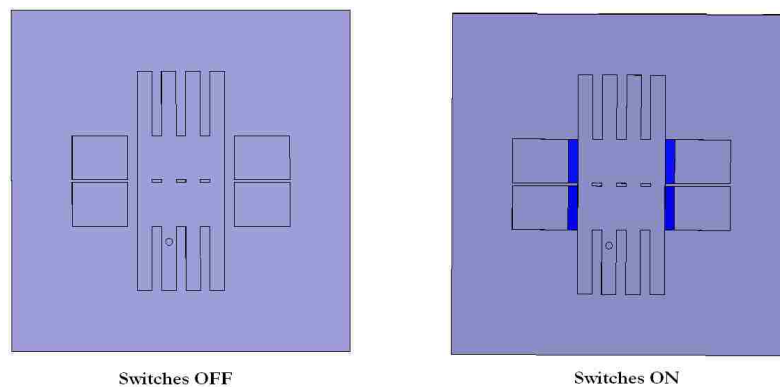


Fig. 6.6 The optimized antenna structure when the switches are all ON or all OFF

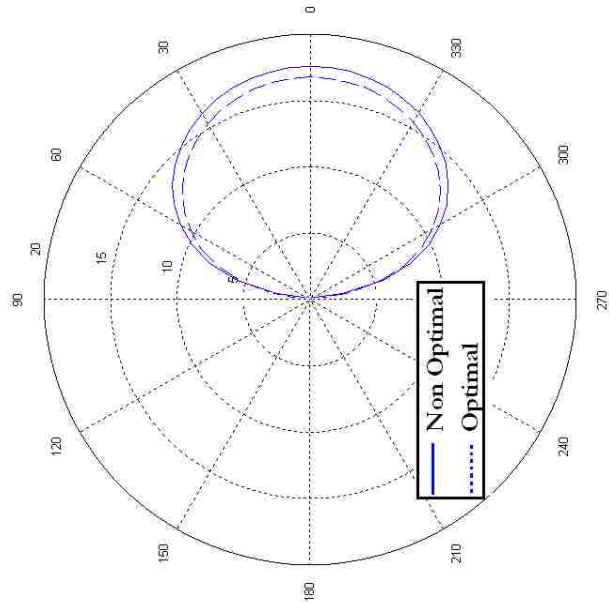


Fig. 6.7 The radiation pattern for the non optimal and the optimal antenna when the switches are open, thus proving that the removal of redundant parts did not disturb the antenna radiation characteristics

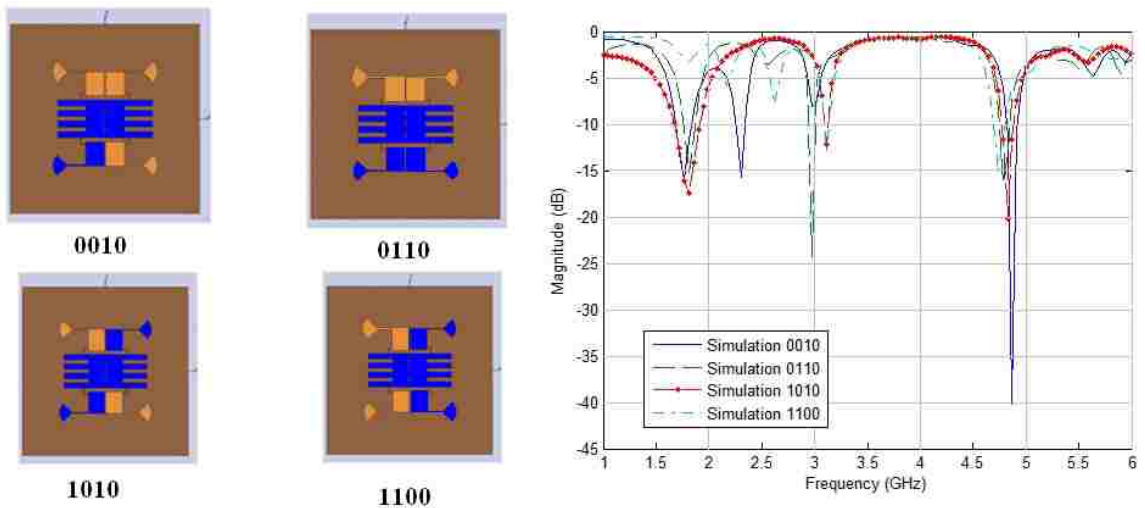


Fig. 6.8 Different S11 for 4 different configurations of the optimized antenna. The activated parts are shown in Blue on the left .

Example 6.3:

Here we consider the switch reconfigurable antenna shown in Fig. 6.9 [23, 47]. The structure of this antenna and its design procedure were discussed in Section 3.3. The graph model of this antenna is according to rule 1.a of Section 4.4.

This antenna is required to have in addition to its original frequencies of operation when all the switches are off 3 more configurations as follows:

Configuration 1: 1 GHz, 3.5 GHz, 4.5 GHz

Configuration 2: 2.35 GHz, 3.5 GHz, 4.5 GHz

Configuration 3: 1 GHz, 2.5 GHz, 5 GHz

These frequencies represent a lot of practical applications such as WIMAX, WIFI, and GPS. When all the switches are off this antenna resonates at 3 GHz, 3.5 GHz and 4.5 GHz.

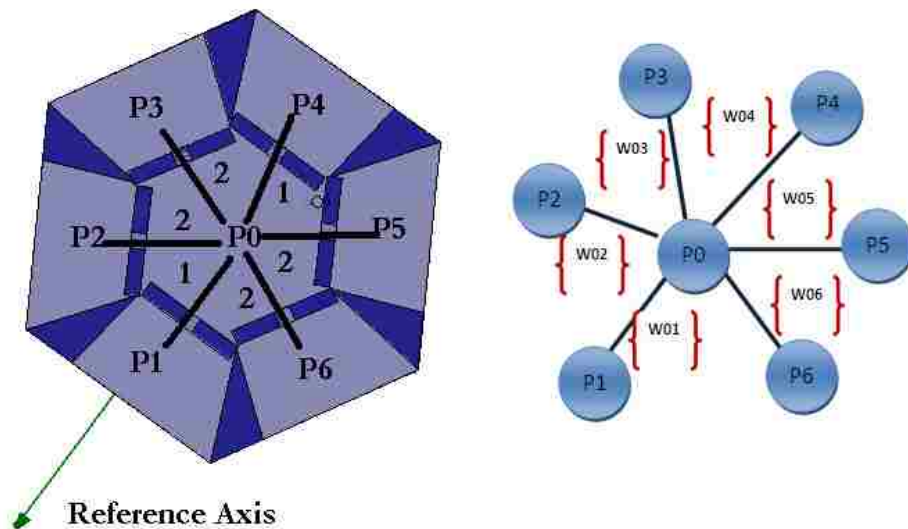


Fig. 6.9 Antenna in [23] and its graph model

The application of Eq.6.3 a,b to the graph model of this antenna shows that this antenna has a minimum bound of 22 configurations, while the required configurations are 4.

$$NUP = \frac{N(N-1)}{2} = \frac{7(7-1)}{2} = 21$$

$$NAC = NUP + 1 = 22$$

The application of Eq.6.3 c, reveals that at most 3 vertices are needed in the graph model to achieve these 4 configurations required.

$$NAC = 4$$

$$N = \left\lceil \frac{1 + \sqrt{1 + 8 \times (NAC - 1)}}{2} \right\rceil = \left\lceil \frac{1 + \sqrt{1 + 8 \times (4 - 1)}}{2} \right\rceil = 3$$

The number of switches used has to be reduced to 2 to remove redundant switches. The general shape of the antenna as a six armed hexagon can't be disturbed to preserve the radiation properties especially when all switches are OFF. The designer has to optimize by simulations the placement of the 2 switches to achieve the required frequencies and configurations. The placement of these switches as well as the graph model of the optimized antenna is shown in Fig. 6.9. The S11 plot of this antenna for all possible configurations is shown in Fig.6.10. Switches are spared and the radiation characteristics are preserved since the antenna's topology is not altered. The radiation pattern at 2.8 GHz in the E plane is shown in Fig. 6.11 when all switches are OFF.

Since this antenna has 6 parts added to a mid section, it has many possible configurations. In another scenario if this antenna was required to achieve 10 possible configurations, the number of required switches is then according to Eq. 6.3 c equals to 5:

$$NAC = 10$$

$$N = \left\lceil \frac{1 + \sqrt{1 + 8 \times (NAC - 1)}}{2} \right\rceil = \left\lceil \frac{1 + \sqrt{1 + 8 \times (10 - 1)}}{2} \right\rceil = 5$$

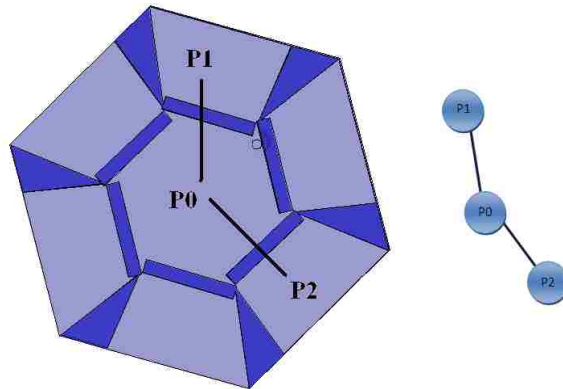


Fig. 6.10 The optimized structure with its graph model

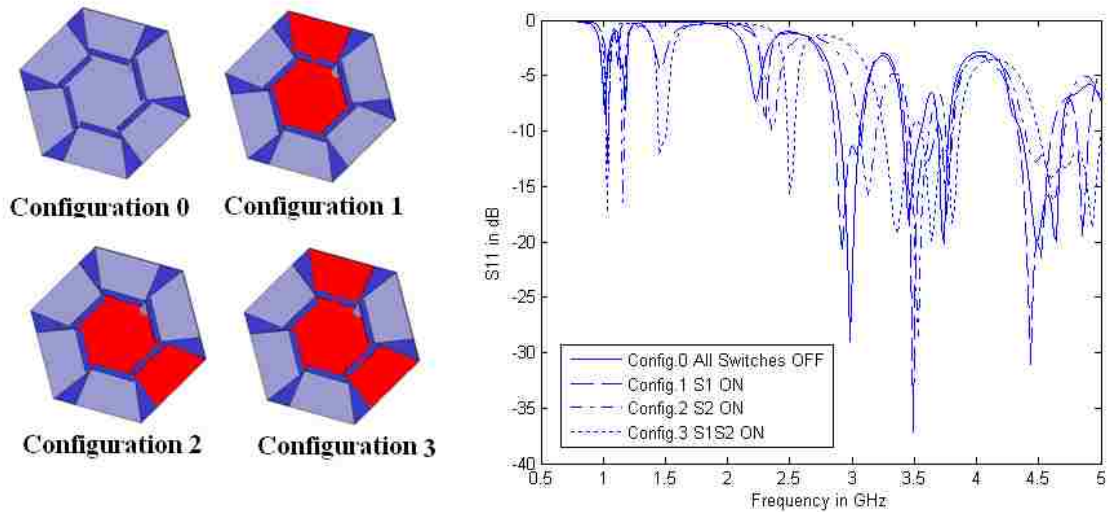


Fig. 6.11 The S11 plot for required configurations. The activated parts are shown in red on the left

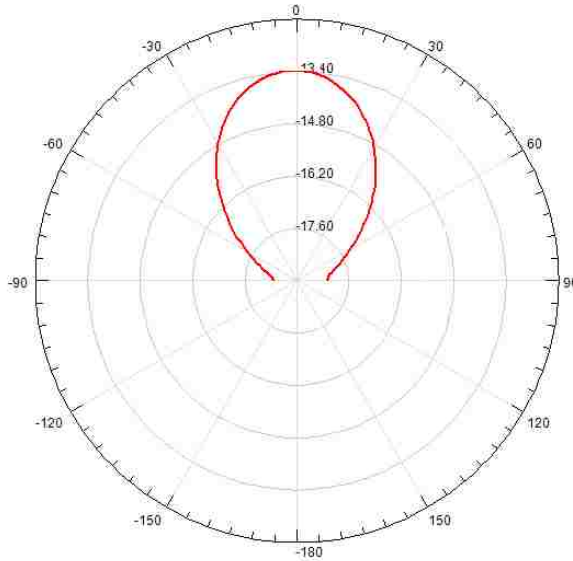


Fig. 6.12 The E-plane radiation pattern for the antenna at 2.8 GHz when all switches are
OFF

Example 6.4:

In this example the antenna [71] is a MEMS-reconfigurable pixel antenna which provides two functionalities: reconfiguration of its modes of radiation and reconfiguration of the operating frequency. The proposed antenna uses a 13×13 matrix of metallic pixels interconnected through MEMS switches in which circular patches of different radius are mapped.

Each metallic pixel has dimensions 1.2×1.2 mm and they are separated 2 mm from each other, to provide enough space to allocate the MEMS switches and interconnecting lines. The MEMS switches around each pixel are activated or deactivated depending on the DC voltage that is supplied to these pixels. The DC connectivity is done

through bias lines that connect the pixels to the back side of the substrate, as shown in Fig.6.12. In order to interconnect two metallic pixels, the voltage difference among them has to be around 30V. The metallic pixels and the bias lines are connected through RF (Radio Frequency) resistive lines made of Ni-Chrome alloy. These lines are able to stop the RF signals while allowing the DC signal to go through. The substrate used is a Quartz substrate of dimensions 2×2 in, and thickness of 1.575 mm with a dielectric constant of 3.78.

This antenna can generate five orthogonal radiation patterns at approximately any frequency between 6 and 7 GHz. These patterns are those generated by the modes $n=1$, $n=2$ and $n=0$, all of them with $\phi_0 = 0^\circ$, $n=1$ with $\phi_0 = 90^\circ$, and $n=2$ with $\phi_0 = 45^\circ$ [72]. At any fixed frequency between 6 and 7 GHz, five radiation states can be selected. This multimode functionality of this antenna is a useful feature for Reconfigurable MIMO (Multiple-Input Multiple-Output) systems using antenna diversity techniques [71]. The simulated θ and ϕ of the flattened 3-D far field pattern for the $n=1$, $n=1$ with $\phi_0 = 90^\circ$, $n=2$, $n=2$ with $\phi_0 = 45^\circ$ and $n=0$ modes are shown in Fig.6.13.

This antenna exhibits frequency tuning as well as pattern/ polarization diversity for fixed frequencies. Herein the pattern / polarization diversity characteristic is only taken into consideration for a fixed frequency. *The optimization approach introduced in Section 6.3 takes into consideration one reconfiguration function at a time.* The antenna structure is shown in Fig.6.14 with the different possible connections. Fig.6.15 shows the different

configurations required from the antenna to achieve the different radiation pattern characteristics shown in Fig.6.13. It is noted that the required configurations are only 5.

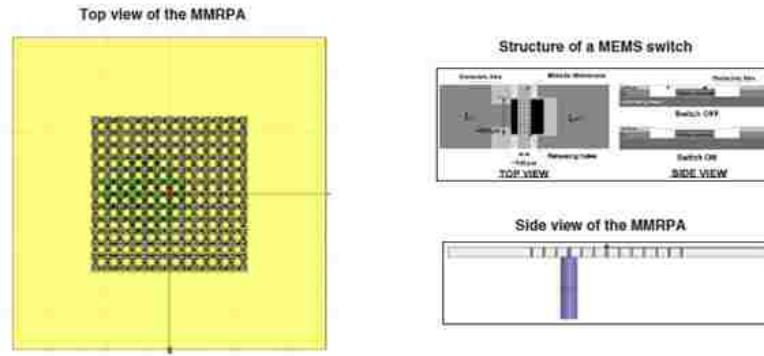


Fig. 6.13 Structure of the multifunctional MEMS-reconfigurable pixel antenna (antenna1)

[71]

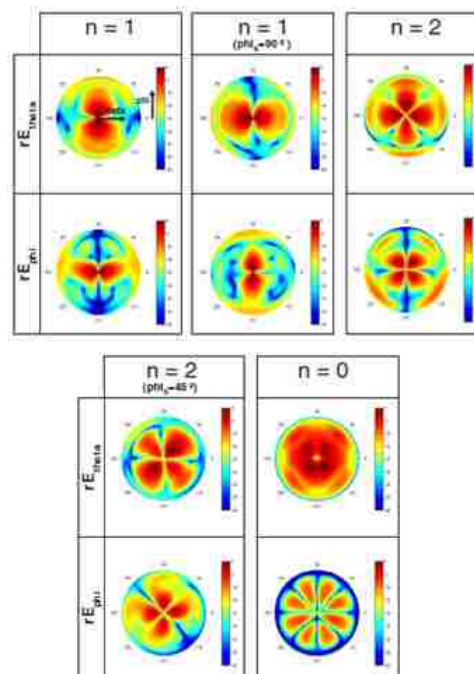


Fig. 6.14 Flattered 3-D radiation pattern with respective antenna configurations [71]

To graph model this antenna the different parts constituting its structure are considered as vertices. These vertices are connected by weighted undirected edges. The graph model of the different antenna configurations required is shown in Fig.6.15 and follows rule 1.a of Section 4.4.

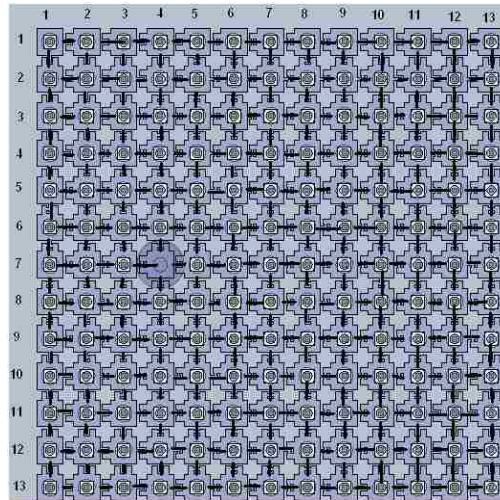


Fig. 6.15 The antenna structure with all possible connections

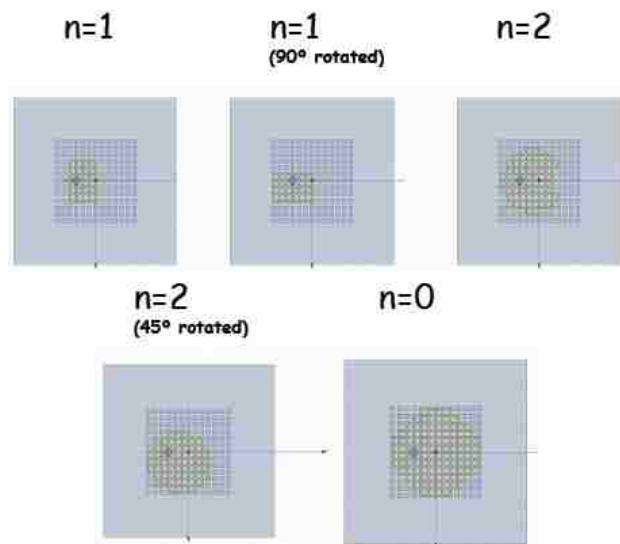


Fig. 6.16 Different configurations required from the antenna [71]

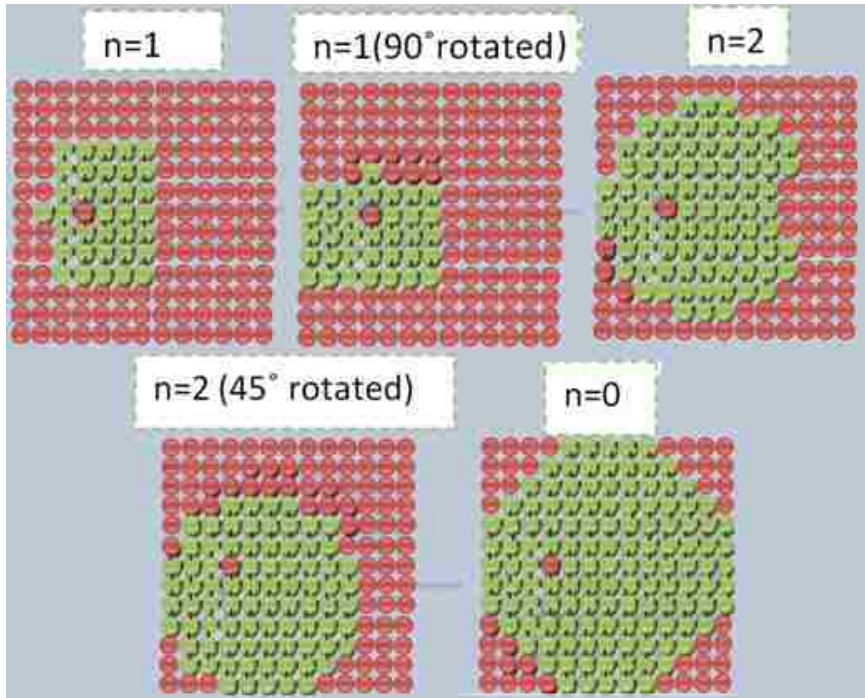


Fig. 6.17 The graph model of the antenna in [71] for all possible configurations

Since the number of required configurations is only 5 applying Eq. 6.3.c to this antenna will give us the number of parts required to achieve the desired configurations.

$$N = \left\lceil \frac{1 + \sqrt{1 + 8 \times (NAC - 1)}}{2} \right\rceil = \left\lceil \frac{1 + \sqrt{1 + 8 \times (5 - 1)}}{2} \right\rceil = 4$$

The number of configurations required to achieve 5 different antenna functions is only 4. The shape of the antenna with four parts will be very different from the one shown in Fig.6.14 and needs to be simulated and investigated extensively. The antenna designer in [71] required an optimization of the number of switches used while keeping the same topology of the antenna.

In order to preserve the same antenna topology, redundant connections have to be identified and redundant switches are eliminated afterwards. By comparing the different graph models of Fig. 6.16 one notices that edges connect only certain vertices and the rest of the vertices remain idle in all 5 configurations. To identify the different necessary sections of the antenna that achieve the desired behaviour, the adjacency matrix representation of the graph is used assuming the edges are not weighted. A part connected by an edge has a value 1 while a part that is not connected by any edge is represented by 0. The adjacency matrix representation for all possible configurations is shown in Table 6.1.

All connections	$\begin{bmatrix} 1 & 1 & 1 & 1 & 1 & 1 & 1 & 1 & 1 & 1 & 1 & 1 & 1 & 1 \\ 1 & 1 & 1 & 1 & 1 & 1 & 1 & 1 & 1 & 1 & 1 & 1 & 1 & 1 \\ 1 & 1 & 1 & 1 & 1 & 1 & 1 & 1 & 1 & 1 & 1 & 1 & 1 & 1 \\ 1 & 1 & 1 & 1 & 1 & 1 & 1 & 1 & 1 & 1 & 1 & 1 & 1 & 1 \\ 1 & 1 & 1 & 1 & 1 & 1 & 1 & 1 & 1 & 1 & 1 & 1 & 1 & 1 \\ 1 & 1 & 1 & 1 & 1 & 1 & 1 & 1 & 1 & 1 & 1 & 1 & 1 & 1 \\ 1 & 1 & 1 & 1 & 1 & 1 & 1 & 1 & 1 & 1 & 1 & 1 & 1 & 1 \\ 1 & 1 & 1 & 1 & 1 & 1 & 1 & 1 & 1 & 1 & 1 & 1 & 1 & 1 \\ 1 & 1 & 1 & 1 & 1 & 1 & 1 & 1 & 1 & 1 & 1 & 1 & 1 & 1 \\ 1 & 1 & 1 & 1 & 1 & 1 & 1 & 1 & 1 & 1 & 1 & 1 & 1 & 1 \\ 1 & 1 & 1 & 1 & 1 & 1 & 1 & 1 & 1 & 1 & 1 & 1 & 1 & 1 \\ 1 & 1 & 1 & 1 & 1 & 1 & 1 & 1 & 1 & 1 & 1 & 1 & 1 & 1 \\ 1 & 1 & 1 & 1 & 1 & 1 & 1 & 1 & 1 & 1 & 1 & 1 & 1 & 1 \\ 1 & 1 & 1 & 1 & 1 & 1 & 1 & 1 & 1 & 1 & 1 & 1 & 1 & 1 \end{bmatrix}$
Mode n=1	$A = \begin{bmatrix} 0 & 0 & 0 & 0 & 0 & 0 & 0 & 0 & 0 & 0 & 0 & 0 & 0 & 0 \\ 0 & 0 & 0 & 0 & 0 & 0 & 0 & 0 & 0 & 0 & 0 & 0 & 0 & 0 \\ 0 & 0 & 0 & 0 & 0 & 0 & 0 & 0 & 0 & 0 & 0 & 0 & 0 & 0 \\ 0 & 0 & 1 & 1 & 1 & 1 & 1 & 0 & 0 & 0 & 0 & 0 & 0 & 0 \\ 0 & 0 & 1 & 1 & 1 & 1 & 1 & 0 & 0 & 0 & 0 & 0 & 0 & 0 \\ 0 & 0 & 1 & 1 & 1 & 1 & 1 & 0 & 0 & 0 & 0 & 0 & 0 & 0 \\ 0 & 1 & 1 & 1 & 1 & 1 & 1 & 0 & 0 & 0 & 0 & 0 & 0 & 0 \\ 0 & 0 & 1 & 1 & 1 & 1 & 1 & 0 & 0 & 0 & 0 & 0 & 0 & 0 \\ 0 & 0 & 1 & 1 & 1 & 1 & 1 & 0 & 0 & 0 & 0 & 0 & 0 & 0 \\ 0 & 0 & 1 & 1 & 1 & 1 & 1 & 0 & 0 & 0 & 0 & 0 & 0 & 0 \\ 0 & 0 & 0 & 0 & 0 & 0 & 0 & 0 & 0 & 0 & 0 & 0 & 0 & 0 \\ 0 & 0 & 0 & 0 & 0 & 0 & 0 & 0 & 0 & 0 & 0 & 0 & 0 & 0 \\ 0 & 0 & 0 & 0 & 0 & 0 & 0 & 0 & 0 & 0 & 0 & 0 & 0 & 0 \end{bmatrix}$

constantly which eliminates the need for switches. Switches will only be used to connect the sections together. *Parts belonging to the same sections are always connected together and there is no need for switches inside each section.* Some antenna parts are never connected to achieve polarization diversity and they are shown in black in Fig. 6.17. *Using this technique the number of switches will be reduced considerably by more than 100 switches.* This technique preserved the antenna topology while reducing the number of switches used. A comparison of the S11 parameter between the original antenna and the antenna with reduced number of switches is shown in Fig. 6.19 for the mode $n=0$ proving that the technique did not disturb the antenna radiation characteristics. The radiation pattern at 5.83 GHz for $\phi=0^\circ$ and $\phi=90^\circ$ is shown in Fig. 6.20.

Example 6. 5:

This antenna shown in Fig. 6.17 was re-designed and optimized iteratively in Section 5.3. Herein the iterative optimization result is verified through Eq.6.4.

The antenna is required to have 3 configurations for each monopole length resulting in a total of 6 configurations. The graph model of the antenna follows rule 1.a of section 4.4 and is shown in Fig.6.17 for all possible connections. Applying Eq.6.4 to the antenna reveals that:

$$NUP = \frac{N(N-1)}{2} = \frac{6(6-1)}{2} = 15$$

$$NAC = NUP + 1 = 16$$

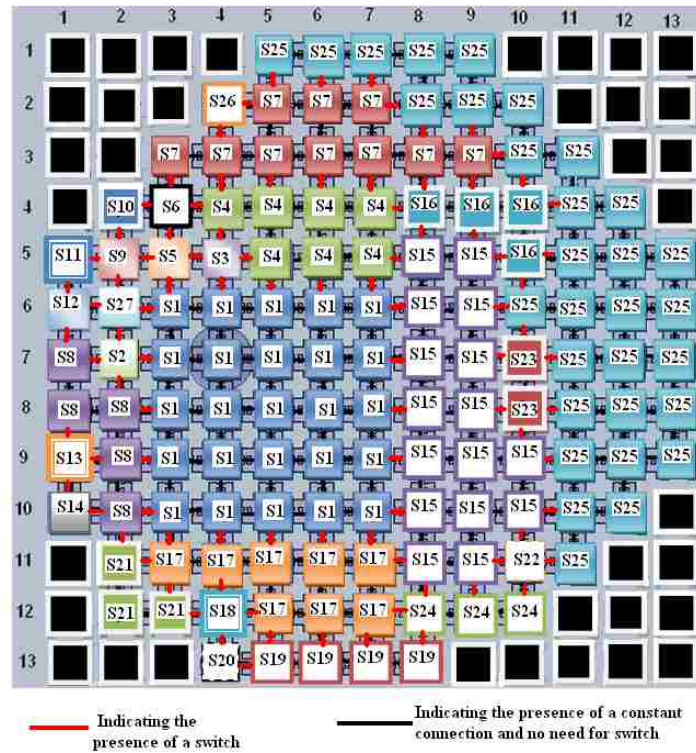


Fig. 6.18 Different antenna sections in different colors . The black parts represent the idle parts (parts never connected to achieve polarization diversity)

It is clear that this antenna exhibits redundancy since $16 > 6$ configurations. To optimize this antenna, Eq. 6.4.c is applied as follows:

$$NAC = 6$$

$$N = \left\lceil \frac{1 + \sqrt{1 + 8 \times (NAC - 1)}}{2} \right\rceil = \left\lceil \frac{1 + \sqrt{1 + 8 \times (6 - 1)}}{2} \right\rceil = 4$$

The optimized antenna structure has 4 parts instead of 6 and two switches are

eliminated. The optimized antenna resembles the original one in Fig. 5.15, except that it has only 4 total parts instead of 6. *The results herein verify the results obtained in Example 5.1 of section 5.3.* The graph model of the optimized structure is shown in Fig. 6.18.

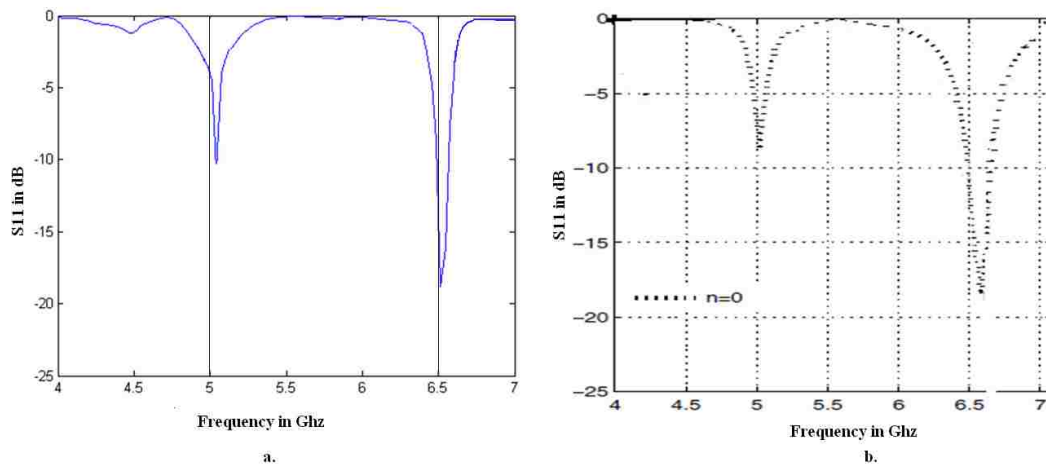


Fig. 6.19 A comparison of the S11 parameter between the original antenna and the antenna with reduced number of switches for the mode $n=0$ a. Reduced number of

switches b. Original antenna

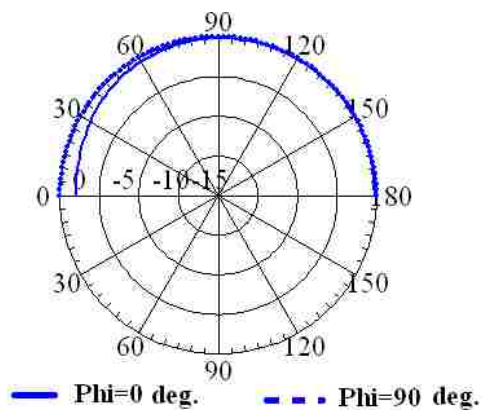


Fig. 6.20 The Antenna radiation pattern at 5.83 GHz for $\phi=0$ deg. and 90 deg.

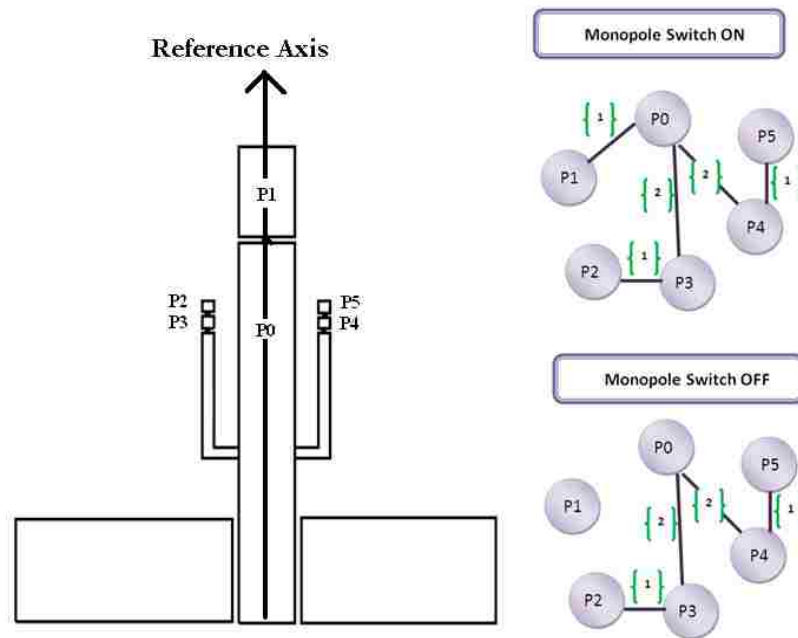


Fig. 6.21 Structure and graph model of the antenna in [20]

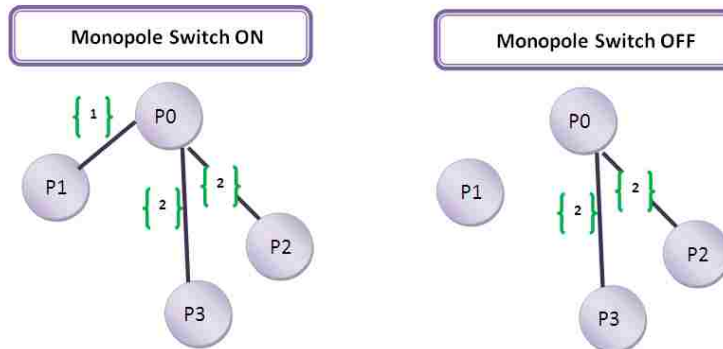


Fig. 6.22 Optimized antenna graph model for all switches ON

Example 6.6:

The antenna shown in Fig.6.19 [5], was discussed in Example 5.2 of Section 5.3.

This antenna was re-designed and optimized iteratively in section 5.3. Herein the

iterative optimization result is verified through Eq.6.3. The graph modeling of this antenna following rule 1.b of section 4.4, is shown in Fig. 6.19.

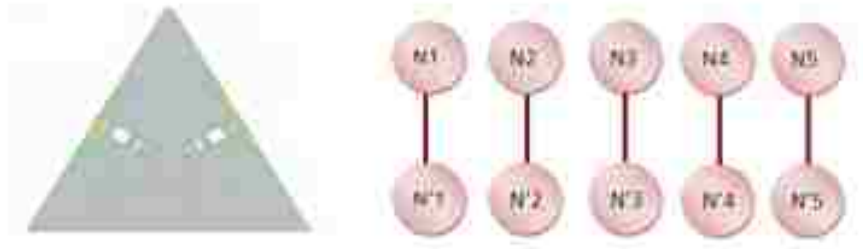


Fig. 6.23 Antenna structure in [5] and graph model for all possible connections

Applying Eq. 6.3 to the graph model of the antenna shown in Fig. 6.19 gives us 11 possible antenna configurations.

$$NAC = \frac{N}{2} + 1 = \frac{20}{2} + 1 = 11$$

The number of configurations required in [5] is only 5 so by applying Eq. 6.3.b we end up with 8 vertices.

$$NAC = 5$$

$$N = 2 \times (NAC - 1) = 2 \times (5 - 1) = 8$$

These 8 vertices represent the 8 end points of 4 switches according to rule 1.b of section 4.4. *The optimal design includes 4 switches. The results herein verify the results*

in Example 5.2. The graph model of the optimal antenna is shown in Fig.6.20. Each vertex in this design represents an end point of a switch in the antenna structure.



Fig. 6.24 Graph of the optimized antenna topology for all possible connections

6.4 A Chart Representation of The Optimization Approach

The optimization approach shown in section 6.2 can be represented graphically in the chart of Fig.6.22.

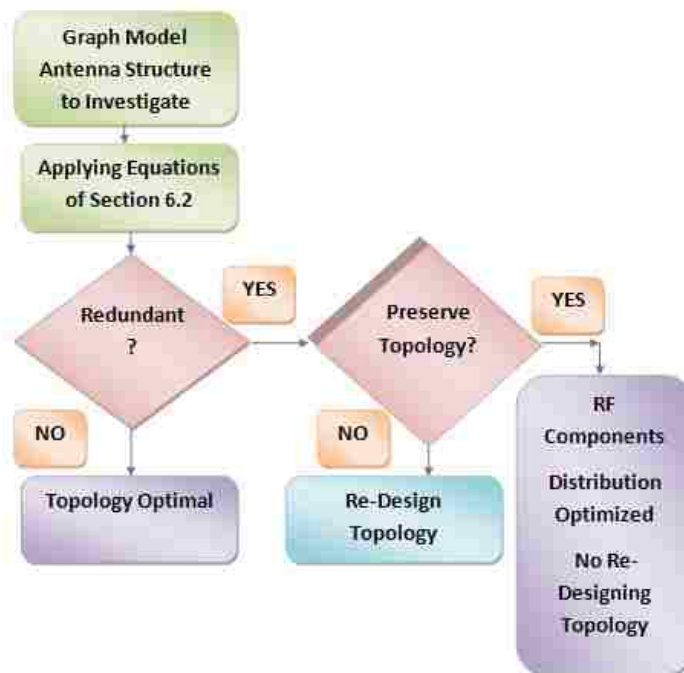


Fig. 6.25A chart representing the optimization approach

6.5 A Comparison Between the Optimization Approach of Section 6.2 and The Iterative Approach of Section 5.2 :

The approach in Section 6.2 is based on Eq. 6.3, 6.4 and 6.5 that are derived based on the guidelines of Section 4.4. These equations minimize redundancies in reconfigurable antenna parts, by specifying the number of needed elements. All these equations are subject to the radiation characteristics constraints of the antennas they are optimizing.

The approach in Section 5.2 is an iterative approach based on removing parts from the antenna and simulating the structure after altering the dimensions. The new structure is required to maintain the desired reconfigurable functionality as the redundant antenna. This process is repeated until the functionality is lost and then the last valid configuration is considered optimal since it is the last one preserving the functionality.

In Section 6.3 examples are presented to apply the approach of Section 6.2. A comparison between example 6.2 and the example in Section 5.2 reveals a complete analogy between the results, structure and topology. That proves that this antenna is optimized.

The results obtained in example 6.5 and 6.6 verify the results obtained in examples 5.1 and 5.2 respectively of Section 5.3. *These verifications prove the optimization effect of the approach in Section 6.2.*

This approach presented here is easy to grasp with less computational

requirements. The efficiency and validity of such approach is proven and it is comparable to the iterative approach presented in Chapter 5. *These two approaches can't be compared to any other optimization technique since they are the first methods to address redundancies in reconfigurable antenna systems.*

6.6 A Comparison Between The Application of Graph Models and Neural Networks On Reconfigurable Antennas:

Neural Networks (NN) are applied because closed-form solutions do not exist. It is also beneficial to apply NN when enough measured data can be obtained to train them. In the case of reconfigurable antennas, a prototype has to be fabricated and measured. A training database is then established. This database is used to train a NN, and then this NN is used for faster antenna synthesis.

For example applying Neural Networks to the antenna in [7-10], results in the association of different antenna configurations with different frequency responses called clusters. Fig.6.21 shows a schematic of this antenna with the different switches. An example of an antenna cluster is shown in Fig. 6.22.

One can also associate the current paths in an antenna system using the training database of a NN with the different clusters. The different current paths representations for different clusters are shown in Fig. 6.23.

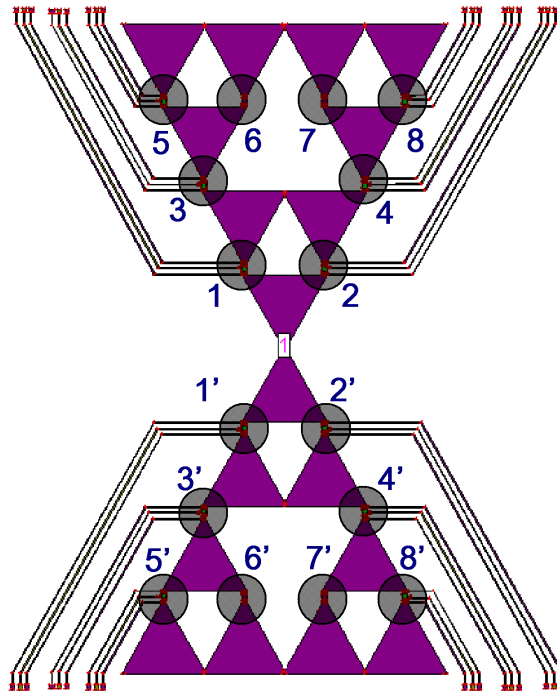


Fig. 6.26 A schematic representation of the antenna in [7-10] with different switches

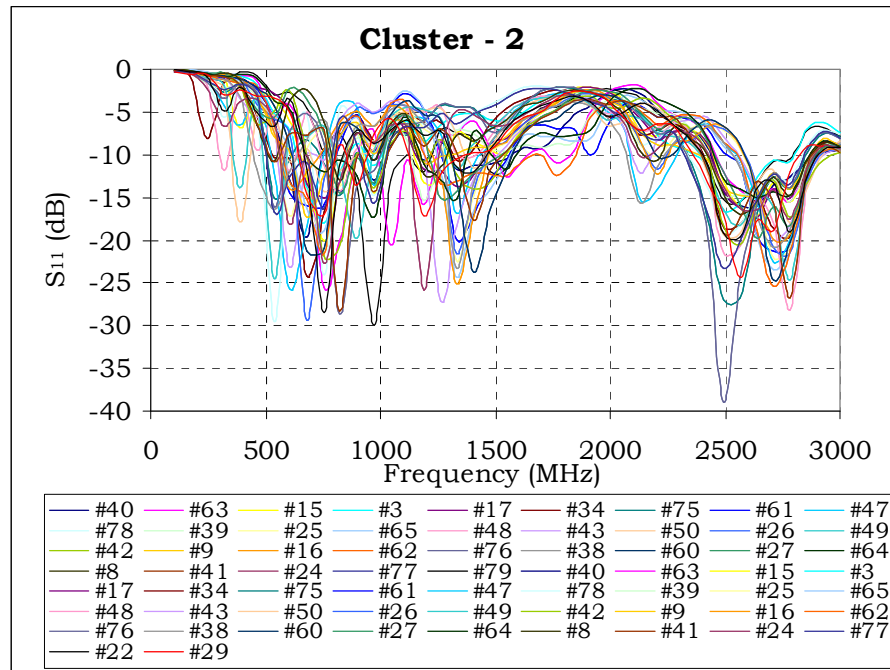


Fig. 6.27 Antenna's frequency response's cluster 2

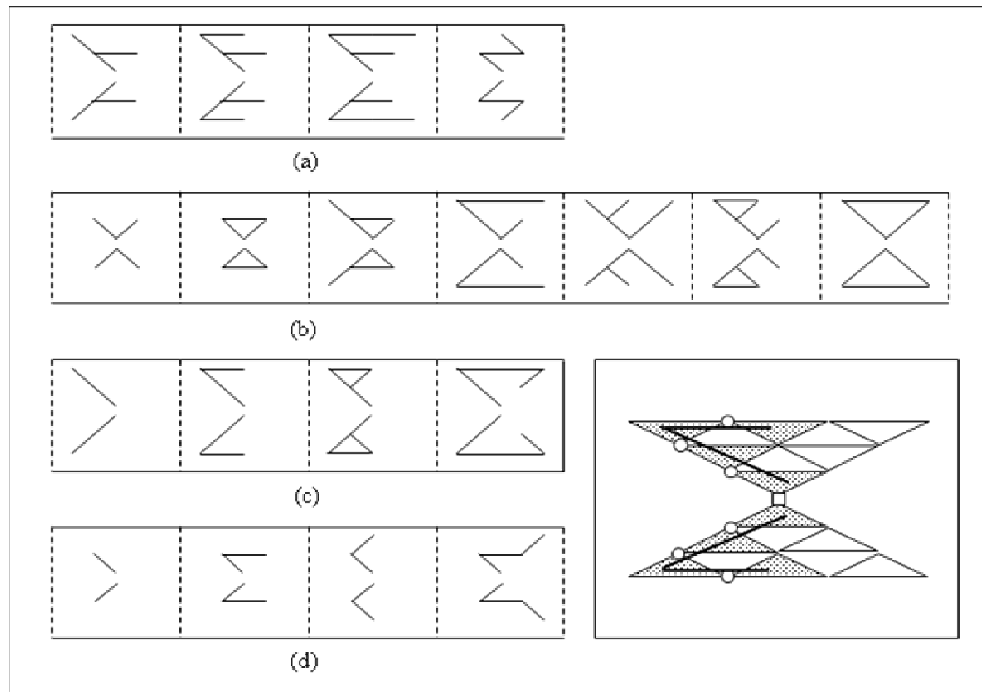


Fig. 6.28 Antenna's different cluster representations (current paths representations)

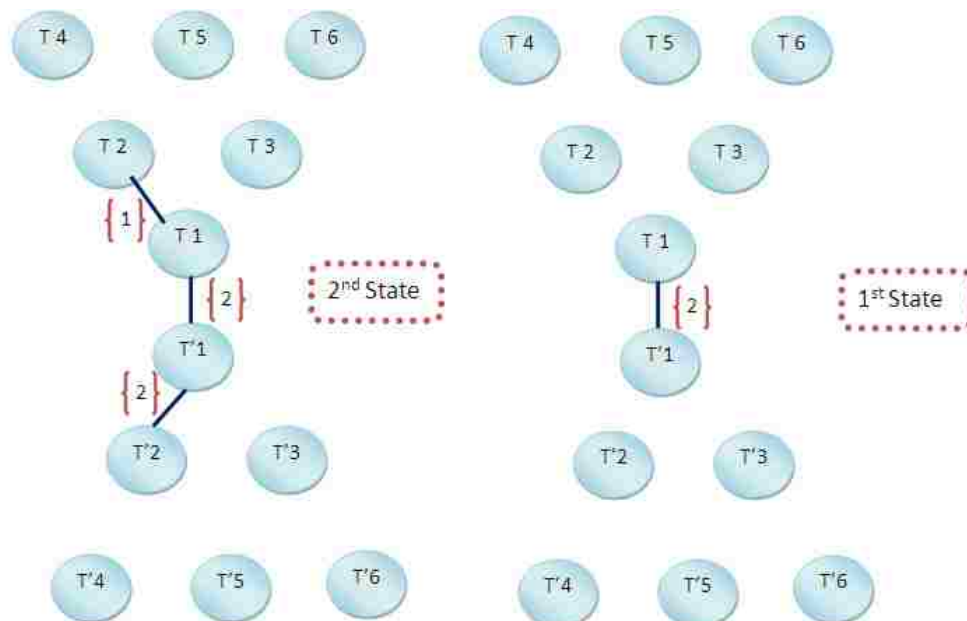
By comparing the current paths representation of Fig.6.23 to the graph model representation of Fig.6.24, similarity is noticed. However in the graph model approach the representation is a starting point of the analysis while in NN the representation is the end of the analysis. Based on these graph models the reconfigurability function is optimized and redundant elements are removed. For example for the antenna in [7-10], a lot of configurations are found equivalent which adds to the robustness of the antenna. Based on Eq. 6.3 this antenna can at least have 67 possible configurations, which is very close to the NN analysis that proposed a minimum of 70 possible configurations

$$NUP = \frac{N(N-1)}{2} = \frac{12 \times 11}{2} = 66$$

$$NAC = NUP + 1 = 67$$

If the number of configurations required from this antenna is less than 67 in any application, then switches may be removed to reduce the number of unused configurations. *This antenna presents a very robust design with many possibilities.* A lot of applications can benefit from this topology, however if the number of applications required is limited, this antenna may be reduced and some switches may be spared.

The difference between the NN approach and the graph models approach is that NN facilitates the synthesis of an antenna while graph models can use this synthesis to optimize its structure and reduce redundancies.



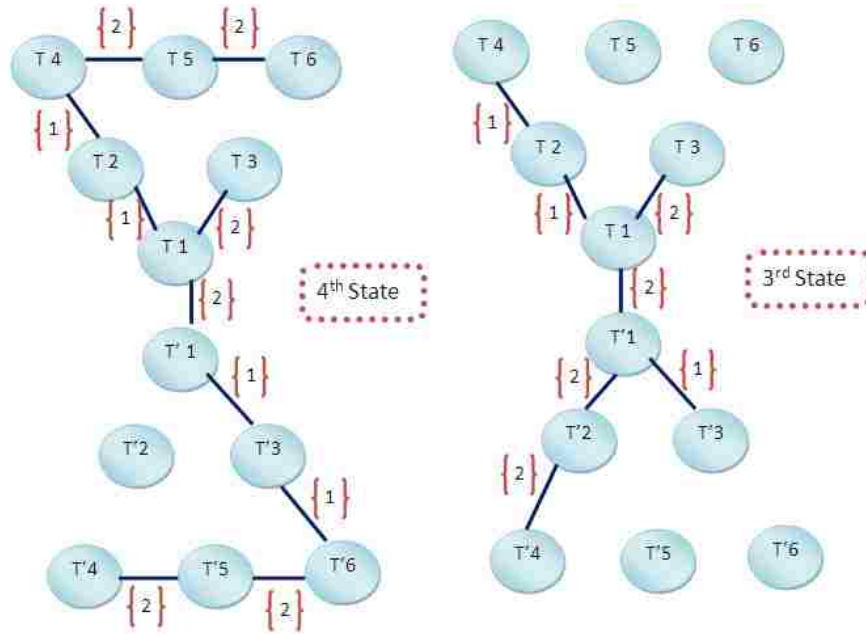


Fig. 6.29 Graph model for the antenna in [7-10]

6.6

Discussion:

In this chapter a handy optimization method based on graph models is presented. This technique optimizes reconfigurable antennas in the sense of removing redundant parts. It minimizes the structure complexity of a reconfigurable antenna leading to cost and losses reduction. The optimization and the complexity minimization facilitate control and the development of the associated programming process for reconfigurable antennas.

In the next chapter the optimization approach and graph models are utilized to address the reliability and complexity issues of reconfigurable antennas. The existing correlation between the reliability and complexity parameters of an antenna structure is investigated. The reconfigurable antenna system uncertainties as well as the probability of error are discussed.

CHAPTER 7

RECONFIGURABLE ANTENNAS UNCERTAINTIES, RELIABILITY AND COMPLEXITY ANALYSIS

7.1 Introduction:

The increased involvement of RF components in the reconfiguration of antenna structures has increased the complexity of antenna systems and left designers trying to reach a compromise between enhanced performance and increased system complexity. The optimization technique presented in Chapter 6 maintained performance while reducing the general complexity.

The probability of failure for any RF component that may be incorporated on an antenna has been reduced due to the technological advancement of the last decade. Also these components have an indefinite normal functioning under standard circumstances.

Standard circumstances are pre-defined by the factory where temperature, humidity and other environmental factors are taken into consideration. Companies clearly specify that if the designer wishes to implement their RF components such as switches under some abnormal conditions, they will provide the probability of failure of their products under these unusual conditions. However reconfigurable antennas with all the incorporated RF components may be installed in unknown environments such as on satellites, airplanes where easy access to such antennas is not available.

The changes in the antenna surroundings may not be predictable most of the time and preserving the antenna's continuous operation is of great importance, which raises the question of the reliability of the whole antenna system and not the electronic components themselves. Regardless of the components' probability of failure, overcoming any error in the reconfigurable antenna is important to the whole system.

Redundancy in a system was used to increase its reliability of that system [73-74]. However, by optimizing the structure of a reconfigurable antenna we have reduced redundancies and removed unnecessary switches. The study of the reliability of our optimized systems becomes important since redundancy was reduced and in some cases eliminated.

In this chapter the issue of reconfigurable antenna uncertainties and the effect of the optimization approach on their reliability are addressed. Solutions are proposed to increase the robustness of reconfigurable antennas as well as an algorithm for assuring the reliability of a reconfigurable antenna system is presented. The general complexity and the correlation between the reliability and complexity of a reconfigurable antenna is also addressed.

7.2 Review of Reliable Circuits Using Less Reliable Relays [73]:

In [73] it is assumed that the components have good reliability and that their probability of error is less than $1/6$, the amount of redundancy required in circuits for a given improvement in reliability is around 67 to 1 [73]. The circuits described in [73] have

a probability of error that approaches 0. The probability of failure remains constant as time passes and the relays are considered not to wear out with age [73].

The first kind of failure allowed in [73] is the failure of a relay contact to close, which in actual relays is often the case due to a particle of dust preventing electrical closure. The second type of failure is the failure of a contact to open, which in actual relays is usually due to the welding action of the current passing through the contacts.

If the relay is energized the contact is closed with probability a , open with probability $1-a$. If the relay is not energized the contact is closed with probability c and open with probability $1-c$. If $a > c$ the contact is called a make contact, if $a < c$ the contact is called a break contact. *Different contacts are assumed to be statistically independent.* A relay of this type governed by probabilities a and c are called *crummy relays* in [73]. Their probability operation is represented in Fig.7.1. The representation is similar to the representation of the noisy binary channel with capacity=0 if and only if $a=c$.

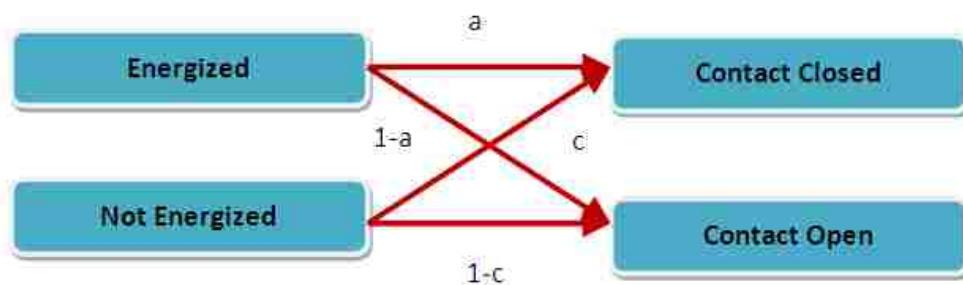


Fig. 7.1 Schematic representation of the transition probabilities

In a general way the analysis given in [73] depends on constructing networks of

contacts which act like a single contact, but with greater reliability than the contacts of which they are composed.

7.3 Review of Switches Used On Reconfigurable Antennas:

RF MEMS in [1] are not restricted for antenna applications instead these types of switches can be used for any reconfigurable integrated circuit. These RF MEMS as described in [1] enable new systems capabilities. The electrostatic microswitch, with superior performance characteristics is also addressed and 2 application possibilities are proposed – The quasi-optical beam steering and the electrically reconfigurable antennas [1].

In [75] RF MEMS capacitive switches are constructed on microwave-laminate printed circuit boards. The technology proposed promises the potential of further monolithic integration with antennas on the same PCBs to form reconfigurable antennas without the concerns of mismatching among components [75].

The typical RF MEMS topology used in most designs can be limiting for highly dynamic applications [10]. Such applications require great deal of reconfigurability. Three sets of RF MEMS with different actuation voltages are used to sequentially activate and deactivate parts of a Sierpinski fractal antenna [10]. The implementation of such a concept allows for direct actuation of the electrostatic MEMS switches through the RF single feed, without the need for individual dc bias lines. The antenna is fabricated on liquid crystal

polymer substrate and constitutes the first integrated RF MEMS reconfigurable antenna on a flexible organic polymer substrate.

Air-bridged RF-MEMS in single pole single through transmission (SPST) are proposed in [76] for antenna applications. In [77] tunable RF MEMS are proposed for the development of reconfigurable antennas fabricated on sapphire substrate with a barium strontium Titanate dielectric.

The problem of integrating commercially packaged RF MEMS into a radiation pattern reconfigurable antenna arose in [31] where not only the simple open /closed behavior of the switches has to be addressed but also their impact on the radiation characteristics.

Also In [78] the reliability of RF MEMS is addressed due to the effect of carbon contamination. The deployment of RF MEMS devices into many commercial and military applications is concluded to be limited by poor reliability [78]. Understanding the function degradation of RF MEMS is still an ongoing study and certainly not an easy one as explained in [78].

7.4 Reconfigurable Antennas Switches Uncertainties:

The complete reliability of a system using RF components is not a realistic goal. A designer can't predict all the conditions that may or may not occur in the environment where components such as switches are placed, also these switches may wear out with age.

Most publications in this area do not reflect the reliability issue of systems relying on switches and few designers investigate the effect of some elements in the environment on the good operation of the system as in [78].

In a switch-reconfigured antenna, the malfunction of a switch affects the performance of the system drastically. However the probability of error of these switches is almost 0 under nominal conditions. For example let's take the p-i-n diode AN-712, the application notes for such a p-i-n diode can be found in Appendix A. This diode is governed by Eq.7.1

$$T_{rr} = T_L \log\left(1 + \frac{I_F}{I_R}\right) \quad (7.1)$$

Where T_{rr} is the switching speed, T_L is the minority carrier lifetime, I_F is the forward current and I_R is the reverse current.

If for any reason I_R goes to 0 then the switching speed will go to infinity and switching will never occur. If the temperature goes beyond 150 ° then also the p-i-n diode becomes defective. The question is not however about the possibility of failure of these devices; instead it is about the probability of failure of these devices.

If switches are to be used to reconfigure an antenna, the environment in which this antenna is installed must be studied by the switch designer beforehand. If the system's environmental conditions exceed the normal conditions that govern the commercial switches, new types of switches have to be designed based on the specific conditions under which their system exists.

Nevertheless no matter how small the probability of failure of a switch is, this probability exists. Suppose we have a switch S properly biased. The biasing techniques are supposed to be working at all time and suitable for the good functioning of the particular switch. There exist two types of switch failures as previously discussed in section 7.2. The first kind of failure is the failure of a switch contact to close. The second type of failure is the failure of a contact to open. The reasons behind these failures are left undefined since we have different types of switching devices. The switch closes with a probability a and opens with a probability $1-a$. The representation is shown in Fig. 7.2.

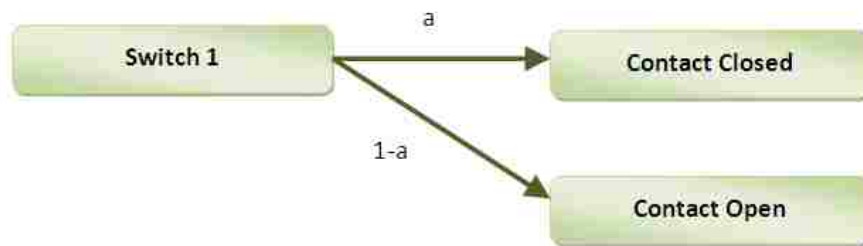


Fig. 7.2 Schematic representation of the transition probabilities

Firstly, Assuming that the switch does not deteriorate with age and that the probability of closing the switch is always a and opening it is always $1-a$. Then events are discrete and the uncertainty of this function achieving its required purpose is defined from [79] by:

$$H(X) = -\sum_{x \in X} p(x) \log(p(x)) \Rightarrow H(S1) = -a \log a - (1-a) \log(1-a) \quad (7.2)$$

Secondly, assuming that the switch is deteriorating with time following a slowly decreasing exponential function $\lambda e^{-\lambda x}$, $x > 0$, $\lambda = \text{constant}$. The exponential function is just an example to prove the concept. The uncertainty regarding the switch function $h(S)$ will now be defined [79] as:

$$h(X) = h(f) = - \int_S f(x) \log(f(x)) dx \Rightarrow h(S1) \approx \log \frac{e}{\lambda} \text{ bits} \quad (7.3)$$

In Eq. 7.2 and 7.3 only one existing switch is taken into consideration. However, for N switches as shown in Fig. 7.3, the uncertainty about each switch individually is the same however the uncertainty that the whole system is failing is the sum of all the respective uncertainties if this failure is only due to defected switches.

$$H(\text{System}) = \sum_{i=1}^N H(S_i) \quad (7.4)$$

Where N is the total number of switches. This equation is valid for the discrete and continuous case of S . $H(S_i)$ was defined in Eq. 7.2 for the discrete case with probability $(a, 1-a)$ and Eq.7.3 for the continuous case.

7.5 The Effect of The Optimization Approach On The Reconfigurable Antennas'

Reliability:

The optimization technique removes redundant switches and so according to Eq.7.4 decreases the uncertainty of the reconfigurable antenna system.

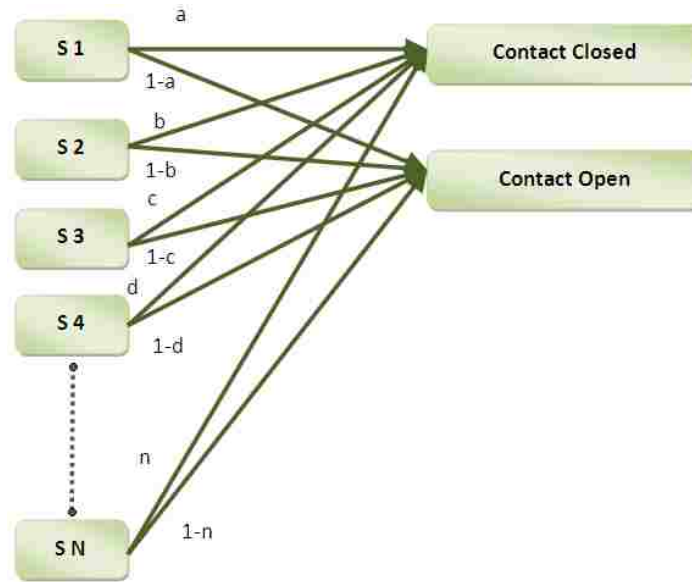


Fig. 7.3 Schematic representation of the transitional probabilities for multiple switches

7.5.1 Reconfigurable Antenna Equivalent Configurations:

In a switch-reconfigured antenna, many switching configurations might yield the same antenna frequency behavior without affecting the other antenna radiation properties. Equivalent configurations can't be predicted and they are deduced from simulations. These equivalent configurations constitute back up configurations to achieve the same antenna performance at a certain frequency.

Example 7.1:

The antenna shown in Fig.7.4 [23] resonates at 5 GHz for 8 different configurations. The 8 different configurations are shown in Table 7.1 and a comparative S11 plot is shown in Fig. 7.5. These configurations are not equivalent at other frequencies.

7.5.2 The Effect of The Optimization Technique On The Equivalent

Configurations:

Reducing the number of switches decreases the number of equivalent antenna configurations at different frequencies but it also removes some undesired configurations. It is a compromise between number of equivalent configurations and additional configurations. The reliability is not largely affected. The cost a designer pays in terms of reliability is tolerable as we show in Example 7.2 as opposed to the price he/she pays if the optimization technique is not applied.

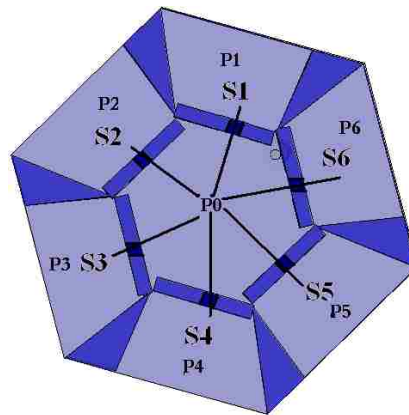
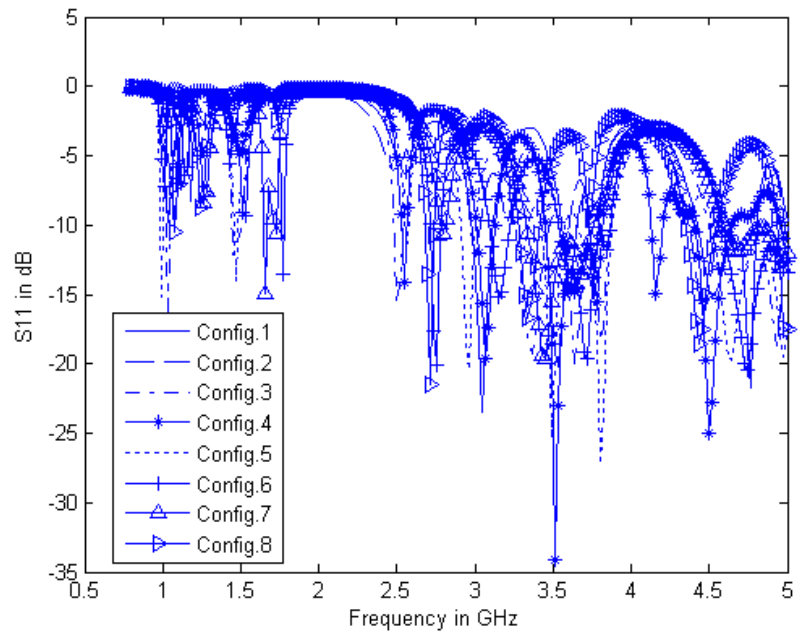


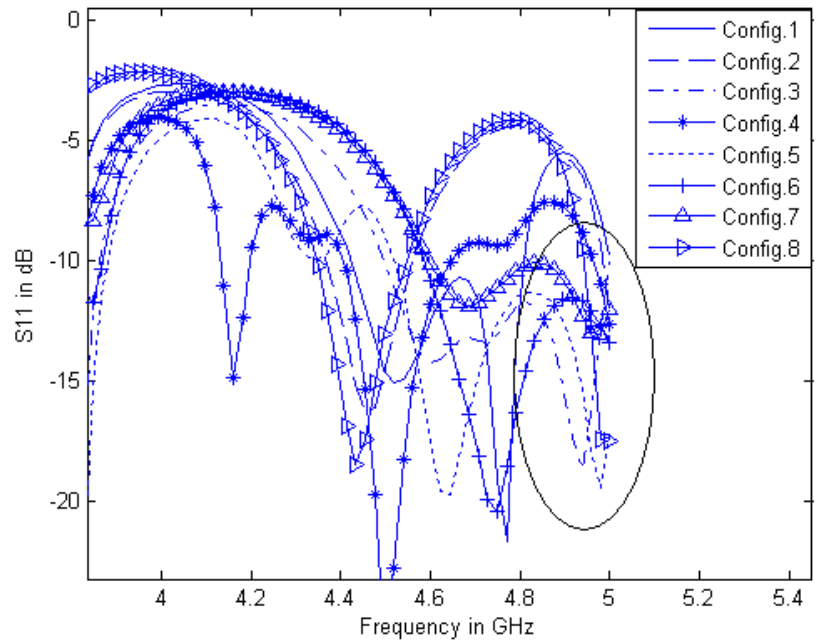
Fig. 7.4 Antenna structure in [23]

Example 7.2:

Here an antenna that was previously optimized in chapters 5 and 6 is studied. The optimized antenna is shown in Fig.7.6. The different antenna configurations for different antenna resonances are shown in Table 7.2.



a.



b.

Fig. 7.5 S_{11} plot for the antenna in [23] for the different configurations in Table

7.1 a. Zoomed Out. b. Zoomed In at 5 GHz

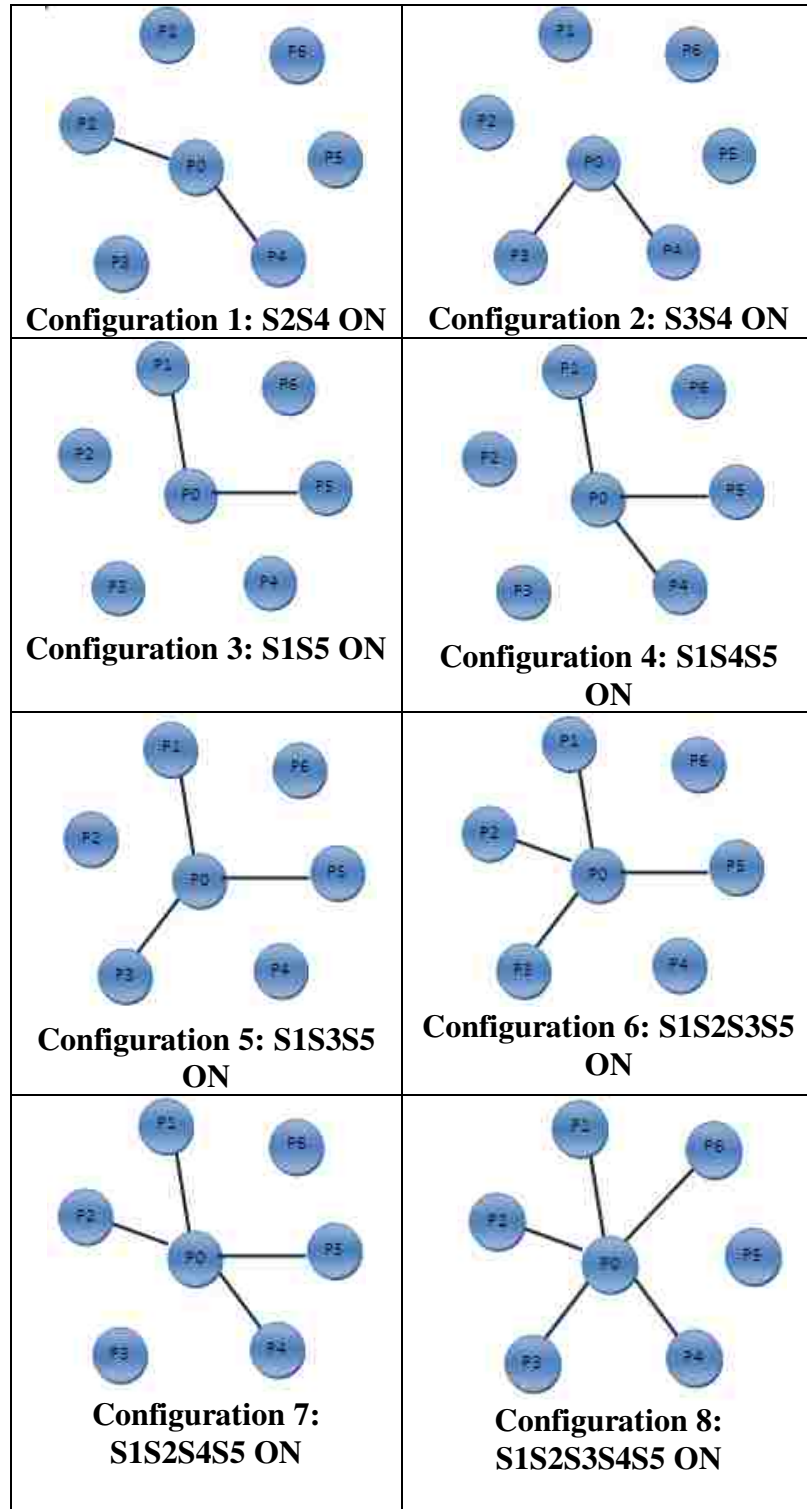


Table 7.1 The different configurations of the antenna in [23] leading to operation at 5 GHz



Fig. 7.6 The optimized antenna

F= 1.7							
F= 1.8							
F= 1.9							
F= 2.05							
F= 2.325							
F= 2.35							
F= 2.425							
F= 2.6							
F= 2.825							
F= 2.875							
F= 2.9							
F= 3.05							
F= 3.1							
F= 3.2							
F= 5.15							

F= 5.2								
F= 5.275								
F= 5.3								

Table 7.2 Different antenna configurations for different resonances (All frequencies are in GHz)

It is shown in Table 7.2 that this antenna even after optimization shows a lot of equivalent configurations for different frequencies. Even though the optimization technique reduced the number of switches it didn't add to the non reliability of the system at certain frequencies. It is also important to point out that certain frequencies are only achievable by one configuration only.

7.5.3 How To Increase The Robustness of A Reconfigurable Antenna:

Some helpful methods are proposed here to avoid any negative effect the optimization technique has on the reliability of a reconfigurable antenna system.

Method 1: The no switch configuration

The first method advises the designer before hand to prioritize the frequencies needed. The frequency with the highest priority should have more than one equivalent configuration. If we look at Table 7.2 we can deduce that the frequency with the biggest number of equivalent configurations is $f=5.2$ GHz. It

has 7 equivalent configurations including the no switch configuration or “all switches off” configurations. A good designing method would be to design the antenna with all switches off to operate at the most important frequency or frequencies. In that case, and under the worst possible scenario of all switches breaking down at the same time the most important frequency will always be achievable.

Method 2: The back-up switch

In addition to method 1, if a certain frequency is needed at all times and the design doesn't include enough back-up configurations. This method proposes the installation of a back-up switch. The back-up switch can be installed at any point in the antenna system as long as its presence achieves the desired frequency.

Example 7.3:

Taking the optimized antenna in Fig. 7.6, this antenna operates at 2.05 GHz for only one configuration (S1 ON only) as shown in Table 7.2. Installing a back-up switch as shown in Fig.7.7 and activating Switches (S2 and S3) will constitute a back up configuration as shown in Fig. 7.7. The graph model of such system is represented in Fig.7.8 where P0 is replaced by P'0 and new vertices are added to account for the presence of such a switch. The placement of the switch depends entirely on the designer and is not relevant in any way as long as the presence of that switch achieves the desired function.

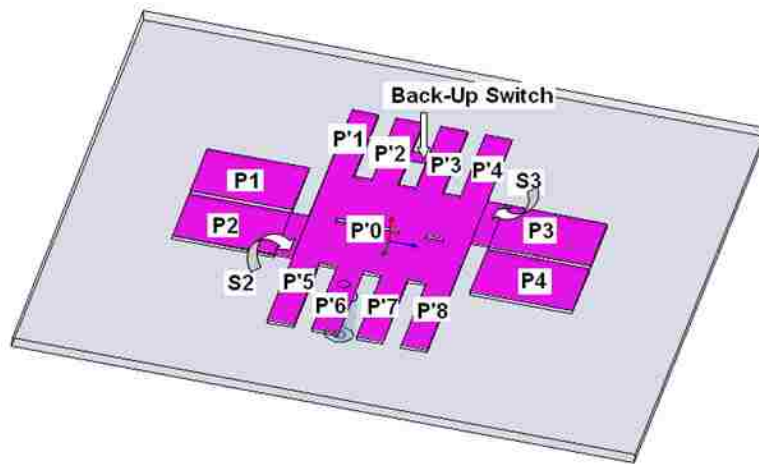


Fig. 7.7 Antenna in Back-Up switch 2.05 GHz equivalent configuration

The return loss plot is shown in Fig.7.9. Installing back-up switches will not add to the redundancy of the system since it is creating a robust antenna that can operate at desired frequencies with very high reliability. The robustness of this antenna can be increased by applying these two methods proposed in this section.

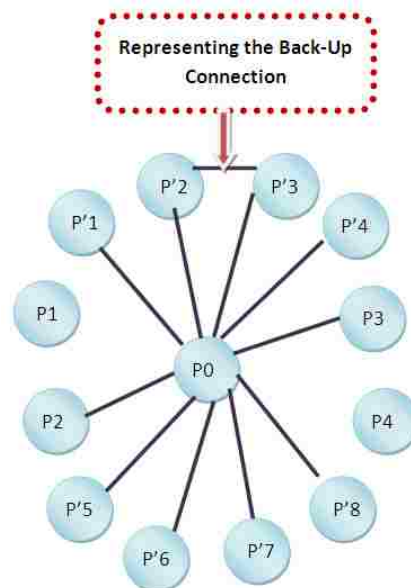


Fig. 7.8 Graph model of the equivalent configuration in Fig.7.7

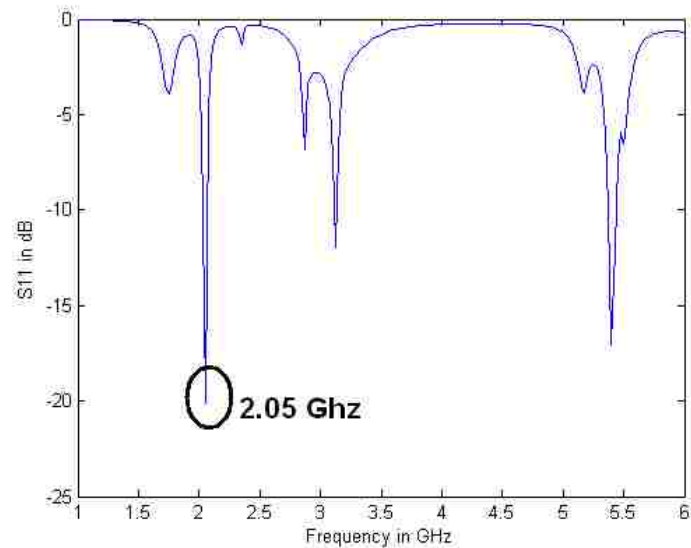


Fig. 7.9 The antenna's return loss showing clear operation at 2.05 GHz

7.5.4 The Reliability Assurance Algorithm:

The designer needs before applying this algorithm to create a library similar to Table 7.2 where all the possible configurations for all the desired frequencies are included. The designer installs switches or RF components on an antenna structure for a specific purpose of tuning a certain frequency or achieving a certain antenna reconfiguration function. There shouldn't be redundant switches after the implementation of the optimization technique and though the algorithm should be easily computable and not extensive nor infinite.

Neural Networks can also be used as in Section 6.5 and in [7-10] to determine the library of equivalent configurations. The use of NN speeds up the library assembly process for large structures.

The designer should include in his library the back-up switch configuration if such configuration existed for specific frequencies. The algorithm is described below and a schematic representation is shown in Fig 7.10.

Step 1: Identify defected switch

Step 2: Identify desired frequency

Step 3: In the library table create a pointer at row i corresponding to the desired frequency

Step 4: In the library table create a pointer at column j corresponding to the defected configuration

Step 5: Move the pointer j to the placement $j+1$

Step 6: Search for a possible edge representing a connection from the defected switch

Step 7: If no connection is found, use configuration in the column $j+1$

Step 8: if a connection is found Repeat Step 5 and 6

Step 9: If no solution was found, declare frequency unachievable

7.6 Reconfigurable Antenna Reliability Formulations:

Reconfigurable antennas reliability depends on the antenna's frequency of operation and its environment of operation. One way of calculating reliability is to relate that reliability to the number of alternative configurations that the antenna has at a certain frequency and the probability of achieving all these configurations. This correlation is also

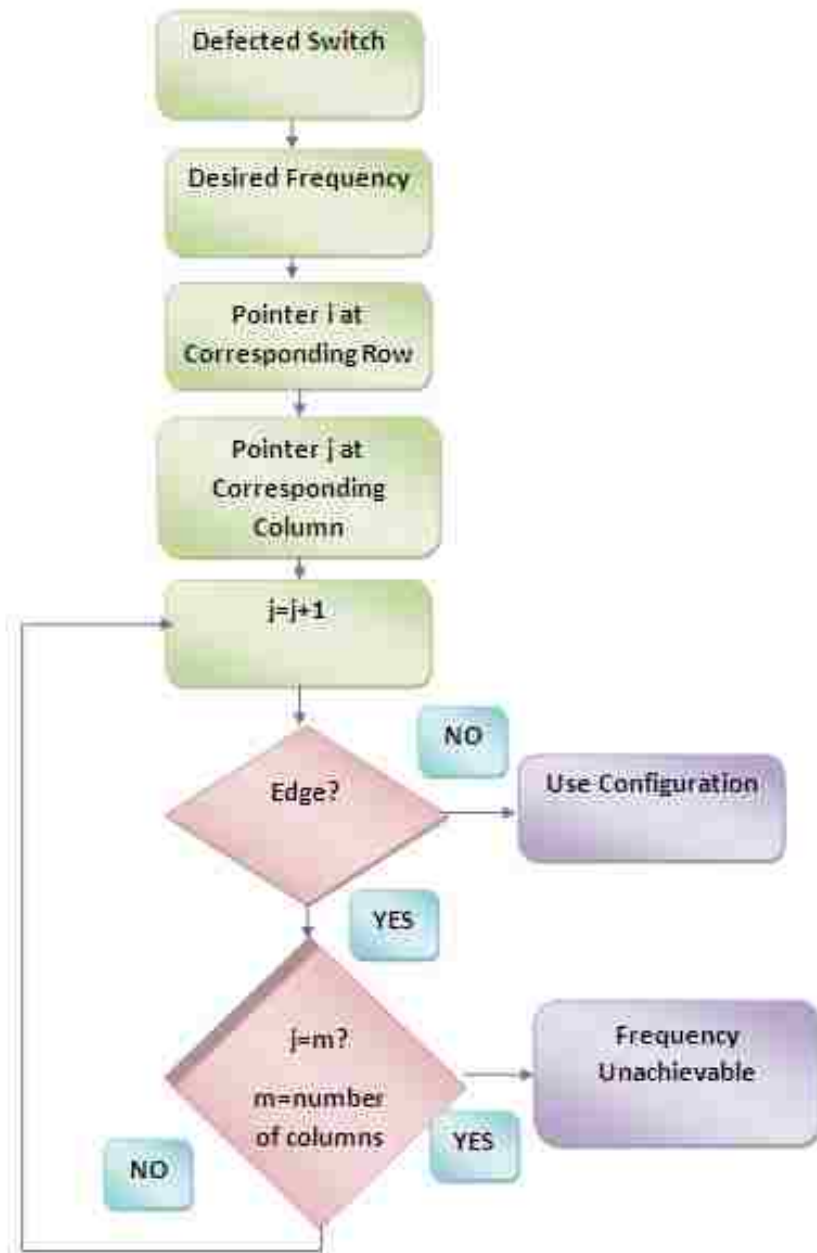


Fig. 7.10 A schematic representation of the algorithm

inversely proportional to the number of edges achieving these constellations. In other words the reliability is higher if the number of configurations is higher but it gets decreased by the number of edges or connections to achieve these configurations. The optimum solution will be to have many alternative configurations with a small number of connections. Eq. 7.5 shows this relation:

$$R(f) = \frac{\sum_{i=1}^{Nc(f)} \sum_{j=1}^{NE_i(f)} P(E_{ij})}{\sum_{i=1}^{Nc(f)} NE_i(f)} \times 100 \quad (7.5)$$

where:

$R(f)$ = The reconfigurable antenna reliability at a particular frequency f

$NC(f)$ = The number of configurations achieving the frequency f

$NE(f)$ =The number of edges for different configurations at the frequency f

$P(E)$ = Probability of achieving the edge E

Example 7.4:

Let's take the antenna shown in Fig.7.6. Let's calculate the antenna's reliability at 2.9 GHz. According to Table 7.2, at 2.9 GHz the antenna has 3 equivalent configurations achieving this particular frequency. Taking the probability of achieving each edge in each configuration equal to 0.98 then according to Eq. 7.5:

$$\begin{aligned}
R(2.9GHz) &= \frac{\sum_{i=1}^3 \sum_{j=1}^{NE_i(2.9)} P(E_{ij})}{\sum_{i=1}^3 NE_i(2.9)} \times 100 \\
&= \frac{\sum_{j=1}^{NE_1(2.9)} P(E_{1j}) + \sum_{j=1}^{NE_2(2.9)} P(E_{2j}) + \sum_{j=1}^{NE_3(2.9)} P(E_{3j})}{NE_1(2.9) + NE_2(2.9) + NE_3(2.9)} \times 100 \\
&= \frac{P(E_{11}) + P(E_{12}) + P(E_{21}) + P(E_{22}) + P(E_{23}) + P(E_{31}) + P(E_{32}) + P(E_{33}) + P(E_{34})}{2 + 3 + 4} \times 100 \\
&= \frac{9 \times 0.98}{9} \times 100 = 98\%
\end{aligned}$$

Example 7.5:

Let's take the antenna shown in Fig.7.6 and calculate the antenna's reliability at 1.7 GHz. Let's assume that the probability for making a connection with switch 1 is 0.999 and the probability for making a connection with switch 2 is 0.998 and the probability of making a connection with switch 3 is 0.900. According to Eq. 7.5 the reliability at 1.7 GHz is:

$$\begin{aligned}
R(1.7GHz) &= \frac{\sum_{i=1}^1 \sum_{j=1}^{NE_i(1.7)} P(E_{ij})}{\sum_{i=1}^3 NE_i(2.9)} \times 100 = \frac{\sum_{j=1}^{NE_1(1.7)} P(E_{1j})}{NE_1(1.7)} \times 100 \\
&= \frac{P(E_{11}) + P(E_{12}) + P(E_{13})}{3} \times 100 \\
&= \frac{0.999 + 0.998 + 0.900}{3} \times 100 = 96\%
\end{aligned}$$

It is important to note that the reliability of an antenna at a frequency that can be achieved without switching or with a no-switch configuration is always 100 % since it is imminent to the uncertainties of switches. An example of such 100% reliable antenna is the antenna in Fig.7.6 at 5.2 GHz.

7.7 Reconfigurable Antenna General Complexity:

The increase in the number of edges in a graph modeling a reconfigurable antenna adds to the complexity of the system. Therefore the complexity is calculated from the size of the graph which is represented by the number of edges existing in that particular graph for all possible connections. This definition of complexity is different than other definitions of complexity such as computational complexity.

$$C = NE \tag{7.6}$$

Where NE represents the number of edges for all possible connections.

The removal of redundant elements results in reduction of the general complexity of the hardware as well as the software controlling the reconfiguration technique. We will show below some examples where the complexity was decreased using our optimization technique.

Example 7.6:

The antenna [71] shown in Fig. 7.11 was discussed and optimized in Example 6.3

of Section 6.3 in Chapter 6. The graph model of the original antenna is shown in Fig.7.11. After optimizing the antenna and preserving the same topology the different sections of the antenna are shown in Fig.7.12. The general complexity of the antenna before optimization is: $C = NE = 312$, however after optimization C was reduced to $C=166$.

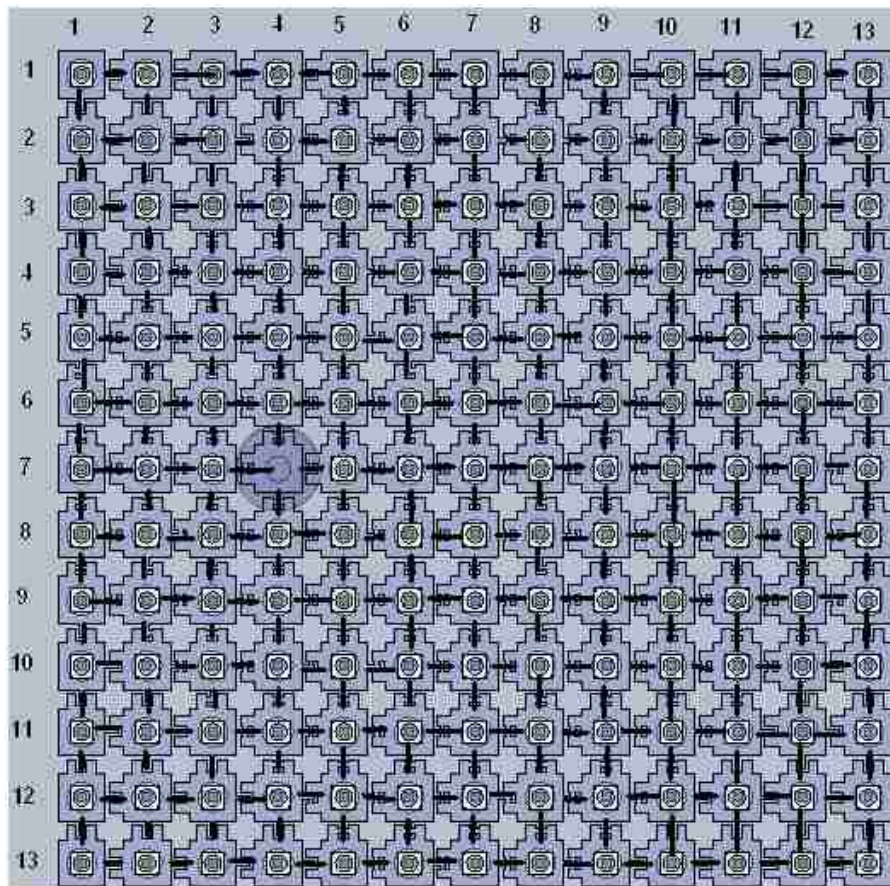


Fig. 7.11 The antenna in [71] as well as its graph model for all possible configurations

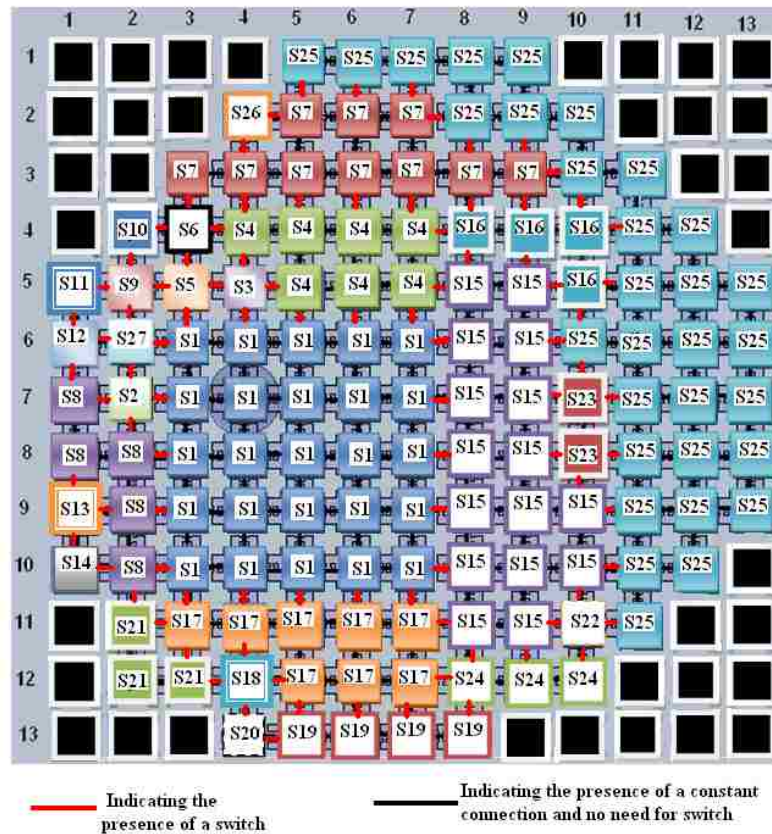


Fig. 7.12 Different antenna sections

Example 7.7:

The antenna [20] shown in Fig.7.13 was discussed in section 6.3 was found to be redundant. The graph modeling of the redundant structure is shown in Fig. 6.14. Applying the optimization technique, results in the graph model of Fig.6.15 representing the optimal antenna configuration.

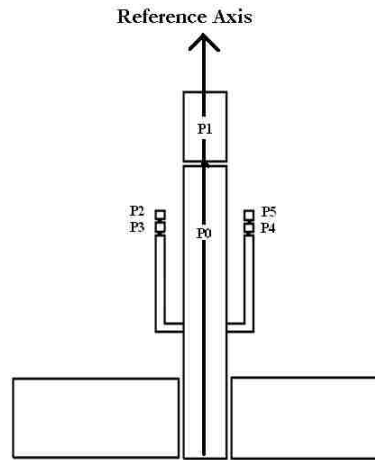


Fig. 7.13 Redundant structure in [20]

The general complexity of the antenna with redundancy (before optimization) is according to Eq. 7.6: $C=5$; however the general complexity of the structure after optimization is : $C=3$.

Example 7.8:

The general complexity of the non optimized structure of Fig.7.6 is $C=8$ according to Eq.7.6; however the general complexity of the optimized topology is $C=4$.

7.8 The Correlation Between The Complexity and The Reliability of A Reconfigurable

Antenna:

It is true that the optimization technique has reduced the general complexity of reconfigurable antenna systems; however an antenna having many different configurations at different frequencies of operation reveals the question of the complexity at each particular frequency. Eq. 7.7 defines such frequency dependent complexity.

$$C(f) = \underset{i=1,NC(f)}{Max} (NE_i(f)) \quad (7.7)$$

where :

$C(f)$ represents the complexity of the antenna system at a frequency f

$NC(f)$ represents the number of equivalent configurations at a frequency f

$NE_i(f)$ represents the number of edges at the configuration i for a frequency f

Example 7.9:

As an example let's take the antenna shown in Fig.7.4. The different configurations of this antenna at 5 GHz are shown in Table 7.1. The complexity of this antenna at 5 GHz is according to Eq.7.7:

$$C(5GHz) = \underset{i=1,8}{Max}(NE_i(5)) = Max(2,2,2,3,3,4,4,5) = 5$$

Example 7.10:

Taking the optimized antenna shown in Fig.7.6 . The different configurations of this antenna are shown in Table 7.2 for different frequencies. The complexity of this antenna at 5.2 GHz is according to Eq.7.7:

$$C(5.2GHz) = \underset{i=1,7}{Max}(NE_i(5.2)) = Max(1,1,1,2,2,2,0) = 2$$

A correlation can be established between the complexity of an antenna at a frequency f and its reliability at that same frequency. That correlation can be derived from Eq. 7.5 and it is shown below in Eq.7.8:

$$R(f) = \frac{\sum_{i=1}^{Nc(f)} \sum_{j=1}^{NE_i(f)} P(E_{ij})}{C(f) + \sum_{k=1}^{N'C(f)} NE_k(f)} \times 100 \quad (7.8)$$

where :

$C(f)$ is calculated in Eq.7.7

$N'C(f)$ is the number of equivalent configurations at a frequency f without one configuration of the configurations with maximum edges.

From Eq. 7.8 we can deduce that the reliability of a reconfigurable antenna at a frequency f is inversely proportional to the complexity of that antenna structure at the same frequency f .

Example 7.11:

Taking the same antenna from example 7.5 of section 7.6 and recalculating reliability according to Eq. 7.8 reveals:

$$C(2.9GHz) = \text{Max}(NE_i(2.9)) = \text{Max}(2,3,4) = 4$$

$$\begin{aligned} R(2.9GHz) &= \frac{\sum_{i=1}^3 \sum_{j=1}^{NE_i(2.9)} P(E_{ij})}{C(2.9) + \sum_{k=1}^2 NE_k(2.9)} \times 100 = \frac{\sum_{j=1}^{NE_1(2.9)} P(E_{1j}) + \sum_{j=1}^{NE_2(2.9)} P(E_{2j}) + \sum_{j=1}^{NE_3(2.9)} P(E_{3j})}{4 + NE_1(2.9) + NE_2(2.9)} \times 100 \\ &= \frac{P(E_{11}) + P(E_{12}) + P(E_{21}) + P(E_{22}) + P(E_{23}) + P(E_{31}) + P(E_{32}) + P(E_{33}) + P(E_{34})}{4 + 2 + 3} \times 100 \\ &= \frac{9 \times 0.98}{9} \times 100 = 98\% \end{aligned}$$

7.9 Applying Fano's Inequality to Switch-Reconfigured Antennas:

In [79] the authors discuss Fano's Inequality as a way of evaluating the probability of error in a system. Suppose that a random variable Y is known and we wish to guess the value of a correlated random variable X . Fano's Inequality relates the probability of error in guessing the random variable X to its conditional entropy $H(X/Y)$ [79]. This inequality is based on a function generation, an estimation of X and then evaluating the probability of error of that estimation. According to Eq. 2.132 in [79] the probability of error can be written as:

$$Pe \geq \frac{H(X/Y) - 1}{\log|X|} \quad (7.9)$$

where $X \rightarrow Y \rightarrow \hat{X}$

In our case, X represents the switches performance in an antenna system. Each switch has a probability of switching success or failure. If N is the number of switches then we have 2^N values of X . We assume that Y is unknown to us and though is independent with X and Eq. 7.9 becomes:

$$Pe \geq \frac{H(X) - 1}{\log|X|} \quad (7.10)$$

Example 7.12 :

An antenna has 2 switches with probabilities of failure of 0.25 for the first switch

and 0.2 for the second switch. Then the probability of an error happening in that antenna related to switch malfunction is:

$$Pe \geq \frac{-0.25 \times \log_2(0.25) - 0.75 \times \log_2(0.75) - 0.2 \times \log_2(0.2) - 0.8 \times \log_2(0.8) - 1}{\log_2(4)}$$

$$\Rightarrow Pe \geq \frac{1.5332 - 1}{2} = 0.266$$

Also according to Eq. 2.143 of [79] shown below, we can calculate the entropy of error of an antenna system as shown in Eq.7.11

$$H(Pe) + Pe \times \log(m - 1) \geq H(X) \quad (7.11)$$

Where m is the number of values X can have.

7.10 Discussion:

Reducing the complexities of reconfigurable antennas facilitates the automation and control process of such systems. Using methods to increase the reliability of reconfigurable antennas sets the way to design more robust systems. In the next chapter conclusions are drawn from this work and steps are defined for future continuation.

CHAPTER 8

CONCLUSIONS AND FUTURE WORK

8.1 Conclusions:

In this work three major reconfigurable antenna's research characteristics are addressed. The first aspect is the design of reconfigurable antennas. These antennas are reviewed, classified and grouped. They are categorized into different groups based on their reconfiguration techniques and they are classified based on their reconfigurability properties. Previous reconfigurable antenna designs, their reconfiguration techniques and their applications are reviewed. A new reconfiguration method based on slot rotation is introduced. This technique redistributes surface currents by rotating slots in an antenna system. The slot rotation process is optimized and processed to be automated through an FPGA. FPGA is also used to activate p-i-n diodes installed on a microstrip antenna to connect and disconnect different sections together. Other new designs are also presented to adapt with the evolution of reconfigurable antennas.

Graph models are introduced and guidelines for using graphs to model reconfigurable antennas are also addressed. Each Group of antennas with a specific reconfiguration technique is modeled in a distinctive manner. The adaptation of graph models to reconfigurable antennas not only helps in the automation process of these antennas but also in the new design methodology proposed in this work. This methodology based on graph models presents an iterative strategy for designing a

constraint-satisfying reconfigurable antenna. Steps that lead to optimal designs are proposed.

The second aspect is the optimization of reconfigurable antennas. A new optimization technique based on graph models is presented. This approach optimizes redundancy in a reconfigurable antenna structure. It helps antenna designers remove any redundant elements from their designs. This optimization approach reduces costs, losses and complexity in a reconfigurable antenna design while maintaining the same performance level.

The third aspect is the analysis of reconfigurable antennas. Two major concerns are addressed. The first issue is reconfigurable antenna systems reliability regardless of the reliability of the electronic components installed on these antennas to achieve reconfiguration. The second issue is the complexity of these antennas. The correlation between these two parameters contributes in achieving an efficient design. Two methods are proposed to overcome failures in reconfigurable antennas due to any failure in its reconfiguration technique or due to any effect from the surrounding environment. The probability of performance error in a reconfigurable antenna system is investigated using Fano's Inequality and information theory.

Reconfigurable antenna designers need to answer a very important question: will they be able to achieve their design objectives in the most efficient and less expensive way. This work tries to answer this question knowing that a designer has to always compromise between improved performance of an antenna and an increased complexity in its structure.

8.2 Future Work:

Future work is proposed to revolve around the following points:

- New reconfiguration techniques applied to new designs.
- Improving and optimizing of the automation process of existing reconfiguration techniques
- Improving and evolving the performance of optimal reconfigurable antennas based on graph models and algorithms.
- Extending graphs to model reconfigurable antennas with many different techniques and reconfiguration properties.
- Extending the information theoretical study starting from Fano's Inequality and the calculation of uncertainties and reliability done in this work.
- Using Information theory to address new issues in reconfigurable antenna designs such as Markov processes.
- Applying the reliability assurance algorithm developed in Chapter 7 on an actual programmable device such as an FPGA to ensure the continuous functioning of reconfigurable antennas at all times.

The development of research areas such as reconfigurable antennas will lead to a future where antennas self correct errors, overcome failures and self-reconfigure to adjust for the upcoming changes of the surrounding environment. Antennas installed in not easily reachable platforms will be controlled from a remote station and continuous functioning must and will be guaranteed.

APPENDIX A

APPLICATIONS NOTES FOR P-I-N DIODES [80]

A.1 Application Notes:

The p-i-n diode structure consists of an Intrinsic “I” region sandwiched between heavily doped P+ and N+ regions as shown in Fig. A.1. The Intrinsic region is a very lightly doped, high resistivity material which controls the fundamental properties of the p-i-n diode.

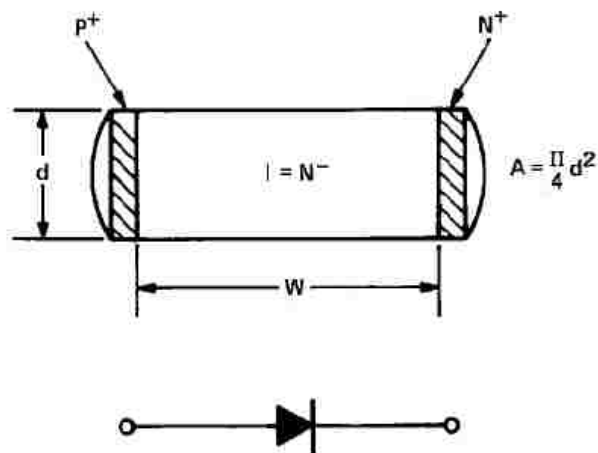


Fig. A.1 Basic p-i-n diode structure [80]

The p-i-n diode essentially operates in two modes. The “ON” state, where the diode is forward biased and the “OFF” state, where the diode is reverse biased. When the p-i-n diode is forward biased, the charge “Q” which consists of electrons and holes is injected into the intrinsic “I” region from heavily doped P+ and N+ regions.

At lower charge injections (IF) the diode presents high impedance. As forward current is increased more charge is injected into the “I” region which lowers the diode impedance. With more charge injection, further reduction in the p-i-n diode impedance occurs until the p-i-n diode saturates and no longer responds to an increase in charge injection. Therefore, a p-i-n diode in the “ON” state is basically an Electronically Variable Resistance which is controlled by a DC current.

When a p-i-n diode is subjected to a reverse bias, the electric field generated in the “I” region depletes the mobile charges and the diode presents high impedance represented by a high parallel resistance “ RP ” shunted by a high impedance junction capacitance “ CJ ”. The electron and hole charges have finite lifetime “ TL ” known as the minority carrier lifetime. p-i-n diodes are rectifiers, but the finite lifetime of these minority carriers permits RF current flow in excess of the DC forward bias without significant variation of the total charge accumulated, and thus without significant resistance change which causes distortion.

The doping profile of an ideal p-i-n diode structure is shown in Fig. A.2.b. Due to donor and acceptor concentration, diffusion takes place and the resultant ionized impurity atoms create the space charge as shown in Fig. A.2.c. This fixed charge region is known as the depletion region [80].

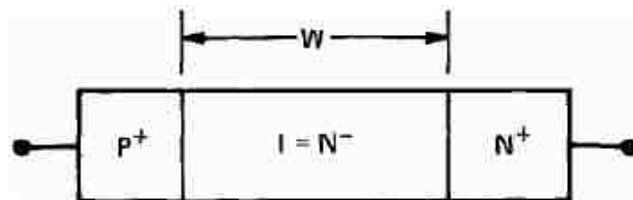


Fig. A.2.a Basic structure [80]

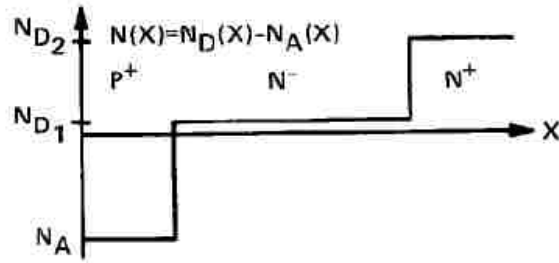


Fig. A.2.b Doping profile [80]

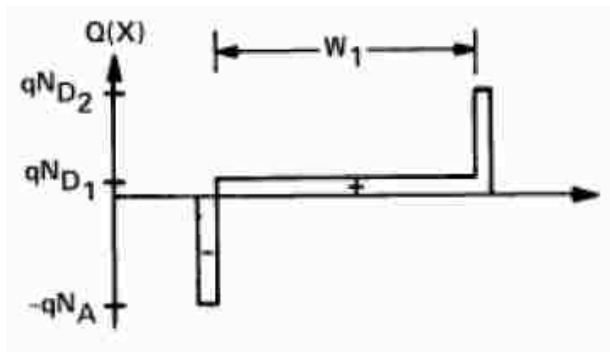


Fig. A.2.c Space-charge profile [80]

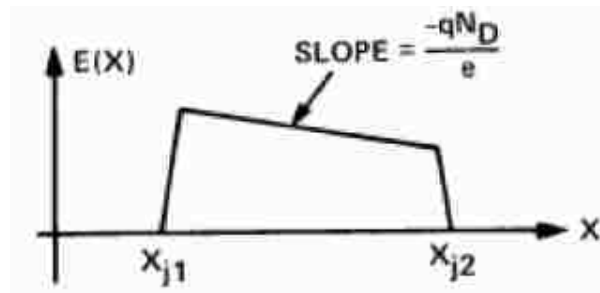


Fig. A.2.d Electric field profile

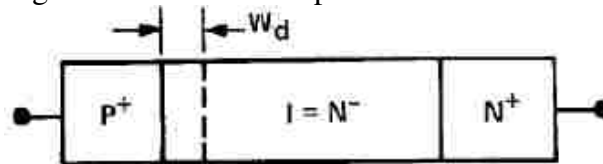


Fig. A.2.e Zero bias depletion [80]

The relationship between the charge distribution and the electrostatic potential is given by Poisson's equation:

$$\frac{d^2\psi}{dx^2} = \frac{qN_A}{\epsilon_0\epsilon_R} \quad (A.1)$$

$$\frac{d^2\psi}{dx^2} = \frac{-qN_D}{\epsilon_0\epsilon_R} \quad (A.2)$$

Where:

q= electron charge

ϵ_0 =free space dielectric constant

ϵ_R =relative dielectric constant

N_A =acceptor doping density

N_D = "I" region donor density

Using Poisson's equation one can integrate the charge distribution of Fig. A.2.c to determine the electric field across the depletion region shown in Fig. A.2.d. If the doping in the "I" region of the p-i-n diode is sufficiently low and the width is small, the zero bias depletion region may extend all the way to the N+ region. Such devices are known as zero punch-through devices. The depletion region WD at zero bias is shown in Fig. A.2.e. With the application of reverse bias voltage, the depletion layer widens. The voltage at which this depletion boundary penetrates the N+ region is called the punch-through voltage (VPT). At bias voltages equal to or greater than the punch through voltage, the "I" region

becomes free of all mobile carriers. Because the N+ region is heavily doped, the depletion region movement into the N+ region is almost negligible.

A.2 Minority Carrier Lifetime :

The carrier lifetime of a p-i-n diode is a very important parameter not only from the diode design standpoint but also from the circuit designer's standpoint. The carrier lifetime "TL" is a property of the semiconductor material. When the p-i-n diode is forward biased, injection of electrons and holes occurs from the N+ and P+ contacts respectively. These carriers have a finite lifetime before they recombine. Recombination takes place through interaction with the crystal lattice. Impurities in the "I" region and at the P+ and N+ region. Carrier lifetime is the average time before electrons and holes recombine.

The carrier lifetime in a p-i-n diode controls the switching speed "TRR". Switching speed is defined in a time domain; it is defined as the time to switch the diode from a low impedance forward bias state to a high impedance reverse bias state and it is the slower of the two states of the p-i-n diode in a switching application. Perhaps the best way to understand the switching speed is to examine its relationship with diode minority carrier life time "TL" and its forward and reverse current ratio (IF/IR) in the following equation:

$$T_{rr} = T_L \log\left(1 + \frac{I_F}{I_R}\right) \quad (A.3)$$

The switching waveform is shown in Fig. A.3. This equation is important because it predicts the variation of switching time with minority carrier lifetime and "IF/IR" ratio.

Drivers with higher value of “IR” or with “spike leading edge” of their wave form are used to minimize the switching speed.

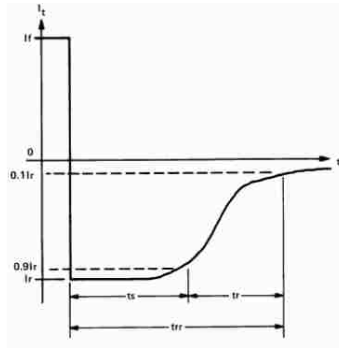


Fig. A.3 Switching transient of a p-i-n diode [80]

The fundamental lower limit of a minority carrier lifetime in a p-i-n diode is the transit time “ T_T ”, where the carrier crosses the “I” region with saturated velocity switching speed “ V_s ”.

$$T_T = W / V_s \quad (A.4)$$

$$V_s = 107 \text{ cm/sec}$$

W = “I” region length in cm

Breakdown Voltage:

The electrical field in the p-i-n diode is essentially constant as shown in Figure A.2.d. Breakdown voltage is the integration of the electric field in the “I” region as

Follows:

$$V_b = \int_0^W E(x) dx \quad (A.5)$$

Since $E(X)$ is constant, the breakdown voltage is simply given by:

$$V_B = E * W \quad (A.6)$$

The theoretical electrical field in the intrinsic “I” region should be 14 volt/micron, but in practice the electrical field is lower (12 volt/micron) due to actual geometry of the p-i-n diode being different from the infinite parallel plate model assumed in the calculation. In order to avoid the nonlinear effects with the RF signal, the bias voltage must be sufficient to prevent the diode junction from beginning to go into conduction. Typically, the bias can be substantially less than the peak RF voltage owing to charge flow delay mechanisms. At HF frequencies, however, the bias **MUST** equal the RF. Exact requirements depend on application and diode I region thickness; experimentation is necessary.

$$V_B > 2V_{RF}(Peak) + V(Bias) \quad (A.7)$$

REFERENCES

- [1] E.R.Brown “RF-MEMS Switches For Reconfigurable Integrated Circuits” *IEEE Transactions on Microwave Theory and Techniques*, Vol. 46 Issue 11 Part 2, pp. 1868-1880, Nov 1998.
- [2] C.A.Balanis “Modern Antenna Handbook”, John Wiley and Sons, 2008.
- [3] J.C.Langer, J. Zou, C.Liu, and J.T. Bernhard “Micromachined Reconfigurable Out Of Plane Microstrip Patch Antenna Using Plastic Deformation Magnetic Actuation” *IEEE Microwave and Wireless Components Letters*, Vol. 13 No 3, pp. 120-122, March 2003.
- [4] A.E. Fathy, A. Rosen, H.S.Owen, F. McGuinty, D.J. Mcgee, G.C. Taylor, R. Amantea , P.K. Swain, S. M. Perlow and M. Elsharbiny “ Silicon-based reconfigurable antennas- concepts, analysis, implementation and feasibility ” *IEEE Transactions on Microwave Theory and Techniques* , Vol. 51, Issue 6, pp. 1650-1661, June 2003.
- [5] L. M. Feldner, C. D. Nordquist , and C. G.Christodoulou, “RFMEMS Reconfigurable Triangular Patch Antenna”, *IEEE AP/URSI International Symposium*, Vol 2A, pp.388-391, July 2005.
- [6] N. Behdad and K. Sarabandi “ Dual-Band reconfigurable antenna with a very wide tunability range” *IEEE Transactions on Antennas and Propagation*, Vol. 54, Issue 2, Part 1, pp. 409-416, Feb. 2006.
- [7] D. E. Anagnostou, Z.Guizhen, M.T. Chrysomallis, J.C. Lyke, G.E. Ponchak, J. Papapolymerou, and C. G. Christodoulou “Design, fabrication and measurement of an RF-

MEMS-based self –similar reconfigurable antenna” , *IEEE Transactions on Antennas and Propagation*, Vol. 54, Issue 2, Part 1, pp. 422-432, Feb 2006.

[8] A.Patnaik, D. E. Anagnostou, C.G. Christodoulou and J.C. Lyke “ Neurocomputational analysis of a multiband reconfigurable planar antenna” , *IEEE Transactions on Antennas and Propagation*, Vol. 53, Issue 11, pp. 3453-3458, Nov. 2005.

[9] A.Patnaik, D. E. Anagnostou, C.G. Christodoulou and J.C. Lyke “ A frequency reconfigurable antenna design using neural networks” , *IEEE Antennas and Propagation society international symposium*, Vol. 2A, pp.409-412, July 2005.

[10] N. Kingsley, D. E. Anagnostou, M.Tentzeris and J. Papapolymerou “ RF MEMS sequentially reconfigurable sierpinski antenna on a flexible organic substrate with novel DC-biasing technique ” , *Journal of microelectromechanical systems*, Vol. 16, Issue 5, pp.1185-1192, Oct. 2007.

[11] D.Piazza, N.J. Kirsch, A. Forenza, R.W. Heath and K.R. Dandekar “Design and evaluation of a reconfigurable antenna array for MIMO systems” , *IEEE Transactions on Antennas and Propagation*, Vol. 56, Issue 3, pp. 869-881, March 2008.

[12] C.S. Deluccia, D.H. Werner, P.L.Werner, M.Fernandez Pentoja and A.R. Bretones “A novel frequency agile beam scanning reconfigurable antenna”, *IEEE Antennas and Propagation society international symposium*, Volume2, pp. 1839-1842, June 2004.

[13] F. Ghanem, P. S. Hall, and J. R. Kelly “Two port frequency reconfigurable for cognitive radios”, *IEEE Electronic Letters*, Volume 45, Issue 11, pp. 534-536, May 2009.

- [14] A.C.K. Mak, C.R. Rowell, R.D. Murch and C.L. Mak “ Reconfigurable multiband antenna designs for wireless communication devices ” *IEEE Transactions on Antennas and Propagation*, Vol. 55, Issue 7, pp. 1919-1928, July 2007.
- [15] A. Cidronali, L. Lucci, G. Pelosi, P. Sarnori and S. Selleri “A reconfigurable printed dipole for quad-band wireless applications”, *IEEE Antennas and Propagation society international symposium*, pp. 217-220, July 2006.
- [16] M. A. Ali and P. Waheed “A reconfigurable yagi-array for wireless applications ”, *IEEE Antennas and Propagation society international symposium*, Vol 1, pp. 446-468, June 2002.
- [17] L.M. Feldner, C.T. Rodenbeck, C.G. Christodoulou and N. Kinzie “ Electrically small frequency-agile PIFA-as-a-package for portable wireless devices” *IEEE Transactions on Antennas and Propagation*, Vol. 55, Issue 11, pp. 3310-3319, Nov. 2007.
- [18] W.H. Weedon, W.J. Payne and G.M. Rebeiz “ MEMS-switched reconfigurable antenna” *IEEE Antennas and Propagation society symposium* , Vol. 3, pp. 654-657, July 2001.
- [19] S. Xiao, B.Z. Wang, X. S. Yang and G. Wang “ Reconfigurable microstrip antenna design based on genetic algorithm” *IEEE Antennas and Propagation society symposium* , Vol. 1, pp. 407-410, June 2003.
- [20] V. Zachou, C.G. Christodoulou, M.T. Chrisomallis, D. Anagnostou and S.E. Barbin, “Planar Monopole Antenna With Attached Sleeves”, *Antennas and Wireless Propagation Letters*, Vol. 5 No 1, pp. 286-289, Dec. 2006.

- [21] J.M. Zendejas, J.P.Gianvittorio,Y.Rahmat-Samii and J.W.Judy “Magnetic MEMS Reconfigurable Frequency Selective Surfaces”, *Journal of Microelectromechanical Systems*, Vol. 15, No. 3,pp. 613-623, June 2006.
- [22] J. Costantine, C.G. Christodoulou “A new reconfigurable antenna based on a rotated feed” *IEEE international symposium on antennas and propagation*, pp. 1-4, July 2008.
- [23] J. Costantine, C. G. Christodoulou, S. E. Barbin, “A New Reconfigurable Multi Band Patch Antenna”, *IEEE IMOC Conference*, Salvador, Brazil, pp.75-78,October 2007.
- [24] B.Poussot, J.M.Laheurte, L.Cirio, O. Picon, D.Delcroix and L.Dussopt “ Diversity measurements of a reconfigurable antenna with switched polarizations and patterns ” *IEEE Transactions on Antennas and Propagation* , Vol. 56, Issue 1, pp. 31-38, Jan. 2008.
- [25] T.L.Roach, G.H.Huff and J.T. Bernhard “ Enabling high performance wireless communication systems using reconfigurable antennas ” *Military Communications Conference* , pp. 1-6, Oct. 2006.
- [26] M.T.Oswald, S.C.Hagnes,B.D.Van Veen and Z. Popovic “ Reconfigurable single-feed antennas for diversity communications ” *IEEE Antennas and Propagation society international symposium* , Vol. 1, pp. 469-472, June 2002.
- [27] B.A.Cetiner, H.Jafarkhani, Jiang-Yuan Qian, Hui Jae Yoo, A. grau and F.De Flaviis “ Multifunctional reconfigurable MEMS integrated antennas for adaptive MIMO systems” *IEEE Communications Magazine* , Vol. 42, Issue 12, pp. 62-70, Dec. 2004.
- [28] H.Aissat, L. Cirio, M. Grzeskwiak, J.M. Laheurte and O. Picon “ Reconfigurable circularly polarized antenna for short-range communication systems ” *IEEE Transactions*

on *Microwave Theory and Techniques* , Vol. 54, Issue 6, Part 2, pp. 2856-2863, June 2006.

[29] C.W. Jung, Ming Cher Lee, G.P.Li and F.De Flaviis “Reconfigurable scan beam single arm spiral antenna integrated with RF MEMS switches” *IEEE Transactions on Antennas and Propagation*, Vol. 54, Issue 2, Part 1, pp. 455-463, Feb. 2006.

[30] F.Yang and Y.Rahmat Samii “Patch antenna with switchable slots (PASS): reconfigurable design for wireless communications” *IEEE Antennas and Propagation Society International Symposium* , Vol. 1, pp. 462-465, 2002.

[31] G. H. Huff and J.T. Bernhard “Integration of packaged RF MEMS switches with radiation pattern reconfigurable square spiral microstrip antennas” *IEEE Transactions on Antennas and Propagation*, Vol. 54, Issue 2, Part 1, pp. 464-469, Feb. 2006.

[32] Nikolaou, S., Bairavasubramanian, R., Lugo, Jr., C., Carrasquillo, I., Thompson, D.C., Ponchak, G.E., Papapolymerou, J., and Tentzeris, M.M., “Pattern and frequency reconfigurable annular slot antenna using PIN diodes,” *IEEE Transactions on Antennas and Propagation*, vol. 54, pp. 439–448, Feb. 2006.

[33] J.T.Bernhard “*Reconfigurable Antennas*”,Morgan and Claypool Publishers, 2007.

[34] Angus C. K. Mak, Corbett R. Rowell, Ross D. Murch, and Chi-Lun Mak “Reconfigurable Multiband Antenna Designs for Wireless Communication Devices”, *IEEE Transactions on Antennas and Propagation*, Vol. 55, No. 7, pp. 1919-1928, July 2007

[35] Xue-Song Yang, Bing-Zhong Wang, Weixia Wu, “Pattern Reconfigurable Patch Antenna with Two Orthogonal Quasi-Yagi Arrays”, *IEEE Antennas and Propagation Society International Symposium 2005*, Vol 2B, pp. 617-620, July 2005.

- [36] E. Ebrahimi, P.S.Hall “A Dual Wide-Narrowband Antenna For Cognitive Radio”, *Third European Conference on Antennas and Propagation 2009*, pp. 809-812, March 2009.
- [37] J.M. Zendejas, J.P.Gianvittorio, Y.Rahmat-Samii and J.W.Judy “Magnetic MEMS Reconfigurable Frequency Selective Surfaces”, *Journal of Microelectromechanical Systems*, Vol. 15, No. 3, pp. 613-623, June 2006.
- [38] J.R. Kelly, P.S.Hall, P.Gardner “Integrated Wide-Narrowband Antenna For Switched Operation”, *Third European Conference on Antennas and Propagation 2009*, pp. 3757-3760, March 2009.
- [39] S. Nikolau, K.Boyon, P.Vryonides “ Reconfiguring Antenna Characteristics Using PIN Diodes”, *Third European Conference on Antennas and Propagation 2009*, pp. 3748-3752, March 2009.
- [40] C. G. Christodoulou, J. H. Kim, J. Costantine, S.E. Barbin “ Reconfigurable RF and Antenna Systems”, *SBMO/IEEE MTT-S International Microwave and Optoelectronics Conference*, pp. 17-20, Nov.2007.
- [41] D. E. Anagnostou “ RF-MEMS Self-Similar Antennas : Design, Analysis, and Measurements: Synthesis Using a Neural Network Technique”, Ph. D Thesis, University of New Mexico, Department of Electrical and Computer Engineering , May 2005
- [42] N.Jin, F.Yang, Y. Rahmat Samii “A Novel Patch Antenna With Switchable Slot (PASS): Dual-Frequency Operation With Reversed Circular Polarizations”, *IEEE Transactions on Antennas and Propagation*, Vol. 54, No. 3, pp. 1031-1034, March 2006

- [43] J. Costantine, S. al-Saffar, C.G.Christodoulou, K.Y.Kabalan, A. El-Hajj “ The Analysis of a Reconfiguring Antenna With a Rotating Feed Using Graph Models”, *IEEE Antennas and Wireless Propagation Letters*, Accepted for Future Publication, Volume PP pp. 1-1, 2009.
- [44] J.Costantine, K.Y.Kabalan, A. El Hajj and M. Rammal “New Multi-Band Microstrip Antenna Design for Wireless Communications” *IEEE Antennas and Propagation Magazine*, Vol. 49, Issue 6, pp. 181-186, Dec. 2007.
- [45] J.Costantine, K.Y. Kabalan, A. El Hajj and C.G. Christodoulou“ New Multi_Band Design for a Microstrip Patch Antenna ” *The Second European Conference on Antennas and Propagation*, pp. 1-4, Nov. 2007.
- [46] Y. Tawk, C. G. Christodoulou “A Cellular Automata Reconfigurable Microstrip Antenna Design”, *IEEE Antennas and Propagation Society International Symposium 2009*, pp. 1-4, June 2009.
- [47] J. Costantine, Y.Tawk, C.G.Christodoullou, S.E. Barbin “ A Star Shaped Reconfigurable Patch Antenna”, *IMWS 2009 International Microwave Workshop Series on Signal Integrity and High-Speed Interconnects*, pp. 97-100, Feb.2009.
- [48] D. Ressiguiet, J. Costantine, Y.Tawk, C.G.Christodoulou “ A Reconfigurable Multi-Band Antenna Based on Open Ended Microstrip Lines”, *Third European Conference on Antennas and Propagation 2009*, pp. 792-795, March 2009.
- [49] Pong P. Chu “*RTL Hardware Design Using VHDL*” John Wiley and Sons Inc., Hoboken, NJ, 2006.

- [50] IEEE Standard Test Access Port and Boundary-Scan Architecture, http://standards.ieee.org/reading/ieee/std_public/description/testtech/1149.11990_desc.html
- [51] Spartan-3E FPGA Starter Kit Board User Guide, http://www.xilinx.com/support/documentation/boards_and_kits/ug230.pdf
- [52] T.H.Cormen, C.E.Leiserson, R.L.Rivest,C.Stein “Introductions to Algorithms”,MIT press, 2001.
- [53] E. Klavins “Programmable Self Assembly” IEEE Control Systems Magazine, Vol. 27, No.4, pp. 43-56, Aug. 2007
- [54] J. Costantine, C.G. Christodoulou, S.E.Barbin “Mapping Reconfigurable Antennas Using Graphs” The NASA/ESA conference on adaptive hardware and systems, pp. 133-140, June 2008.
- [55] John Clark, Derek Alan Holton “*A First Look At Graph Theory*”, World Scientific Publishing Company, 1991.
- [56] Gary Chartrand “*Introductory Graph Theory*”, unabridged edition, Dover Publications, 1984.
- [57] E. Klavins “Programmable Self Assembly” IEEE Control Systems Magazine, Vol. 27, No. 4, pp. 43-56, Aug. 2007.
- [58] E. Klavins, R. Ghrist, D. Lipsky “Graph Grammars for Self Assembling Robotic Systems” IEEE International Conference on Robotics and Automation, Vol. 5, pp. 5293-5300, April 2004

- [59] N. Napp, S. Burden, E. Klavins “The Statistical Dynamics of Programmed Assembly” IEEE International Conference on Robotics and Automation, pp. 1469-1476, May 2006
- [60] E. Klavins “Self-Assembly From the point of view of its pieces” American Control Conference, pp.7, June 2006
- [61] J. A. Bossard, D.H. Werner, T.S.Mayer, R.P.Drupp “A Novel Design Methodology for Reconfigurable Frequency Selective Surfaces Using Genetic Algorithms” *IEEE Transactions on Antennas and Propagation*, Volume 53, Issue 4, pp. 1390-1400, April 2005.
- [62] Zhang Min, Luo Xiao-Wu, Wang Guang-Hui “Preliminary Research of the Reconfigurable Antenna Based on Genetic Algorithms” *2004 third International Conference on Computational Electromagnetics and its Applications* , pp. 137-140, Nov. 2004.
- [63] D.E. Skinner, J.D. Connor, S. Y. Foo, M.H. Weatherspoon, and N. Powell “Optimization of Multi-Band Reconfigurable Microstrip Line-Fed Rectangular Patch Antenna Using Self-Organizing Maps” *IEEE 10th Annual Wireless and Microwave Technology Conference (WAMICON)*, pp. 1-4, Apr. 2009.
- [64] A. Akdagli, K. Guney, B. Babayigit “Clonal Selection Algorithm for Design of Reconfigurable Antenna Array with Discrete Phase Shifters” *Journal of Electromagnetic Waves and Applications*, Vol. 21, Number 2, pp. 215-227, 2007.
- [65] C.M. Coleman, J.E. Rothwell, and J.E. Ross “Investigation of Simulated Annealing, Ant-Colony and Genetic Algorithms for Self-Structuring Antennas” *IEEE Transactions on Antennas and Propagation*, Vol. 52, Issue 4, pp. 1007-1014, Apr. 2004.

- [66] J.D.Connor “*Antenna Array Synthesis Using the Cross Entropy Method*” Ph.D. Dissertation, Florida State University, Tallahassee, Fl., USA, June. 2008.
- [67] D. Langoni, M.H. Weatherspoon, E. Ogunti, and S.Y. Foo “An Overview of Reconfigurable Antennas: Design, Simulation, and Optimization” *IEEE 10th Annual Wireless and Microwave Technology Conference (WAMICON)*, pp. 1-5, Apr. 2009.
- [68] J. Costantine, C. G. Christodoulou “Analyzing Reconfigurable Antenna Structure Redundancy Using Graph Models” *IEEE Antennas and Propagation Society International Symposium 2009*, pp. 1-4, June 2009.
- [69] J. Costantine, C. G. Christodoulou, C.T. Abdallah, S.E.Barbin “Optimization and Complexity Reduction of Switch-Reconfigured Antennas Using Graph Models” *IEEE Antennas and Wireless Propagation Letters*, Vol. 8, pp. 1072-1075, 2009.
- [70] V. Balakrishnan “*Schaum’s Outline of Graph Theory: Including Hundred’s of Problems*”, McGraw- Hill Companies Inc, 1997.
- [71] A. Grau, Lee Ming-Jer, J. Romeu, H. Jafarkhani, L.Jofre, F. De Flaviis “ A Multifunctional MEMS-Reconfigurable Pixel Antenna For Narrowband MIMO Communications” *IEEE Antennas and Propagation society international symposium* , pp. 489-492, June 2007.
- [72] RodneyG.Vaughan “Two-port higher mode circular microstrip antennas” *IEEE Transactions on Antennas and Propagation*, Vol.36 Issue 3, pp. 309–321, Mar 1988.
- [73] E. F. Moore and C. E. Shannon, “Reliable Circuits Using Las Reliable Relays” (Part I and Part II), *J. Franklin Inst.*, Vol. 262, No. 3’ (Sept. 1956), 191-208 and No. 4 (Oct. 1956), 281-297.

- [74] N. Pippenger and G. Lin “Fault-Tolerant Circuit-Switching Networks ”, SIAM Journal on Discrete Mathematics, Vol.7, Issue 1 pp. 108-118, June 2004.
- [75] H. Chang , J. Quian, B. A. Cetiner, F. De Flaviis, M. Bachman and G. P. Li “RF MEMS Switches Fabricated on Microwave-Laminate Printed Circuit Boards ”, IEEE Electron Device Letters, Vol. 24, Issue 4, pp. 227-229, April 2003.
- [76] C.W.Jung, and F. De Flaviis “RF-MEMS Capacitive Series of CPW&MSL Configurations For Reconfigurable Antenna Application” , IEEE Antennas and Propagation society International Symposium, Vol. 2A, pp. 425-428, July 2005.
- [77] G. Wang, T. Polley, A. Hunt and J.Papapolymerou “A High Performance Tunable RF MEMS Switch Using Barium Strontium Titanate (BST) Dielectrics for Reconfigurable Antennas and Phased Arrays” , IEEE Antennas and Wireless Propagation Letters, Vol. 4, pp. 217-220, 2005.
- [78] A. Carton, C. G. Christodoulou, C. Dyck and C. Nordquist “Investigating the impact of Carbon Contamination on RF MEMS Reliability ” , IEEE Antennas and Propagation International Symposium, pp.193-196, July 2006.
- [79] T. M. Cover and J. A. Thomas “*Elements of Information Theory*” Second Edition, John Wiley & Sons, 2006.
- [80] www.microsemi.com : Application Notes For PIN Diode